Recent trends in non-invasive on-body chemical sensing

Zhanna Boeva [a,b], Zekra Mousavi [a], Tomasz Sokalski [a], Johan Bobacka [a,*]

[a] Åbo Akademi University, Faculty of Science and Engineering, Johan Gadolin Process Chemistry Centre, Laboratory of Molecular Science and Engineering, Henriksgatan 2, 20500, Turku/Åbo, Finland
[b] GlucoModicum Ltd, Toinen Linja 7, 00530, Helsinki, Finland

ARTICLE INFO

ABSTRACT

Recent advances in non-invasive on-body chemical sensing over the last five years (2018–2022) are summarized in this review. The review illustrates major achievements enabled by chemical sensors and biosensors based on electrochemical and optical transduction that were tested on human subjects. The review is limited to purely non-invasive analysis of body fluids and therefore sampling methods using *e.g.* microneedles and implantable sensors are excluded. Based on the recent literature, major research efforts are currently directed towards epidermal chemical sensors, in particular electrochemical and optical sensors and biosensors for determination of electrolytes, pH and metabolites in sweat. Other types of samples, such as tears, saliva and dermal interstitial fluid, receive less attention. However, glucose monitoring often relies on interstitial fluid as a representative sample. Recent approaches utilize innovative design of chemical sensor and biosensor platforms as well as microfluidic sampling for non-invasive on-body chemical sensing.

1. Introduction

A major trend in analytical chemistry is the transition from centralized laboratory analysis towards distributed chemical analysis in applications such as environmental monitoring and clinical diagnostics. This transition is enabled by the development of compact-size chemical sensors and biosensors with associated microfluidics and wireless connectivity. Wearable chemical sensors for personal health monitoring is a very active research area that aims to revolutionize the field of clinical diagnostics and personal healthcare. Analytes of interest include metabolites, electrolytes, H_3O^+ (pH), hormones, nutrients, proteins, and drugs. For some relevant analytes, such as glucose, lactate, pH, electrolytes, oxygen and CO_2, the chemical sensor technology is relatively mature. However, extensive research is still needed to develop robust chemical sensors and biosensors for several other biomarkers, especially when considering continuous monitoring. The interdisciplinary nature of this extremely challenging and prospective research field is well illustrated in previous authoritative reviews [1–6]. Heikenfeld et al. [1] provide a historical perspective of various mechanical, electrical, optical and chemical sensors, and highlight the barrier properties of human skin (epidermis), which makes non-invasive chemical monitoring particularly challenging. Heikenfeld et al. [2] also discuss the partitioning of analytes between blood and peripheral biofluids such as interstitial

fluid, saliva and sweat, which is essential for selecting the most representative non-invasive sample type. Ray et al. [3] emphasize the advances in chemistry, material science, and engineering that enable the development of integrated wearable sensor technologies. Gao et al. [4] focus on flexible electronic devices and systems for physical and chemical sensing in wearable applications. Kim et al. [5] focus on wearable biosensors based on electrochemical and optical transduction. Furthermore, Sempionatto et al. [6] highlights the combination of modern data analysis with wearable chemical sensors as a tool for biomarker discovery. These reviews provide a broad overview of wearable sensor technologies for on-body measurements that were mostly published until the year 2018 [1–5] and highlight the importance of wearable chemical sensors for biomarker discovery [6]. Due to the rapid progress in this research field, the goal of the present review is to highlight the most recent trends in non-invasive on-body chemical sensing by focusing on wearable chemical sensors and biosensors that were published during the last five years (2018–2022) and tested on human subjects.

On-body chemical sensing enables continuous tracking of biomarkers that are central to human health and wellbeing. Wearable biosensors for continuous glucose monitoring (CGM) is an excellent example that fulfils an enormous need among people with diabetes. CGM eliminates the discomfort related to blood sampling via finger pricking and it allows users to obtain frequent readings of their glucose

---

Abbreviations

AgNWs	silver nanowires
BSA	bovine serum albumin
CFT	carbon fibre thread
CNT	carbon nanotube
Ecoflex	platinum-catalyzed silicone (rubber)
FET	field effect transistor
GOx	glucose oxidase
HIS paper	highly integrated sensing paper
HRP	horseradish peroxidase
ISEs	ion-selective electrodes
ISF	interstitial fluid
ISM	ionophore-based PVC membrane
LIG	lased inscribed graphene
LOx	lactate oxidase
MHA	6-mercaptohexan-1-ol
MHD	magnetohydrodynamics
PANI	polyaniline
PB	Prussian Blue
PDMS	polydimethylsiloxane
PET	Polyethylene terephthalate
PU	polyurethane
PVA	polyvinyl acetate
PVB	polyvinyl butyral
PVC	polyvinyl chloride
rGO	reduced graphene oxide
RM	reference membrane (PVC or PVB based)

concentration. Hence, CGM provides real-time changes and trends in glucose concentrations, which are crucial to manage diabetes more effectively. However, all commercially available CGM devices are still invasive, because they rely on biosensors that are inserted or implanted under the skin to access interstitial fluid (ISF) that is a clinically relevant biological sample. Analysing ISF via microneedles causes less discomfort compared to finger pricking, but is still invasive.

Non-invasive extraction of ISF is possible by reverse iontophoresis and the more recent magnetohydrodynamic sampling method [7], which rely on transport of ISF through the skin without any physical puncture of the skin. However, non-invasive sampling of ISF is not trivial due to the excellent barrier properties of human skin. Therefore, recent research is much focused on non-invasive chemical sensing utilizing alternative human samples, such as sweat, saliva and tears, which are easily accessible as they are naturally excreted from the body, in contrast to ISF. However, the clinical relevance of sweat, saliva and tears is still questioned. As we know from basic analytical chemistry, it is absolutely essential that the sample is representative of the medium that we want to analyse – in this case human blood or tissue. If the biomarker concentration in the sample does not correlate with its concentration in the human body, the analysis is meaningless. This is probably the reason why commercially successful CGM devices mainly rely on the analysis of ISF.

Information about biomarkers in the human body may be obtained non-invasively also via spectroscopic methods, *i.e.* by applying electromagnetic radiation through the skin. This approach solves the sampling issue. However, when considering the chemical complexity of biological media, a major challenge is to find wavelengths of the electromagnetic radiation where only the analyte interacts and responds without any interference from the matrix. Whatever analytical method chosen, non-invasive on-body chemical sensing is still associated with major challenges, which are addressed by many research groups [1–7]. The fast progress and prospective future applications in this branch of analytical chemistry encouraged us to summarize the recent trends in the form of this review.

This review covers recent advances in non-invasive on-body chemical sensing. The focus is on applications in this field over the last five years (2018–2022) in samples like sweat, interstitial fluid, saliva, and tears. The review illustrates major achievements enabled by chemical sensors and biosensors based on electrochemical and optical transduction that have been tested on human subjects. Since the review is limited to non-invasive analysis of body fluids, all sampling methods that require physical skin puncture are excluded. Therefore, even minimally invasive techniques, such as microneedles, are outside the scope of this review. Wearable sensors that record physical parameters such as hearth rate, electrocardiogram (ECG), temperature and physical movements, belong to the class of physical sensors, which are also outside the scope of this review. Typical samples, analytes, wearable

sensors, and detection methods used in non-invasive on-body chemical sensing are summarized in Scheme 1.

2. Epidermal sensors

Epidermal sensors are devices or systems that are designed to be worn on the skin. Due to their ability to continuously monitor a wide range of parameters in a non-invasive and convenient manner, these sensors have the potential to revolutionize healthcare, sports, and other human activities. Potential use scenarios of epidermal sensors in healthcare include remote monitoring of patients, continuous monitoring of vital signs, and early detection of abnormal medical conditions. In sports, epidermal sensors may help athletes to optimize their performance and to prevent injuries by monitoring fatigue levels. In occupational health, epidermal sensors can be used to monitor the exposure of workers to harmful substances or conditions. In research, epidermal sensors enable studies on human physiology and behavior in real-world situations.

Chemical sensors and biosensors based on electrochemical transduction (current, potential, impedance) represent a major group of epidermal sensors that are used to measure *e.g.* electrolytes, metabolites, and drug concentrations in sweat [5,6]. Another type of epidermal sensors uses electromagnetic radiation in the UV–vis–NIR wavelength range to measure and analyse chemical properties. For instance, near-infrared spectroscopy can be employed in non-invasive measurement of blood oxygenation level or glucose concentration by shining light through the skin and measuring the reflectance or transmittance. Likewise, in fluorescence-based sensors particular chemicals or biomolecules are detected by measuring the light emitted after excitation.

Epidermal sensors come in various forms, such as patches, temporary tattoos (stickers), or other wearable devices that contact the skin. They should be biocompatible, flexible, thin, and lightweight to conform to the irregular surface of the skin, allowing for comfortable and unobtrusive wear for prolonged times. Batteries usually power epidermal sensors, while also other energy sources, energy harvesting mechanisms, and wireless energy transfer are used. Additionally, epidermal sensors should be able to communicate wirelessly with external devices for data collection, analysis, and interpretation.

2.1. Sweat

Sweat, also known as perspiration, is the fluid secreted by sweat glands in the skin of mammals. It is mainly composed of water, electrolytes (such as Na^+, K^+, Ca^{2+}, Mg^{2+}, and Cl^-), metabolites (such as lactate, ammonia, and urea), and unmetabolized pharmaceutical drugs [8,9]. Sweating serves several important functions in the body, such as thermoregulation, detoxification, hydration, and sweating promotes skin health [10]. In research works done within the period considered in

Sample type	Analyte	Wearable type	Detection method
Sweat	Glucose / Electrolytes & pH / Lactate / Other biomarkers	Microfluidic patch/textile / Microfluidic device / Wristband / Smart socks and gloves / Tape sensor	**Chemical sensors** - Potentiometry - Colorimetry - Amperometry **Biosensors** - Amperometry - Enzymatic - Immunochemical
ISF	Glucose	Temporary tattoo / Magnetohydrodynamics	
Saliva	Electrolytes	Pacifier / Mouth guard	
Tears	Glucose / Ethanol / pH	Contact lens	

Scheme 1. Typical types of samples, analytes, wearable sensors, and detection methods used in non-invasive on-body chemical sensing.

this review, both classical and novel materials and techniques were used to fabricate electrolyte and pH sensors for wearable applications. The two main transduction methods used were electrochemical and optical. Table 1 shows the concentration ranges of important analytes in sweat, and other biofluids, and their diagnostic importance.

2.1.1. Electrochemical sensors for determination of electrolytes and pH in sweat

All electrochemical sensors mentioned in this section were tested in on-body applications. The sensitivity and working range of the sensors are summarized in Table 2.

2.1.1.1. Fibre and fabric type sensors. A self-healable sensor has the ability to repair or recover its functionality after being damaged. This property provides benefits such as extended life span, reduced maintenance costs and enhanced reliability. Self-healable and wearable sensors with a fast and reversible recovery were presented by Yoon et al. [16] for monitoring Na^+ and K^+ in sweat. The sensors were prepared by covering carbon fibre thread (CFT) with poly(3,4-ethylenedioxythiophene) doped with polystyrene sulfonate (PEDOT:PSS) and further coated with the respective ionophore-based polyvinyl chloride (PVC) membrane (ISM). For the reference part, CFT was covered with Ag,AgCl paste and a reference membrane (RM) composed of polyvinyl butyral (PVB) containing NaCl. Both fibres were subsequently coated with poly(1, 4-cyclohexanedimethanol succinate-*co*-citrate) (PCSC) as the self-healing polymer (SHP). Finally, the indicator and reference fibres were weaved together (Fig. 1A and B). A similar approach was used by the same authors for pH monitoring [17]. In this case, the indicator fibre was prepared by covering CFT with polyaniline (PANI), which is known

to be sensitive to pH changes (Fig. 1C). The obtained fibre-type sensors were knitted into textile garment (Fig. 1D).

Fibre-type substrates are appealing, because the resulting sensors can be woven into garments providing close and comfortable contact with human skin. Additionally, fibre-based sensors can be very flexible thus resisting damage caused by on-body usage.

Wang et al. [18] presented a general concept of making highly flexible electrochemical fabric from carbon nanotube (CNT)-based sensing fibre units that were weaved into the fabric from which a garment was made (Fig. 2A). Sensing fibres were made for potentiometric determination of Na^+, K^+, Ca^{2+}, and pH, as well as for amperometric sensing of glucose. For making the Na^+, K^+, and Ca^{2+} sensors, conventional ionophore-based PVC membranes were used, whereas the pH sensor was based on PANI. The glucose sensor was of the enzymatic amperometric type. The reference electrode was Ag/AgCl/PVB.

In another work, Terse-Thakoor et al. [19], presented a multi sensor thread-based patch for potentiometric determination of Na^+, NH_4^+, and pH, as well as for amperometric lactate monitoring in sweat. The substrate of the sensors was either polyester (PE) or stainless steel (SS) thread covered with carbon black. For Na^+ and NH_4^+ sensors, conventional ionophore-based PVC membranes were used, while PANI was used for the pH sensor. Lactate was measured by an enzyme-based amperometric sensor. This concept is promising because the fibrous textile threads can be directly sewn, woven, or stitched on to any garment to be in close contact with the skin (Fig. 2B)

A novel wearable sweat nanobiosensor based on conductive thread decorated with zinc-oxide nanowires (ZnO NWs) (Fig. 2C and D) was proposed by Zhao et al. [20]. The sensor was used for the potentiometric detection of Na^+ and lactate in sweat. Here, the enzymatic

Table 1

Concentration ranges of essential analytes (mM) and pH (pH units) in blood, ISF, sweat and saliva and their diagnostic importance.

| Analyte/pH	Concentration (mM)/pH value				Diagnostic importance	Ref.
	Blood	ISF	Sweat	Saliva		
pH	7.35–7.45	6.6–7.6	6–6.8	6.7–7.3	Pathogenesis of skin diseases, wound healing	[11–13, 15]
Na^+	135–145	similar to plasma	10–100	27–217	Cystic fibrosis, muscle cramp, hyper/hyponatremia	[6,9]
K^+	3.5–5	similar to plasma	5–15	10s	Hyper/hypokalemia and an indicator of ocular disease	[9,14]
Cl^-	96–106	similar to plasma	10–100	7–18	Cystic fibrosis, lung disease, hyper/hypochloremia, and potentially for hydration status and electrolyte stores	[6,9]
Glucose	3.9–5.5	0.8–6	0.006–0.3	0.03–0.14	Diabetes management, metabolic syndrome	[6,14]
Lactate	0.5–10	2.5–6.6	3.7–50	<3.5	Fatigue level, lactic acidosis, ischemia, sepsis, liver disease and cancer, hydration plan	[6,14]

Table 2

Electrochemical sensors for determination of electrolytes and pH in sweat.

Working electrode	Reference electrode	Analyte	Concentration range	Sensitivity mV/dec	ref
CFT/PEDOT:PSS/ISM/SHP	CFT/Ag,AgCl/RM/SHP	Na^+	0.1–100 mM	60.7	[16]
		K^+	0.1–100 mM	54.8	
CFT/PANI/SHP	CFT/Ag,AgCl/RM/SHP	pH	pH 3.89–10.09	−58.7	[17]
CNT fibre/PEDOT/ISM	CNT fibre/Ag,AgCl/RM	Na^+	10–160 mM	45.8	[18]
CNT fibre/PANI		K^+	2–32 mM	35.9	
		Ca^{2+}	0.5–2.53 mM	52.3	
		pH	pH 4–7	N/A	
PE thread/C/ISM	PE thread/Ag,AgCl/RM	Na^+	1–1000 mM	52.8	[19]
PE/thread C/ISM		NH_4^+	0.1–100 mM	60.6	
SS thread/C/PANI		pH	pH 4–8	−62.3	
Cotton thread, PDMS/C/ZnO-NWs/ISM	Cotton thread, PDMS/Ag,AgCl/RM	Na^+	0.1–100 mM	N/A	[20]
C/PANI, PU fibre	Ag/AgCl	pH	pH 2–7	ca −60	[21]
Au NWs/SEBS fibre/Au/ISM	Au NWs/SEBS fibre/Au/RM	Na^+	$10^{-5} - 10^{-1}$ M	59.2	[22]
		Cl^-	$10^{-5} - 10^{-1}$ M	−57.2	
		pH	pH 4–8	−58.3	
rGO fibre/ISM	rGO fibre/Ag,AgCl/RM	pH	pH 3–8	−55.4	[23]
PDMS/AuNS/CNTs/PANI	PDMS/AuNS/Ag,AgCl/RM	pH	pH 4–8	−71.4	[24]
PDMS/AuNS/CNTs/CoWO$_4$		Glucose	0–0.3 mM	10.89 µA/mM	
PET/C/PEDOT/ISM	PET/C/PEDOT/IL, PM/RM	Na^+	$10^{-4} - 10^{-1}$ M	54.8	[25]
		K^+	$10^{-4} - 10^{-1}$ M	53.9	
PET/C/PEDOT/ISM	PET/C/PEDOT/IL,PM/RM	Na^+	$10^{-4} - 10^{-1.1}$ M	57	[26]
PET/Au/ISM	PET/Ag,AgCl/RM	Na^+	15–120 mM	56	[27]
		Cl^-	15–120 mM	N/A	
PDMS/Au/C/ISM	PDMS/Au/Ag,AgCl/RM	Na^+	0.1–200 mM	60	[28]
		K^+	0.1–100 mM	46	
PU/C/MWCNTs/ISM	PU/IL	Na^+	0.1–100 mM	54.2	[29]
		K^+	0.1–100 mM	56.8	
		Cl^-	1–100 mM	−63.0	
		pH	pH 4–7.5	−50.1	
PET/SilkNCT/PEDOT:PSS/ISM	PET/Ag,AgCl/RM	Na^+	5–100 mM	51.8	[30]
		K^+	1.25–40 mM	31.8	
PDMS/v-AuNW/ISM	PDMS/v-AuNW/Ag,AgCl/RM	Na^+	$10^{-3} - 10^{-1}$ M	58.2	[31]
PDMS/v-AuNW/PANI		K^+	$10^{-3} - 10^{-1.75}$ M	41.5	
		pH	pH 5–8	−56.1	
PET/C/ISM	PET/Ag,AgCl/RM	Na^+	1–1000 mM	19.6	[32]
PET/C/ISM		K^+	1–1000 mM	14.6	
PET/C/PANI/GOx chitosan		Glucose	0.1–50 mM	15.1	
PE/C/PANI	PE/Ag,AgCl/RM	pH	pH 4.5–8.5	−59.1	[33]
PET/Ag/C/F–Ti$_3$C$_2$T$_x$/PANI	PET/Ag,AgCl/RM	pH	pH 1–11	−40.7	[34]
PET/TA-rGO/PDMS	PET/Ag,AgCl/RM	pH	pH 1–10	−53.0	[35]
PET/Au/WO$_3$, PVDF	PET/Ag,AgCl/RM	pH	pH 3–8	−51.77	[36]
Paper/C or Au or Pt/Nafion	Paper/Ag,AgCl/RM	Na^+	$10^{-3.75} - 10^{-0.5}$ M	56.3	[37]
Silanized paper/Gr/ISM	Silanized paper/Gr/RM	Na^+	$10^{-6} - 10^{-1}$ M	55.7	[38]
		K^+	$10^{-6} - 10^{-1}$ M	57.0	
		Cl^-	$10^{-6} - 10^{-1}$ M	−56.7	
		pH	pH 4–7.5	−56	
Leather/Na$_{0.44}$MnO$_2$, GR, DBP, PVDF	Leather/Ag	Na^+	0.21−24.54 mM	58	[39]
PET/Ag/C/ISM	PET/Ag/RM	Na^+	10–1.60 mM	N/A	[40]
PET/Ag/C/PANI		K^+	2–32 mM	N/A	
		pH	pH 4–8	−53.8	
PET/Ag/C/ISM	PET/Ag,AgCl/PVB/RM	Na^+	15–120 mM	56.2	[41]
		K^+	5–40 mM	51.3	
PDMS/AgNWs/rGO/ISM	PDMS/AgNWs/RM	Na^+	10–160 mM	60.1	[42]
PDMS/AgNWs/rGO/ISM		K^+	2–32 mM	64.5	
PDMS/AgNWs/AuNPs/PANI		pH	pH 3–8	−60.0	
Au/Ir/PEDOT/IrO$_x$	N/A	pH	pH 1–9	−53	[43]
NBR/Au/Ag,AgCl	NBRAu/Ag,AgCl/RM	Cl^-	25–200 mM	−52.8	[44]
NBR/Au/PANI		pH	pH 4-7	−60.3	
Textile/Ecoflex/Eco-Gr/ISM	Textile/Ecoflex/Eco-Gr/Ag,AgCl/RM	Na^+	1–1000 mM	58.76	[45]
EIROF	3 M™ EKG electrode	pH	pH 4–8	−32.11	[46]

CFT – carbon fibre thread, PEDOT:PSS – poly(3,4-ethylenedioxythiophene) doped with polystyrene sulfonate, ISM – ionophore-based PVC membrane, SHP – self healing polymer, RM – reference membrane (PVC or PVB based), PANI – polyaniline, CNT – carbon nanotube, PE – polyester, C – carbon, SS – stainless steel, PDMS – polydimethylsiloxane, ZnO NWs – zinc oxide nanowires, PU – polyurethane, AuNWs – gold nanowires, SEBS – styrene-ethylene/butylene-styrene, rGO – reduced graphene oxide, AuNS – gold nanosheets, CoWO$_4$ – cobalt tungstate, PET – Polyethylene terephthalate, SilkNCT – silk fabric-derived nitrogen-doped carbon textile, IL – ionic liquid, PM – polymeric matrix, v-AuNW – vertically aligned gold nanowires, GOx – glucose oxidase, F–Ti$_3$C$_2$T$_x$ – fluoroalkyl silane functionalized Ti$_3$C$_2$T$_x$ Mxene, TA-rGO – Tannin-reduced graphene oxide, WO$_3$ – Tungsten oxide, PVDF – poly(vinylidene fluoride), Gr – graphene, GR – graphite, DBP – dibutyl phthalate, PVB – poly(vinyl butyral), AgNWs – silver nanowires, AuNPs – gold nanoparticles, IrO$_x$ – iridium oxide, NBR – nitrile rubber, Ecoflex – platinum-catalyzed silicone (rubber), Eco-Gr – Ecoflex/Graphene, EIROF – electrodeposited iridium oxide film.

potentiometric determination of lactate was based on measuring the redox potential of the oxidised and reduced tetrathiafulvalene couple (TTF^+/TTF). The TTF^+/TFF ratio changes due to the oxidation of lactate in the presence of LOx according to the reaction:

$$Lactate + 2TTF^+ \rightarrow pyruvate + 2TTF + 2H^+$$
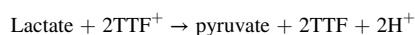
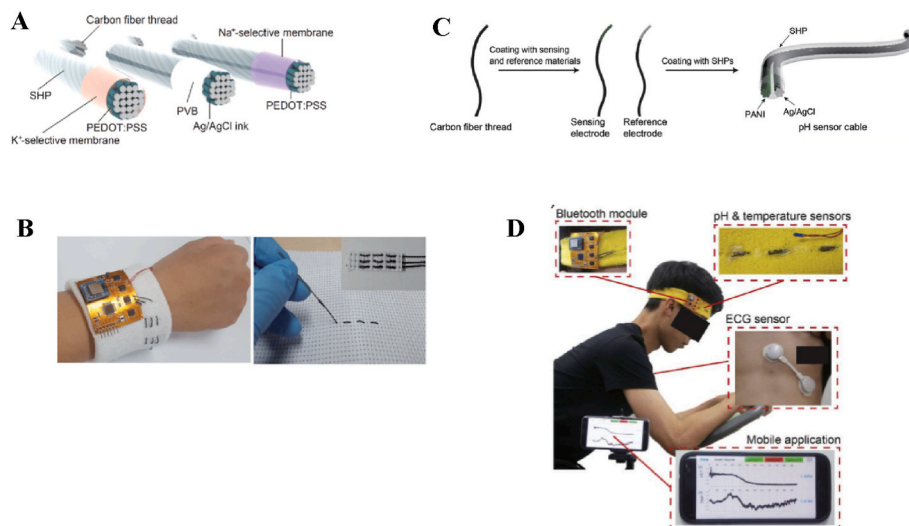Hou et al. [21] reported a highly sensitive and wearable

Fig. 1. Wearable self-healing sweat sensor based on polymer-coated carbon fibre thread. **(A)** Schematic illustration of self-healing ion-sensing and reference thread electrodes. **(B)** Sensor integration in a wristb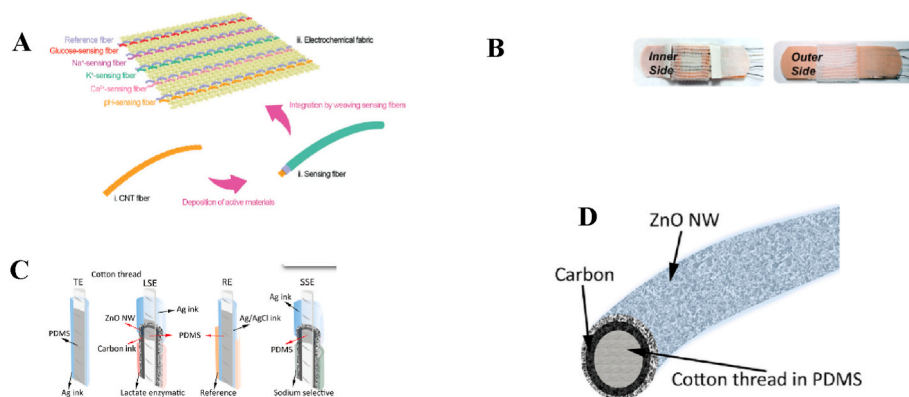and. Adapted with permission from Ref. [16]. *Copyright © 2019, American Chemical Society.* **(C)** Schematic illustration of self-healing ion-sensing and reference thread electrodes. **(D)** Sensor integration in a headband. Adapted with permission from Ref. [17]. *Copyright © 2020, Elsevier.*

Fig. 2. (A) Schematic illustration of the fabrication of the electrochemical fabric by weaving sensing fibres, made by depositing active materials on carbon nanotube (CNT) fibre substrates. Adapted with permission from Ref. [18]. *Copyright © 2018, John Wiley & Sons.* **(B)** Photograph of sweat sensor patch prototype. Adapted with permission from Ref. [19]. *Copyright © 2020 The Authors, some rights reserved. Distributed under a Creative Commons Attribution License 4.0 (CC BY).* **(C)** Cross-section view of electrodes showing different material layers. **(D)** Electrode consisting of cotton thread in PDMS/C/ZnO NW layers. Adapted with permission from Ref. [20]. *Copyright © 2021, Elsevier.*

potentiometric pH sensor based on electrospun flexible PANI/PU fibres. In such a construction, PANI provided pH sensitivity while PU enhanced the mechanical properties. By using this sensor, pH changes below 0.2 pH units could be detected.

Highly stretchable (up to 200 %) fibre-based ion-selective electrodes (ISEs) and reference electrode for determination of Na^+, Cl^-, and pH in sweat were presented by Xu et al. [22]. The electrodes were fabricated by depositing the ISM and RM on stretchable gold fibre substrates (Au NWs) (Fig. 3). The slopes of the resulting ISEs slightly fluctuated upon stretching the fibres between 0 % and 200 % strain. The stretchable fibre electrodes was woven into a garment for on-body sweat monitoring.

A textile integrated potentiometric pH sensor was proposed by Napier et al. [23]. To prepare the sensor, a traditional plasticized PVC-based membrane containing the ionophore, was spray-coated on reduced graphene oxide (rGO) in the form of a fibre (with diameter of 35 or 50 μm and about 15 mm length) to improve the reproducibility of sensor production. Similarly, the reference membrane was spray-coated on the same rGO fibre to make the reference part. Sections of the rGO fibre between pH and reference parts were coated with insulating PU (Fig. 4).

2.1.1.2. Planar type sensors. Planar type sensors are among the most commonly studied flexible sensors as they offer advantages such as a uniform sensing surface and ease of integration. In this case, the most frequently used substrates are polyethylene terephthalate (PET) and polydimethylsiloxane (PDMS).

Oh et al. [24] presented a stretchable (mechanical stability up to 30 % stretching), skin-attachable sensor for the determination of pH and glucose in sweat (Fig. 5). A PANI-based potentiometric sensor was used for measuring pH, while glucose was determined using a non-enzymatic amperometric sensor. The stretchable substrate used for making pH or glucose sensors was PDMS/gold nanosheets (AuNS)/CNT prepared by layer-by-layer deposition. The substrate was covered with PANI and cobalt tungstate ($CoWO_4$) for preparing the pH and glucose sensor, respectively. The Ag/AgCl reference electrode was prepared via chlorination of silver nanowires covered with a PVB-based RM. Due to encapsulation of the sensor with sticky silbione™, the sensor had good adhesion even to wet skin.

A flexible sweat sensing platform (Fig. 6A) for potentiometric Na^+ and K^+ determination was demonstrated by Alizadeh et al. [25]. The Na^+ and K^+ sensors were based on conventional ISMs. For making the
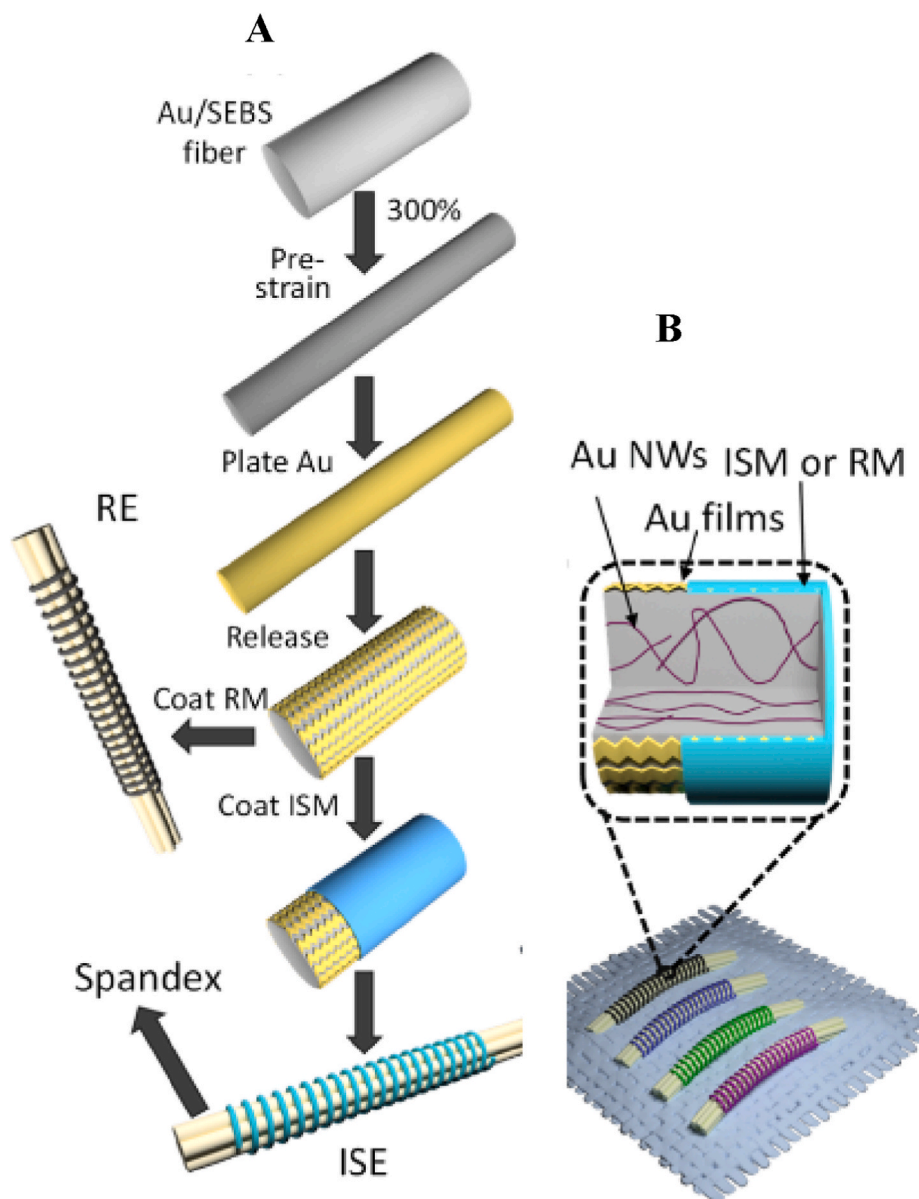
Fig. 3. **(A)** Fabrication process of stretchable Au fibre-based ISE and RE. **(B)** Schematic illustration of the wearable potentiometric ion sensors including three ISEs and RE. Adapted with permission from Ref. [22]. *Copyright © 2020, American Chemical Society.*
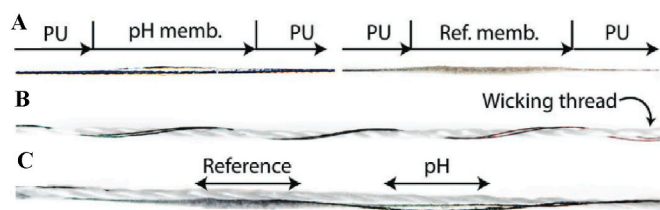

Fig. 4. **(A)** Images of active regions of pH and reference membranes. **(B)** Interconnect region of sensor bundle. **(C)** Active region of sensor bundle. Adapted with permission from Ref. [23]. *Copyright © 2022, John Wiley & Sons.*

reference electrode a PET/carbon ink substrate was covered with PEDOT (as transduction layer) and a RM containing ionic liquid (IL) in a polymeric matrix. The platform was integrated into a patch containing a conformable fluidic system for sweat collection with rapid sweat removal to minimize sensor lag (Fig. 6B). In another publication presented the same year by McCaul et al. [26], the ISE platform (Fig. 6A)

was integrated into a watch-type casing made by 3D printing and used for Na$^+$ measurement in sweat (Fig. 6C).

A flexible PET-based sweat sensing patch was reported by Nyein et al. [27]. The patch comprises four layers: a spiral-patterned microfluidic channel, a pair of parallel Au electrodes for impedance-based sweat-rate sensing, a parylene-C insulation layer, and Na$^+$, K$^+$, Cl$^-$, pH potentiometric sensing electrodes (Fig. 7A). The analyzed data was wirelessly transmitted to a cell phone via Bluetooth (Fig. 7B).

Another soft, flexible, and skin-worn potentiometric device for the detection of Na$^+$ and K$^+$ in sweat was reported by Sempionatto et al. [28]. A microfluidic system permitted effective natural sweat pumping to the detection chamber. The device consisted of a top PDMS layer containing the sensors, a second PDMS layer containing microchannels and an adhesive layer in contact with the skin (Fig. 7C).

PU is another possible substrate for making planar sensors. In a work by Parrilla et al. [29], a flexible device for monitoring Na$^+$, K$^+$, Cl$^-$, and pH in sweat was introduced. The device comprised a sampling cell and multichannel sensors (Fig. 8A). The design of the sampling cell prevented sweat contamination and evaporation problems and provided
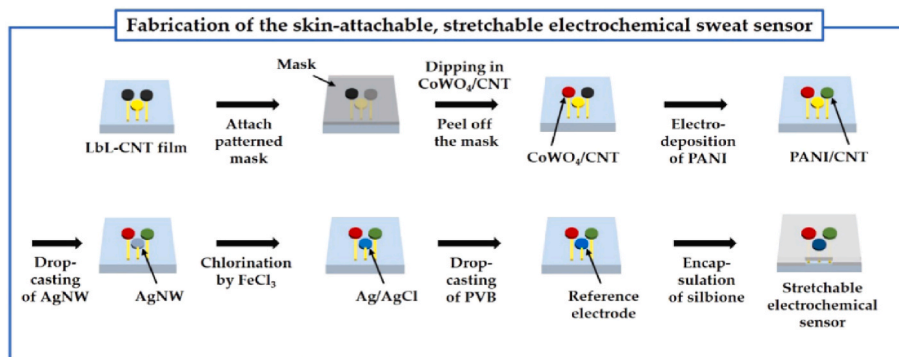
Fig. 5. Fabrication of the skin-attachable, stretchable electrochemical sweat sensor. Adapted with permission from Ref. [24]. *Copyright © 2018, American Chemical Society.*
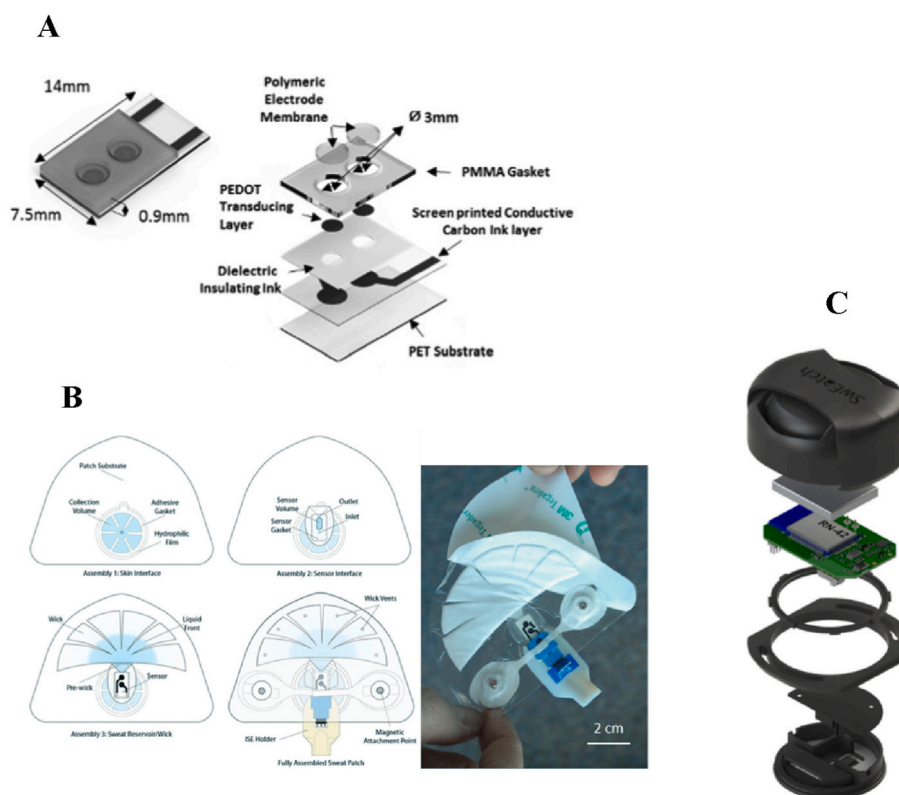

Fig. 6. (A) The assembled and individual components of the ISE platform, including a polymeric electrode membrane, polymethyl methacrylate (PMMA) gasket, PEDOT transducing layer, dielectric insulating ink, screen-printed conductive carbon ink layer, and a PET substrate. **(B)** Schematic illustration and image of fully assembled sweat patch. Adapted with permission from Ref. [25]. *Copyright © 2018, Royal Society of Chemistry.* **(C)** Schematic illustration of the platform integrated into a watch-type device. Reproduced with permission from Ref. [26]. *Copyright © 2018, John Wiley & Sons.*

passive sweat flow (Fig. 8B). The potentiometric sensors were prepared by depositing the respective ionophore-based PVC membrane layers on carbon ink and multiwalled carbon nanotubes (MWCNTs) deposited on the PU substrate. The reference electrode was constructed by using a plasticized PU membrane containing ionic liquid.

He et al. [30] reported a PET based flexible patch with silk fabric-derived nitrogen-doped carbon textile (SilkNCT) for potentiometric monitoring of Na^+ and K^+ in sweat (Fig. 9). The SilkNCT textile provided good electrical conductivity and good water wettability needed for efficient electron transmission and good access to reactants due to the porous and intrinsically N-doped graphitic structure. Other biomarkers (glucose, lactate, ascorbic acid, and uric acid) were also determined by enzyme-based amperometric sensors.

Vertically aligned gold nanowires (v-AuNW) on a PDMS substrate

was reported by Zhai et al. [31]. This substrate was used for the fabrication of a stretchable and wearable epidermal ion-selective electrode array for the potentiometric determination of pH, Na^+ and K^+ in sweat. The ISMs were ionophore-based PVC membranes in the case of Na^+- and K^+-ISEs, while the pH electrode was PANI-based. The analytical performance of the device was maintained under up to 30 % strain. The v-AuNW ISEs could easily be integrated with a flexible printed circuit board for wireless communication.

Mou et al. [32] presented a PET-based epidermal sensor for potentiometric determination of Na^+, K^+ and glucose in sweat (Fig. 10A). For measuring Na^+ and K^+ ions, potentiometric ionophore-based sensors were used, while an enzyme-based glucose sensor was used for potentiometric measurement of glucose. The glucose sensor was prepared by depositing a glucose oxidase layer (GOx) on a PANI-based pH sensor. In
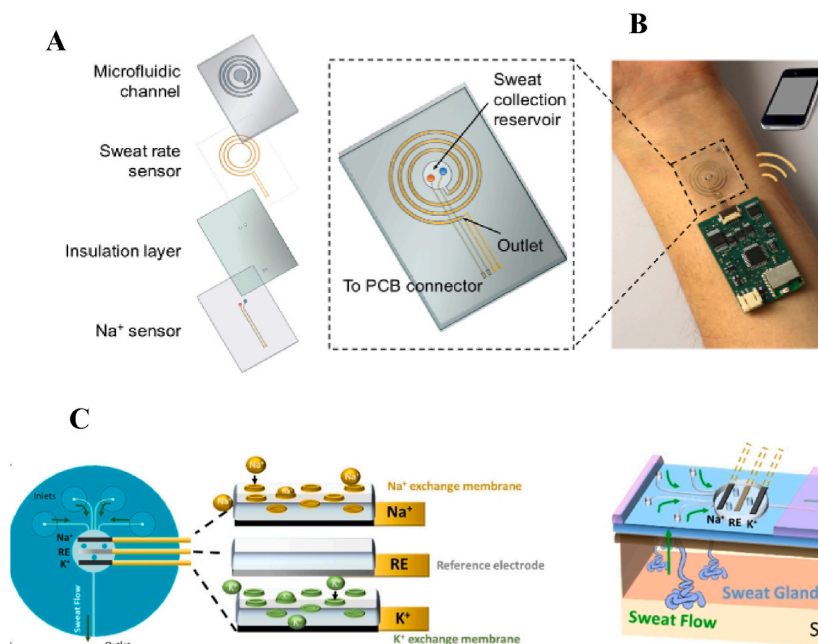
Fig. 7. **(A)** Schematics of a wearable sweat sensing patch and stacked view of the microfluidic device. **(B)** The sweat sensing patch on a human wrist. Adapted with permission from Ref. [27]. *Copyright © 2018, American Chemical Society.* **(C)** Schematic of microfluidic device integrated with the fabricated ISE and schematics of working principle of the epidermal device where the sweat generated by sweat glands is driven from the inlets to the detection chamber. Adapted with permission from Ref. [28]. *Copyright © 2018, John Wiley & Sons.*
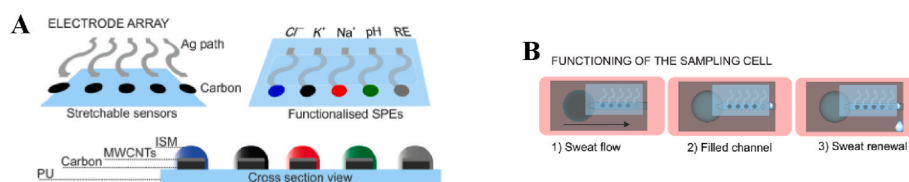

Fig. 8. **(A)** Electrodes before and after functionalization. **(B)** Sweat flow in the sampling cell once it is attached to the skin. Adapted with permission from Ref. [29]. *Copyright © 2019 The Authors, some rights reserved. Distributed under a Creative Commons Attribution NonCommercial License 4.0 (CC BY-NC).*
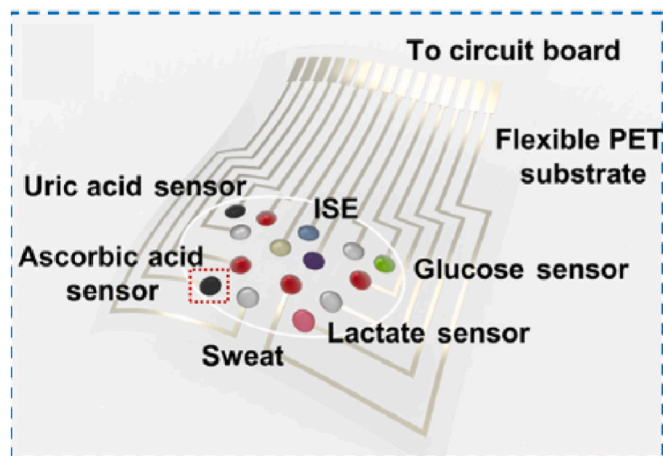

Fig. 9. Illustration of a wearable sweat analysis patch based on SilkNCT with multiplex electrochemical sensor array. Reproduced with permission from Ref. [30]. *Copyright © 2019 The Authors, some rights reserved. Distributed under a Creative Commons Attribution NonCommercial License 4.0 (CC BY-NC).*

this case, GOx catalyzed glucose oxidation thus generating H^+ that was measured by the potentiometric pH sensor (Fig. 10B).

In a lactate biosensor presented by Xuan et al. [33] for on-body

lactate determination, pH and temperature sensors were included to account for the acidity and temperature influence on the lactate measurement.

A flexible, superhydrophobic, and skin-attachable potentiometric pH sensor based on a more recent 2D material (MXene) was presented by Chen et al. [34]. For the sensor preparation, the MXene (fluoroalkyl silane functionalized $Ti_3C_2T_x$), and a PANI membrane were deposited on a PET substrate. This construction improved the sensitivity, reversibility, responsiveness, and environmental stability of the sensor. The pH sensing and reference parts are shown in Fig. 11A. In another flexible potentiometric pH sensor reported by Lin et al. [35], self-adhesive tannin (TA)-graphene supramolecular aggregates were deposited on a PET substrate (Fig. 11B). TA was self-assembled on reduced graphene oxide to form supramolecular aggregates (TA-rGO) which promoted electron transfer from TA to the electrode. The phenolic hydroxyl groups in tannin served as pH responsive sites and provided strong adhesion. Due to the electronic conductivity of TA-rGO, a reference electrode membrane was deposited on top of the PET/TA-rGO substrate. Still another example of a potentiometric pH sensor with PET substrate was given by Tang et al. [36]. The authors used proton lattice intercalated tungsten oxide (H_xWO_3), with high chemical stability, biocompatibility, and low cost, as the pH sensitive and selective material (Fig. 11C).

Synthetic substrates are the most frequently used materials for planar sensor fabrication. However, substrates based on natural materials are also used. Hoekstra et al. [37] proposed a paper substrate for preparation of a wearable patch for potentiometric monitoring of total cation
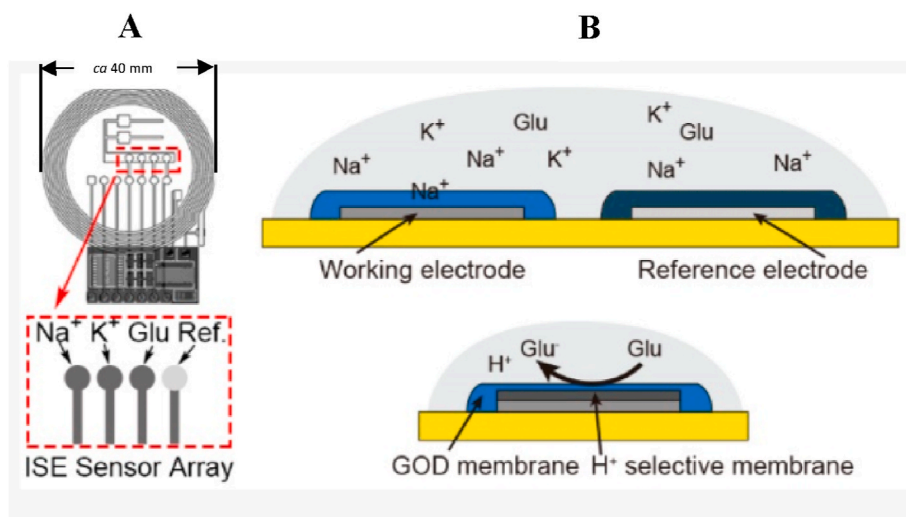
Fig. 10. (A) Illustration of epidermal sensors for non-invasive determination of metabolites and electrolytes. Top view of the assembled epidermal sensor with three potentiometric ion-selective electrodes for determination of Na^+, K^+ and glucose. **(B)** The principle of ISE for detecting Na^+, K^+, and glucose which is based on GOx membrane and H^+-selective membrane. Adapted with permission from Ref. [32]. *Copyright © 2021, American Chemical Society.*
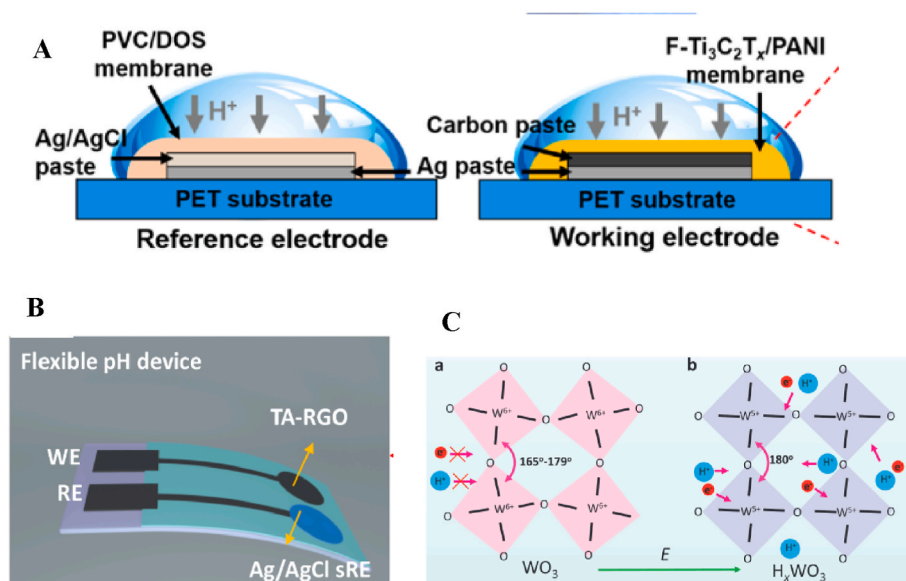

Fig. 11. (A) Illustration of PVC/dioctyl sebacate (DOS)-based Ag/AgCl reference electrode and F–Ti$_3$C$_2$T$_x$/PANI-based working electrode for pH measurements. Adapted with permission from Ref. [34]. *Copyright © 2022, American Chemical Society.* **(B)** Schematic illustration of flexible TA-rGO-based pH device. Adapted with permission from Ref. [35]. *Copyright © 2022, Elsevier.* **(C)** Structures of WO$_3$ before and after proton intercalation (H$_x$WO$_3$). Adapted with permission from Ref. [36]. *Copyright © 2022, John Wiley & Sons.*

content in sweat. The working electrodes were constructed by depositing carbon, gold or platinum on a paper substrate and subsequently covering it with Nafion. For the reference electrode, the paper substrate was covered with Ag,AgCl ink and subsequently PVB containing NaCl. The Na^+ ion was chosen as a model analyte. In this case, the best results (slope, detection limit, linear range, and response time) were obtained with carbon as substrate. The potentiometric results correlated well with the conductometric ones.

Another example of a paper-based potentiometric sensor was presented by An et al. [38]. The flexible integrated four-channel sensor was used for simultaneous monitoring of K^+, Na^+, Cl^- and pH in sweat. The sensor substrate was silanized paper covered with graphene. The ISEs had ionophore-based PVC membranes, and the reference electrode was also based on PVC (Fig. 12).

Leather was used as a substrate by Ghoorchian et al. [39] for

preparing a wearable potentiometric ion sensor for real-time monitoring of Na^+ in human sweat samples. As the sensing material, $Na_{0.44}MnO_2$ was used due to its Na^+ incorporation ability, electrical conductivity, stability, and low fabrication cost. For the flexible Na^+ sensor, the leather substrate was covered with cyanoacrylate glue to increase the surface hydrophobicity. Carbon paste containing $Na_{0.44}MnO_2$, graphite, dibutyl phthalate (DBP), and poly(vinylidene fluoride) (PVDF) was deposited on the substrate. The potentiometric sensor was integrated into a headband textile.

2.1.1.3. Mass production. Low-cost and high-throughput production with controllable size and density of sensors can be achieved using roll-to-roll (R2R) fabrication methods, where a PET substrate is very often used. Bariya et al. [40] reported the mass production of printed electrodes using the roll-to-roll gravure technique on 150 m flexible PET
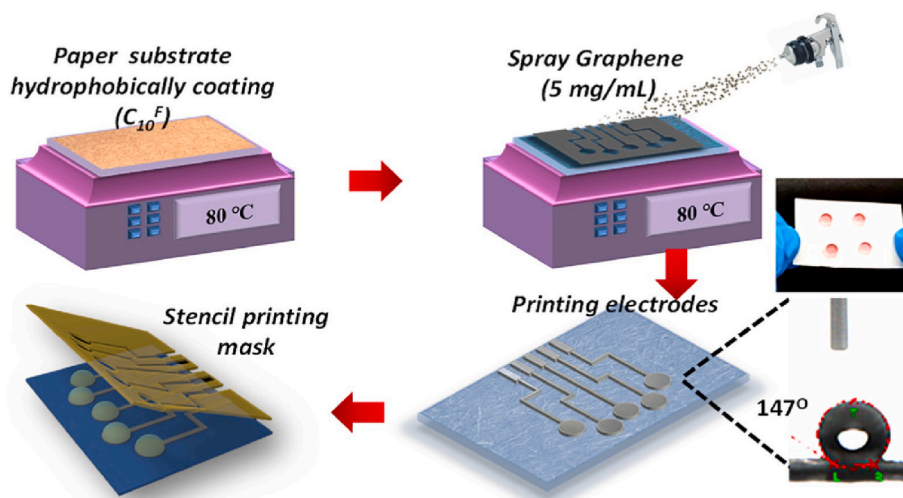
Fig. 12. A schematic representation of the fabrication of paper-based ISEs. Adapted with permission from Ref. [38]. *Copyright © 2019, Elsevier.*

substrate rolls (Fig. 13A and B). For Na^+ and K^+-ISEs, ionophore-based PVC membranes were used and the pH sensor was PANI-based. Importantly, the roll-to-roll gravure technique allowed the production of consistently performing sensors.

In another work, Nyein et al. presented R2R process for the mass production of microfluidic sensing patches [41]. The patch (Fig. 13C–F) permitted sweat capture within a spiral microfluidic channel for measuring sweat rate and analytes such as Na^+, K^+, and glucose in real time. The electrodes and the microfluidic channel were printed on a flexible PET substrate, using silver and carbon inks. The potentiometric Na^+ and K^+ sensors were made using traditional ionophore-based ISMs.

2.1.1.4. Other implementations. Some interesting sensor implementations are shown below. They are ingenious and novel although based on existing technologies. For example, Xu et al. [42] reported a battery-free, all-printed, and stretchable electrode array for measuring Na^+, K^+, pH, and glucose in sweat (Fig. 14A). For all sensors and the reference electrode, PDMS/silver nanowires (AgNWs) was used as substrate. In the case of Na^+ and K^+ sensors, rGO was deposited on top of the substrate and covered with the respective ISM. In the pH sensor, gold nanoparticles (AuNPs) were deposited on top of the PDMS/AgNWs substrate and covered with a PANI layer. For the reference electrode, the same substrate was covered by PVB. The main advantage of this concept is that the sensor itself is battery-free and does not consume any power. For data readout the device is powered by the mobile phone near field communication (NFC) and the data is transmitted wirelessly (Fig. 14B).

Gil et al. [43] reported an ear-worn device meant mainly for measuring cardiovascular parameters and additionally pH and lactate in sweat (Fig. 14D). The sweat rate was estimated using the impedance method. The determination of pH and lactate levels was done using potentiometric and amperometric sensors, respectively. The solid-state pH sensor was of metal/metal oxide type ($Au/PEDOT/Ir/IrO_x$).

A glove-based sensor was presented by Bariya et al. [44]. The sensor was capable of efficiently collecting relatively large volumes (hundreds of μL) of sweat sample in 30 min without the need of physical stimulation. The sensor array was patterned on a nitrile rubber (NBR) glove or finger cots (Fig. 14C). Chloride ion and pH were measured potentiometrically and other analytes (Zn, ascorbic acid, and ethanol) amperometrically. The chloride ion sensor and Ag/AgCl reference electrode were fabricated by depositing Ag,AgCl conductive ink over the Au electrode. The reference electrode was made by the deposition of a thick layer of PVB solution with saturated NaCl over the Ag/AgCl.

Recently, Kil et al. [45] reported fully integrated wireless sweat sensor socks for the real-time monitoring of Na^+ concentration in sweat. For this purpose, highly stretchable and conductive graphene ink was

used for the preparation of the Na^+ sensor. The graphene ink (Eco-Gr) was prepared by a fluid dynamics-assisted exfoliation of graphite that was mixed with elastomeric Ecoflex (Fig. 14E).

2.1.2. Optical sensors for determination of electrolytes and pH in sweat

Although the electrochemical transduction mode is most popular in the case of electrolyte and pH measurements, there are also examples where optical transduction was used, as summarized in Table 3. Kim et al. [47] proposed a soft microfluidic device with valves made from a super absorbent polymer (SAP) and colorimetric assay papers to sample, store and analyse chloride in sweat samples from the skin (Fig. 15A). The colour developed in the assay papers were stabilized by means of non-interacting ions and a surfactant. The device was used on human subjects and the results were compared to those obtained in the laboratory.

A more advanced colorimetric soft patch was presented by Choi et al. [48]. This patch enabled the measurement of temperature, total loss of sweat and its range. Additionally, it allowed for quantitative determination of pH, chloride, glucose, and lactate (Fig. 15B). Precise readout was facilitated by the integrated colour calibration markings. The results from on-body measurements correlated well with the results from the laboratory. In the same year, Promphet et al. [49] presented a flexible textile-based colorimetric sensor for determining pH and lactate in sweat. The sensor was made by depositing three different layers onto a cotton fabric. The layers were: chitosan, sodium carboxymethyl cellulose, and an indicator dye (mixture of methyl orange and bromocresol green) for pH or an enzymatic assay for lactate sensing. Cetyltrimethylammonium bromide (CTAB) was used to prevent fading of the indicator colours.

Another flexible colorimetric sensing patch was developed by Zhang et al. [50]. In this patch, superhydrophilic colorimetric assays were assembled on top of a superhydrophobic substrate generating a large wettability contrast to efficiently concentrate the sweat. This system was used for determining pH, chloride, and calcium ions in sweat (Fig. 15C). A similar approach of contrasting hydrophobic and hydrophilic parts of the sensor was presented by Zhao et al. [51]. In this case, a microfluidic thread/fabric-based analytical device integrated hydrophilic dot-patterns with a hydrophobic surface via embroidering thread into the fabric (Fig. 15D). The thread-embroidered patterns functioned as detection zones for sweat loss, pH, chloride, and glucose. Embroidered reference markers for more accurate colorimetric data readout surrounded the working dots.

2.1.3. Biosensors for sweat analysis

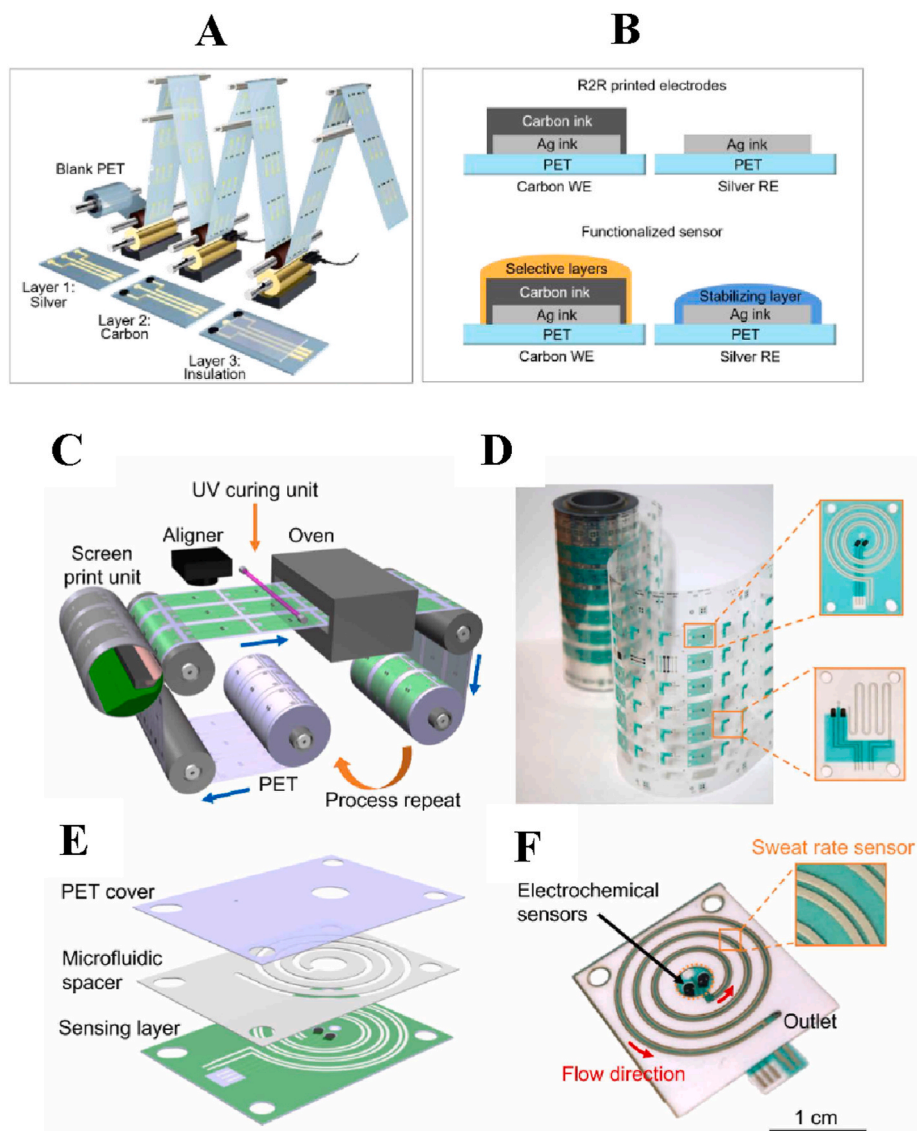Epidermal biosensors for monitoring various analytes in sweat have

Fig. 13. (A) Roll-to-roll (R2R) gravure printing of biocompatible electrode arrays on flexible PET substrate. **(B)** Schematic illustration of the cross-section of printed carbon and silver electrodes after printing and functionalization. Adapted with permission from Ref. [40]. *Copyright © 2018, American Chemical Society*. **(C)** R2R rotary screen printing of a wearable sensing patch. **(D)** Photo of sensing electrode patterns printed using the R2R method. **(E)** Sensing patch consisting of a sensing layer, microfluidic adhesive spacer, and PET cover sheet. **(F)** Illustration of the assembled biosensing patch. Adapted with permission from Ref. [41]. *Copyright © 2019 The Authors, some rights reserved. Distributed under a Creative Commons Attribution NonCommercial License 4.0 (CC BY-NC)*.

attracted significant attention lately, as summarized in Table 4. The popularity of using sweat for non-invasive on-body monitoring is obviously due to the good availability of sweat as a sample. Two methods of sweat production are generally used by researchers: (i) exercise induced sweating and (ii) chemically induced sweat production at rest. Monitoring biomarkers in sweat comes with the challenge of fluidic management and controlling the flow and production rate that affect the analytical sensitivity of a sensing platform in use [13]. Multiple reviews were written recently about sweat detection theory [52], covering chip design, modes of liquid transport, sampling [53], and other persisting challenges of this research direction. Several recent articles report novel methods of fluid quantification and management using *e.g.* nanoliter to microliter flow rate sensors (Fig. 16) [54], super-absorbing polymer [55] and tesla [56] valves, open nanofluidic sensors and hexagonally patterned (hex) wick with fumed silica and with gelatine binder used to couple the hex wick and sensor surface (Fig. 17) [57,58] for creating continuous and blood-correlated sweat biosensing devices, and flow-rate independent measurements of lactate concentration using enzyme/nanozyme approaches (Fig. 18) [59]. Correction of the

biosensor reading based on pH and temperature was recently introduced by Wiorek et al. [60] and Yoon et al. [61] to improve the accuracy of wearable sensor platforms.

The choice of the operational parameters of a biosensor largely depends on the method of detection and signal transduction as well as the nature of the biorecognition element used for the construction of the sensing layer. For example, in case of amperometric biosensors, the choice of potential applied at the working electrode depends on the molecule to be amperometrically detected, which can be a substrate or product of the enzymatic reaction, mediator or catalytic centre of the enzyme [62]. The redox potential of these molecules at which the maximum current density is observed largely depends on the modification of the working electrode. For example, hydrogen peroxide may be reduced at a carbon working electrode modified with Prussian Blue at potentials below 0 V, while hydrogen peroxide can be oxidised at potentials above 0.3 V if the electrode material is chosen to be Pt or its alloys with other metals of the platinum group. The size of the material particles used for modification of the working electrode, their doping degree, and arrangement at the surface of the electrode further affect the
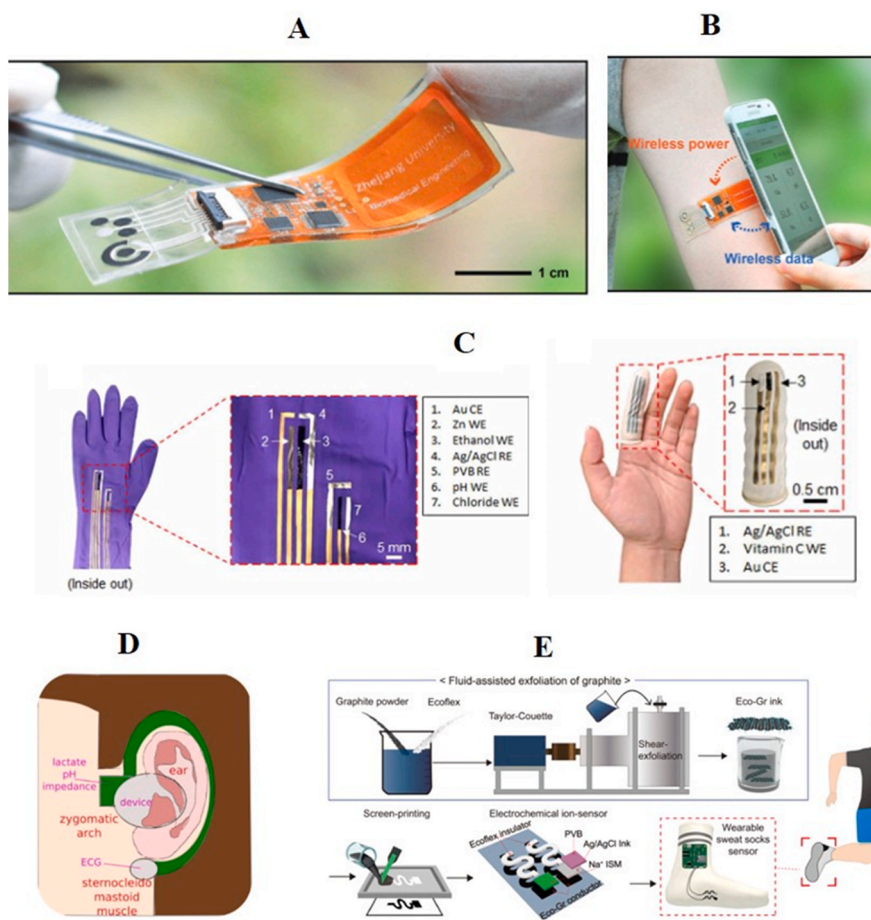
Fig. 14. **(A)** Battery-free, wireless, and epidermal electrochemical system for in situ sweat sensing. **(B)** The sweat-sensing device on a subject's arm, with a smartphone for wireless power and data transmission. Adapted with permission from Ref. [42]. *Copyright © 2019, John Wiley & Sons.* **(C)** Three-electrode system on the inside of a glove and finger cot. Adapted with permission from Ref. [44]. *Copyright © 2020 The Authors, some rights reserved. Distributed under a Creative Commons Attribution NonCommercial License 4.0 (CC BY-NC).* **(D)** Illustration of anatomical features of an ear located sensor for cardiovascular measurement and additional sweat parameters such pH and lactate. Adapted with permission from Ref. [43]. *Copyright © 2019 The Authors. Distributed under a Creative Commons Attribution License 4.0 (CC BY).* **(E)** Preparation of Eco-Gr ink for the fabrication of smart sweat socks. Adapted with permission from Ref. [45]. *Copyright © 2022, American Chemical Society.*

Table 3
Chemical sensors based on colorimetric transduction for detecting electrolytes and pH in sweat.

Analyte	Concentration/pH range	Ref.
Cl^-	0 to >160 mM	[47]
Cl^-	25–100 mM	[48]
pH	5.0–6.5	
pH	1–14	[49]
pH	4.4–7.4	[50]
Cl^-	0–125 mM	
Ca^{2+}	0–15 mM	
pH	5–7.5	[51]
Cl^-	10–150 mM	

choice of the potential applied at the working electrode. Therefore, electrochemical biosensors are typically optimised for multiple parameters, including the potential applied at the working electrode that produces the largest oxidation or reduction current upon addition of the analyte of interest, i.e. highest sensitivity.

Many articles published in the past five years cover various aspects of the research in sweat biomarker monitoring. In attempts to improve sensitivity and lower the limit of detection of the biosensors, carbon nanomaterials, metal nanoparticles, MXenes, conductive hydrogels, and combinations of these materials show promising results. For example,

Xiao et al. [63] used graphene oxide in combination with metal organic frameworks (ZIF-8) as a large surface area carrier to load tyrosinase for amperometric detection of levodopa.

Besides graphene oxide, other 2D materials such as MXenes were used for preparing materials showing high conductivity and enhanced electrocatalytic properties. These materials were used to immobilize biomolecules at the flake or nanowire surface to obtain biosensors with large surface area and enhanced analytical signal. Li et al. [64] developed a highly integrated sensing paper (HIS paper) using $Ti_3C_2T_x$ to create a sweat analysis patch for simultaneous lactate and glucose biosensing (Fig. 19). $Ti_3C_2T_x$ was decorated with methylene blue as a mediator for electron transfer from the enzyme to the conductor and vertically aligned single sheets of MXene allowed for capillary transport of sweat to the biosensor surface. A similar concept, but combining $Ti_3C_2T_x$ with Prussian Blue as a mediator for hydrogen peroxide reduction, was presented by Lei et al. [65]. The biosensor featured typical analytical performance for biosensors based on Prussian Blue in addition to being non-toxic, which is critical to wearable platforms (Fig. 20). $Ti_3C_2T_x$ were also combined with electrocatalytically active ZnO tetrapods and deposited on a stretchable electrode as an electrochemically active transducer layer for the qualitative determination of glucose [66]. The obtained transducer worked at a low applied negative potential of −0.24 V, which allowed to avoid the impact of interfering species present in sweat.
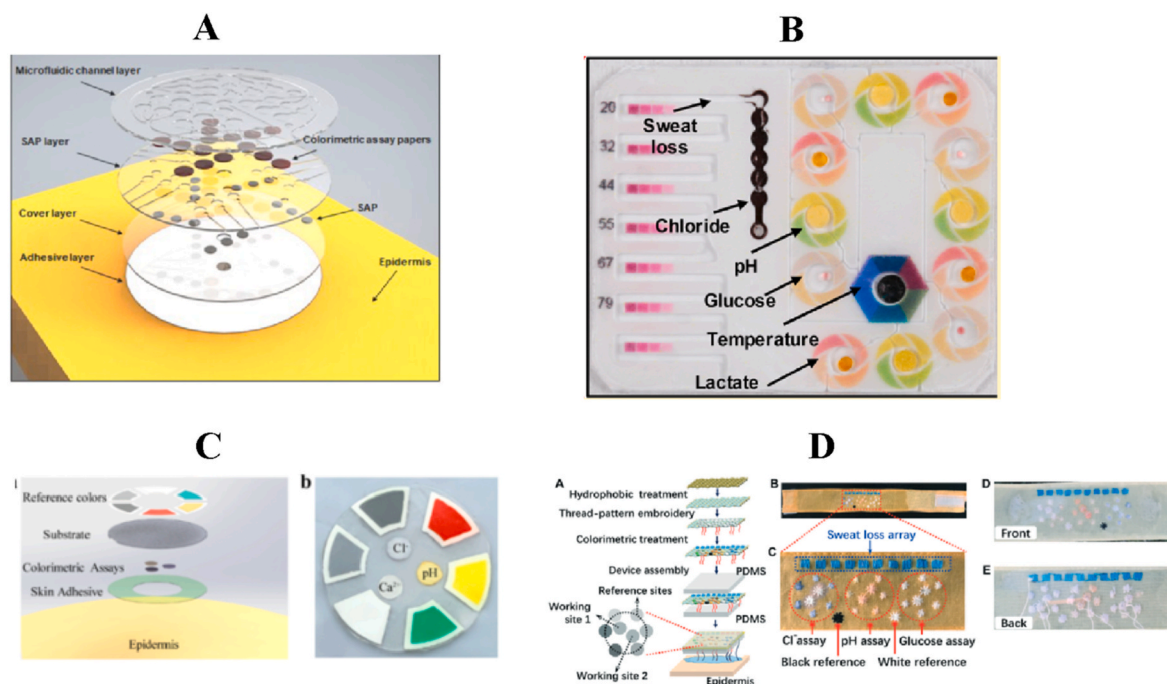
Fig. 15. (A) Schematic illustration of the device structure for optical sweat sensing with flexible valves. Adapted with permission from Ref. [47]. *Copyright © 2018, John Wiley and Sons.* **(B)** Illustration of the microfluidic channels of a colorimetric sweat sensing patch. Adapted with permission from Ref. [48]. *Copyright © 2019, American Chemical Society.* **(C)** Schematic illustration of a stretchable sweat sensing patch, and a patch consisting of colorimetric assays and reference colours. Adapted with permission from Ref. [50]. *Copyright © 2021, American Chemical Society.* **(D)** Schematic illustration of the detection zone in a microfluidic device, images of the thread-embroidered patterns of the detection sites in the band, and front and back side of the detection zone. Adapted with permission from Ref. [51] *Copyright © 2021, Royal Society of Chemistry* (For interpretation of the references to color in this figure legend, the reader is referred to the Web version of this article.)

Among the material science approaches, fabrication of laser inscribed graphene (LIG) as a conductor is an interesting method for fabrication of electrodes and electrode traces for biosensors. Unlike traditional inkjet or screen-printing techniques, laser scribing does not require a solvent and complex formulation of inks. Rather, it converts sp^3 carbon of a substrate material into sp^2 configuration, thus making it electrically conductive. The substrate material can be a flexible film, such as polyimide, suitable for fabrication of wearable analytical devices. The drawback of LIG traces, compared with printed ones, is low conductivity. However, treatment of a substrate with acetic acid improves the yield of sp^2 carbon atoms. Acetic acid-activated LIG enabled fabrication of a fully functional glucose biosensor based on laser scribed electrodes with analytical performance typical for Prussian Blue/GOx enzyme-mediator coupling [67].

Several works focused on the development of multilayer architectures combining for example, carbon nanotubes (CNTs), Nafion, and Pt nanoparticles (PtNPs) serving as an electrocatalyst for electrochemical oxidation of hydrogen peroxide [68]. Interestingly, poly--*m*-phenylenediamine was used as an anti-interference layer sieving molecules larger than H_2O_2 to improve the mediator operational stability and solve the problem of oxidation of electrochemically active molecules at 0.6 V, a typical applied potential for hydrogen peroxide oxidation on Pt. The developed platform was used to detect glucose, lactate, and choline in sweat. Carbon nanotubes were used in a bi-enzyme biosensor to couple Horseradish peroxidase (HRP) with an electrochemical transducer via direct electron transfer enabling mediator-free electron transfer from Glucose oxidase (GOx) via hydrogen peroxide [69]. The wearable biosensor demonstrated very high sensitivity and low oxidation potential, which made the biosensor less susceptible to interfering agents.

In order to improve the analytical performance of the biosensors, a range of 3D materials were used as electrodes for biosensor preparation. A hierarchically organized conductive hydrogel made of PANI, PVA and thermally expanded graphene oxide was used as an electrode for GOx immobilization to achieve high sensitivity and mechanical stability of the resulting wearable biosensor (Fig. 21) [70]. Another approach by Karpova et al. [71] used alkoxysilane polymers to improve the transport properties of the hydrogel used for enzyme immobilization. Eight different polymers for glucose oxidase immobilization were tested and compared with Nafion. It was found that biosensors based on γ-aminopropyltriethoxysilane featured the highest analytical sensitivity to glucose, *i.e.* 0.23 A/(M•cm^2), which is 4–5 times higher than the one for biosensors prepared with Nafion. Further improvement in analyte permeability through the 3D material was achieved by replacing a hydrogel with a porous membrane for the enzyme immobilization and combining it with dendritic nanostructures at the electrode surface [72]. The dendritic structures anchored the porous enzymatic membranes, offered mechanical robustness of the sensor devices, and provided a large surface area to improve stability and sensitivity of the biosensor (Fig. 22).

Textile-based chemical sensors and biosensors are among the most attractive ones. A challenge for such sensors is their fast degradation upon wear and after a few washing cycles. Within the last five years, several design solutions were proposed towards integrating biosensors into cloth. For example, an ordinary cotton fabric was used to make a disposable, biodegradable and functional diagnostic platform, using commercially available Au plasma coated thread, solving the problem with sensor degradation [73]. The diagnostic platform used ferrocene as a mediator coupled with GOx as a proof of concept, featuring excellent analytical performance of the biosensor and a facile fabrication method (Fig. 23).

In another work by Zhao et al. [20], cotton thread was impregnated with PDMS to alter its fluid wicking properties and then covered with a roll-printing process to infer conductivity to the thread. After annealing, ZnO nanowires were grown via a hydrothermal method, followed by deposition of TTF and LOx entrapped in Nafion to create a biosensor. In a similar manner, reference and counter electrodes were fabricated by covering the PDMS-impregnated cotton threads with Ag/AgCl/PVB and

Table 4

Analytical performance of biosensors for biomarker monitoring in sweat.

Biosensor implementation	Analyte	Analytical sensitivity, nA/(µM • cm^2)[a]	Limit of detection, µM[a]	Tested shelf life/operational stability	Reference
Pt/AOx/BSA/chitosan/glutaraldehyde	Ethanol	7.320 ± 0.099	1.7		[57]
PB nanoparticles/γ-aminopropyltriethoxysilane/LOx/carbon black nanoparticles	Lactate	260 ± 25	N/A		[59]
C/PB/GOx/chitosan/Nafion	Glucose	(1.14 ± 0.03) nA/µM	N/A		[60]
Au/rGO/PtNPs/Chitosan-GOx	Glucose	29.10	200	7 days/-	[61]
GOx/PtNP/acetic acid treated LIG	Glucose	65.6	0.3	16 days/-	[67]
Au/GO/ZIF-8@tyrosinase	Levodopa	47 nA/µM	0.45	7 days/-	[63]
MB/Ti$_3$C$_2$T$_x$/Nafion GOx/Chitosan	Glucose	2.4 nA/µM 1.2[c]	17.05	-/14 days	[64]
MB/Ti$_3$C$_2$T$_x$/Nafion LOx/Chitosan	Lactate	0.49 nA/µM 0.24[c]	3.73	-/14 days	[64]
CNT/PB/Ti$_3$C$_2$T$_x$/carbon filter membrane GOx/Chitosan/BSA/ Glutaraldehyde	Glucose	35.3	0.33	-/15 days	[65]
CNT/PB/Ti$_3$C$_2$T$_x$/carbon filter membrane LOx/Chitosan/BSA/ Glutaraldehyde	Lactate	11.4	0.67	-/15 days	[65]
ZnO tetrapods/MXene/GOx/Nafion	Glucose	7.87 ± 2.8	17 ± 1.7	-/10 days	[66]
Au/Cr/MWCNT/Nafion/PtNP/PPD GOx/BSA/Glutaraldehyde	Glucose	59 ± 12	N/A	-/20 h	[68]
Au/Cr/MWCNT/Nafion/PtNP/PPD LOx/BSA/Glutaraldehyde	Lactate	0.79 ± 0.18	N/A		[68]
Au/Cr/MWCNT/Nafion/PtNP/PPD ChOx/BSA/Glutaraldehyde	Choline	68 ± 5	N/A		[68]
Patterned CNT-ethylene-vinyl acetate copolymer/GOx-HRP	Glucose	270 ± 10	3	7 days/-	[69]
polyaniline, PVA, thermally expanded graphene/GOx/chitosan	Glucose	N/A	0.2		[70]
C/PB/GOx/γ-aminopropyltriethoxysilane	Glucose	230	N/A	1 year/25 h	[71]
C/PB/GOx/Al$_2$O$_3$/agarose, glycerol	Glucose	41.8	10	-/20 h	[72]
Au/6-ferrocenylhexanethiol/6-mercaptohexan-1-ol (MHA)/MHA-GOx self-assembly monolayer	Glucose	(0.088 ± 0.010)	0.301	-/6 h	[73]
Carbon/ZnO nanowires/Nafion TTF/LOx/Chitosan/Glutaraldehyde	Lactate	0.94 V/M	3610	-/-	[20]
elastomeric gold fibre/PB/LOx/chitosan	Lactate	19.13	137	-/-	[74]
CNT fibres/PB/chitosan/SWCNT/GOx	Glucose	2.15 nA/µM	N/A	-/-	[18]
Ag/C/GO/PB/PU/LOx/Chitosan	Lactate	0.33 nA/µM[b]	440	-/-	[75]
MWCNT/PB GOx/Chitosan	Glucose	105.93	4.95	22 days/-	[76]
Au nanodendrites/PB/GOx/chitosan	Glucose	8 nA/µM	N/A	-/-	[77]
Au nanodendrites/PB/GOx/chitosan	Lactate	67 nA/µM	N/A	-/-	[77]
Carbon-Prussian Blue/LOx/BSA/Chitosan	Lactate	0.3[b]	N/A	-/10 runs	[79]
Carbon-Prussian Blue/AOx/BSA/Chitosan	Alcohol	0.2[b]	N/A	-/10 runs	[79]
Carbon-Prussian Blue/AOx/BSA/Chitosan	Alcohol	0.7[b]	N/A	-/10 runs	[78]
Au/Au nanodendrites/11-mercaptoundecanoic acid SAM/CYP2B6	Nicotine	4.3 nA/µM	1.6	-/ca 1600 s	[80]
Rh/C/AAO/BSA/glutaraldehyde	Ascorbic acid	3.5 nA/µM[b]	N/A	-/90 min	[81]
Carbon-Prussian Blue/GOx/BSA/agarose	Glucose	46.5 ± 4.1	N/A	-/7500 s	[82]
Carbon/AuNP/Prussian Blue/GOx/CNTs/BSA/Chitosan	Glucose	24.8	7.34	-/9 h	[83]
Carbon/AuNP/Prussian Blue/LOx/CNTs/BSA/Chitosan	Lactate	1.0	1.24 mM	-/9 h	[83]
ZnO/Au/cortisol antibody - di(N-succinimidyl)3,3′-dithiodipropionate self-assembly monolayer (SAM)/ethanolamine	Cortisol	0.25 Ω/ng ml^{-1}	1 pg/ml	-/-	[84]
TTF/CNT/LOx/chitosan/PVC	Lactate	124 mV/(mM•cm^2)	2.1 mM	-/8 days	[86]
TTF/CNT/GOx	Glucose	5.4 mV/(µM•cm^2)	43	-/8 days	[86]
AuNP/GOx/Chitosan	Glucose	1.27	24	16 days/180 h	[87]
AuNP/cortisol antibody - SH-PEG-COOH SAM/BSA	Cortisol	61.2 µA/dec	7.47 nM	-/-	[85]
C/PB/TTF/CNT/LOx/BSA/Chitosan/colorimetric	Lactate	N/A	3.70 mM	-/-	[88]
Toray carbon paper-060 PTFE FcMe$_2$-LPEI/LOx	Lactate	16.4[b]	N/A	-/30 min	[89]
LOx on porous carbon	Lactate	6.14 V/M	N/A	-/2 h	[90]
PDMS/MWCNT/BiVO$_4$/SiO$_2$/GOx/Nafion/PDMS	Glucose	0.2 µA/dec	22.2 pM	28 days/-	[91]
GOx−peroxidase−o-dianisidine colorimetric	Glucose	111.23 A U./mM	0.03 mM	25 days/-	[92]
Au nanorods/KI/GOx/HRP colorimetric	Glucose	241.5 nm/mM	7.2	10 months/-	[93]
Urease/filter paper	Urea	N/A	N/A	-/-	[94]
Creatininase, creatinase, sarcosine oxidase, and peroxidase/µ-reservoirs	Creatinine	N/A	N/A	-/-	[94]
Au nanocluster/MnO$_2$ nanosheets/poly(allylamine hydrochloride)/ uricase luminescent	Uric acid	N/A	136 nM	3 days/-	[96]
PSi/(Au–Ag)NP/GOx/chitosan/PU fluorescent/luminescent	Glucose	3.46 %/mM	N/A	-/10 h	[97]

AOx – Alcohol oxidase, BSA – bovine serum albumin, PB – Prussian Blue, LOx – lactate oxidase, GOx – glucose oxidase, rGO – reduced graphene oxide, PtNP – platinum nanoparticles, LIG – lased inscribed graphene, ZIF - zeolitic imidazolate framework, MB – methylene blue, GO – graphene oxide, CNT – carbon nanotube, MWCNTs – multiwalled carbon nanotubes, PPD - poly-*m*-phenylenediamine, HRP – horseradish peroxidase, ChOx – choline oxidase, PVA – polyvinyl acetate, MHA - 6-mercapto-hexan-1-ol, TTF – tetrathiafulvalene, SWCNT – single walled carbon nanotubes, PU – polyurethane, SAM – self-assembly monolayer, AAO – ascorbic acid oxidase, PVC – polyvinylchloride, AuNP – gold nanoparticles, PEG – polyethylene glycol, FcMe$_2$-LPEI - dimethylferrocene-modified with linear polyethylenimine, PDMS – poly-dimethylsiloxane, (Au–Ag)NP – gold-silver nanoparticles, PSi – porous silica.

[a] Unless otherwise stated.
[b] Estimation based on graphical data provided in the article, when the exact number was not reported.
[c] Calculated based on the numerical data provided in the article.

Ag, respectively. The resulting three electrodes were weaved around with a wicking cotton thread to provide electrolytic contact and function as a three-electrode setup for detection of lactate. The resulting electrochemical platform demonstrated adequate sensitivity to lactate in a real sweat sample. A more sophisticated thread construction was used by Wang et al. [74], where a stretchable thread consisting of an elastomeric gold fibre coated with Prussian Blue/LOx/chitosan was weaved into a textile and used as a working electrode. Correspondingly, other threads
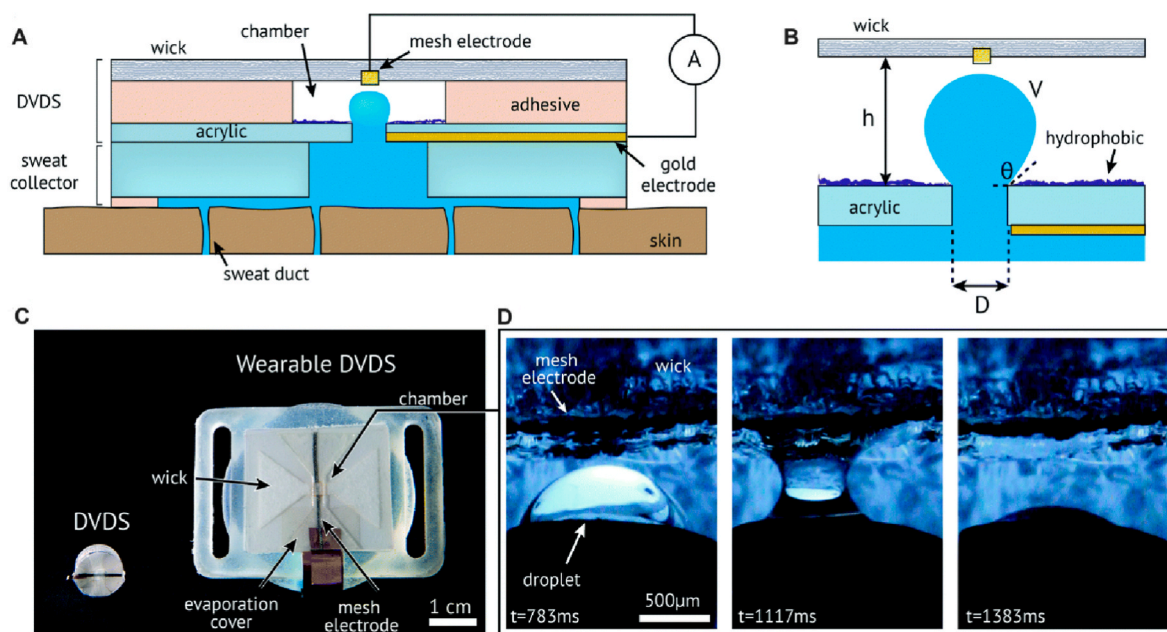
Fig. 16. (A) Side view of a digital volume dispensing system (DVDS) flow sensor coupled to a wearable sweat collector. **(B)** Close-up of the chamber including critical parameters. **(C)** Photo of two different devices including a miniature version (left) and wearable version (right). **(D)** Demonstration of droplet breaking onto the mesh electrode. Reproduced with permission from Ref. [54]. *Copyright © 2019, Royal Society of Chemistry.*
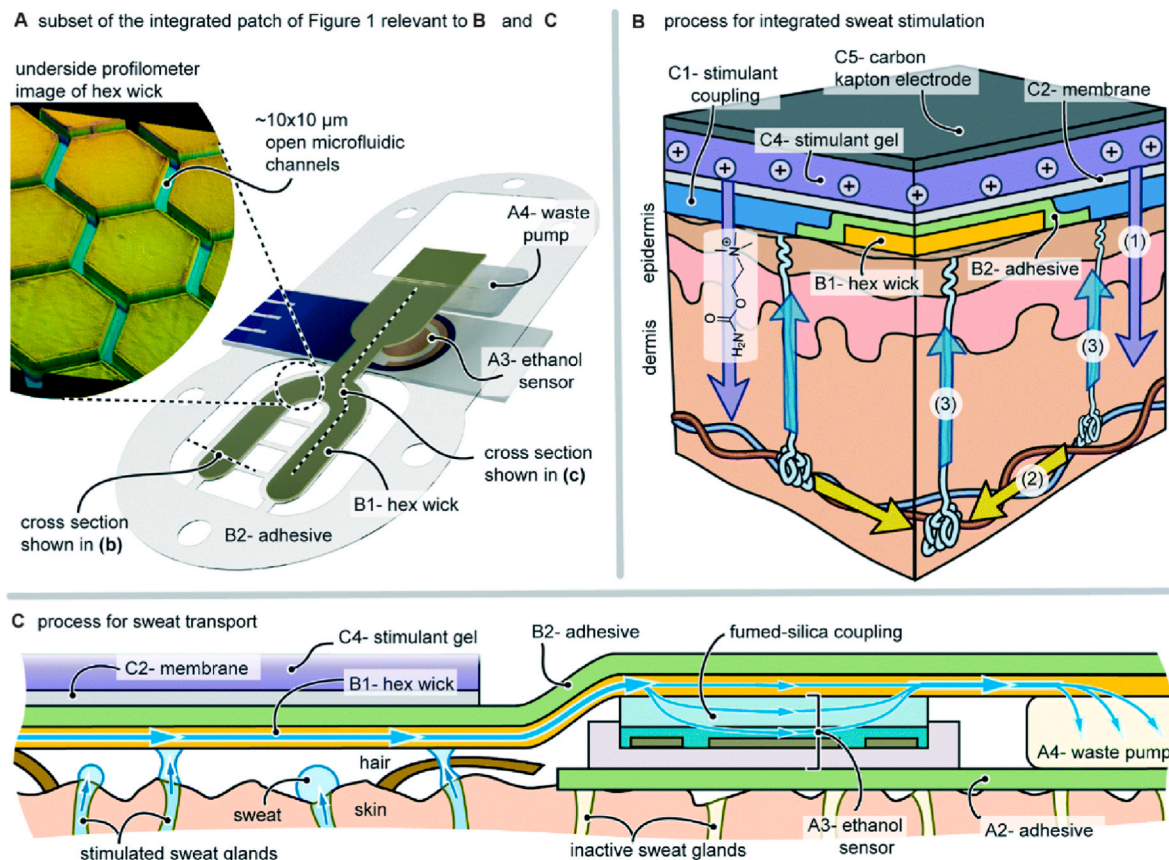

Fig. 17. Operational process of the integrated sweat-ethanol biosensing patch. See Ref. [57] for full explanation. Reproduced with permission from Ref. [57]. *Copyright © 2018, Royal Society of Chemistry.*

made of uncoated elastomer gold fibres and elastomer gold fibres covered with Ag/AgCl were weaved into the same textile to be used as counter and reference electrodes (Fig. 24).

A similar approach was used to cover carbon nanotube fibres with a thin layer of Prussian Blue followed by coating the obtained composite with a chitosan/single walled carbon nanotube (SWCNT)/glucose
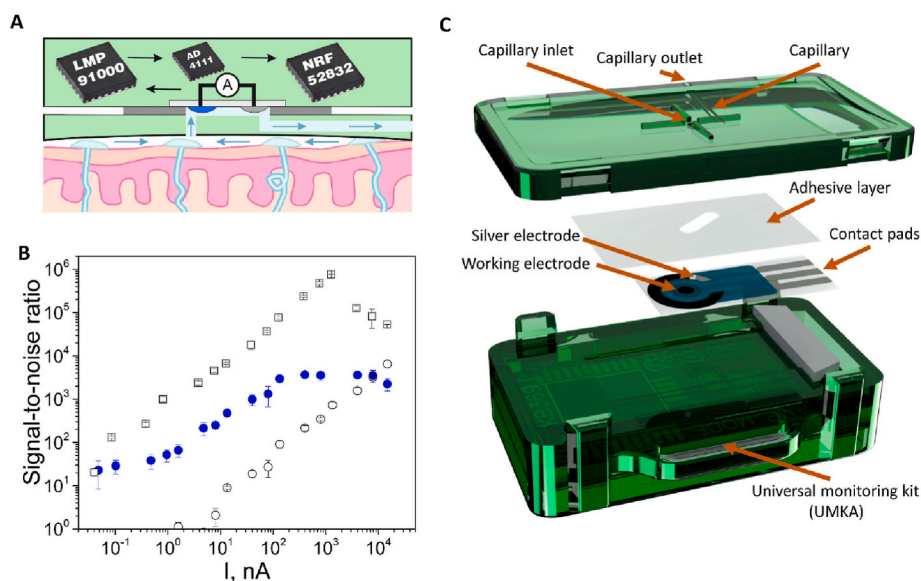
Fig. 18. (A) Scheme of an on-skin wearable universal monitoring kit (UMKA) for continuous sweat monitoring. **(B)** Investigation of electronic noise (signal-to-noise ratio) using galvanic cells discharged on a set of calibrated resistors for the elaborated wearable device UMKA (●), commercial ammeter Tektronix (○) and pico-ammeter Keithley (□). **(C)** UMKA device. For full description of the device and results see Ref. [59]. Reproduced with permission from Ref. [59]. *Copyright © 2022, Elsevier.*
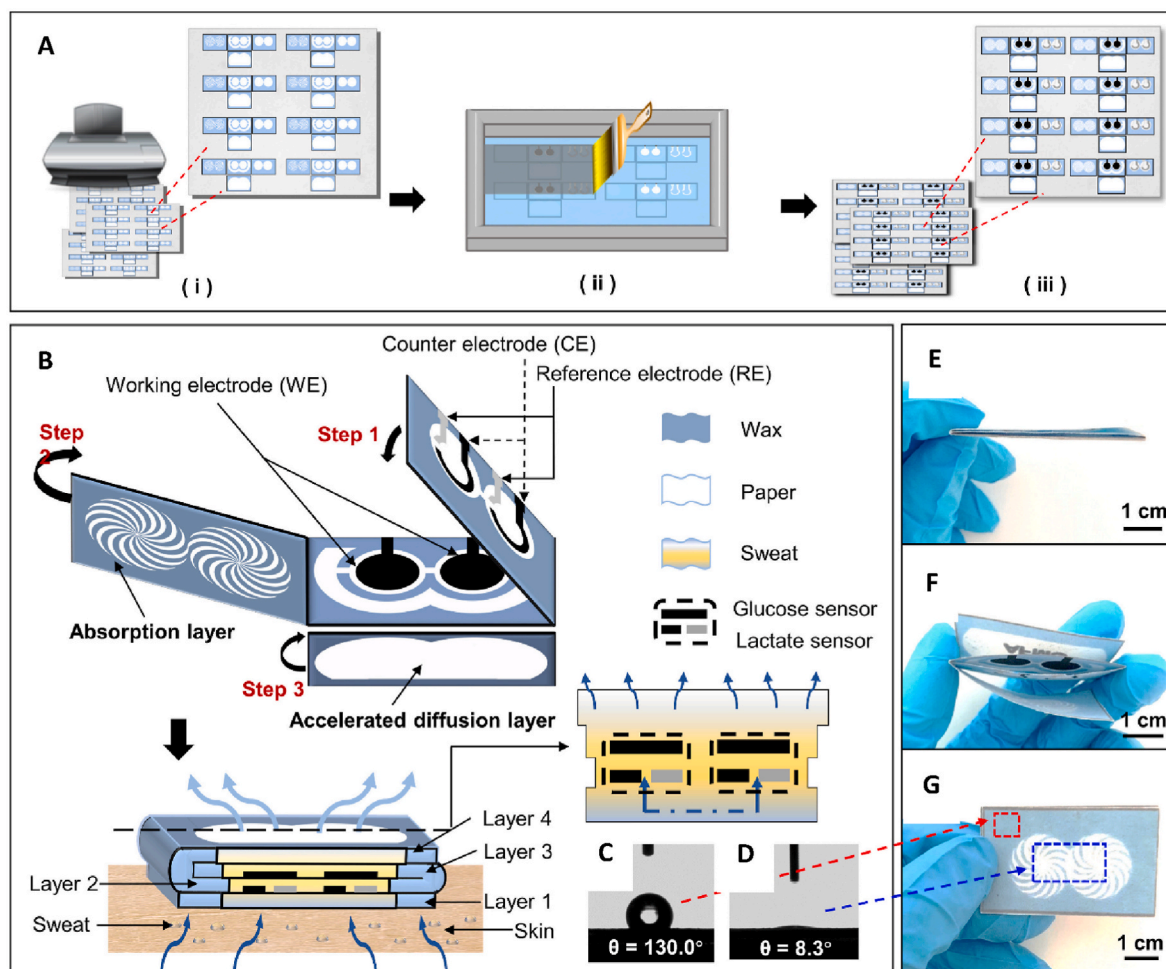

Fig. 19. Schematic illustration and photos of a highly integrated sensing paper (HIS paper). **(A)** Schematic illustration of the fabrication of HIS paper. **(B)** Structural anatomy of HIS paper. **(C, D)** Contact angle tests on hydrophobic and hydrophilic regions of the HIS paper. **(E–G)** Photographs of the foldable HIS paper. Reproduced with permission from Ref. [64]. *Copyright © 2021, Elsevier.*
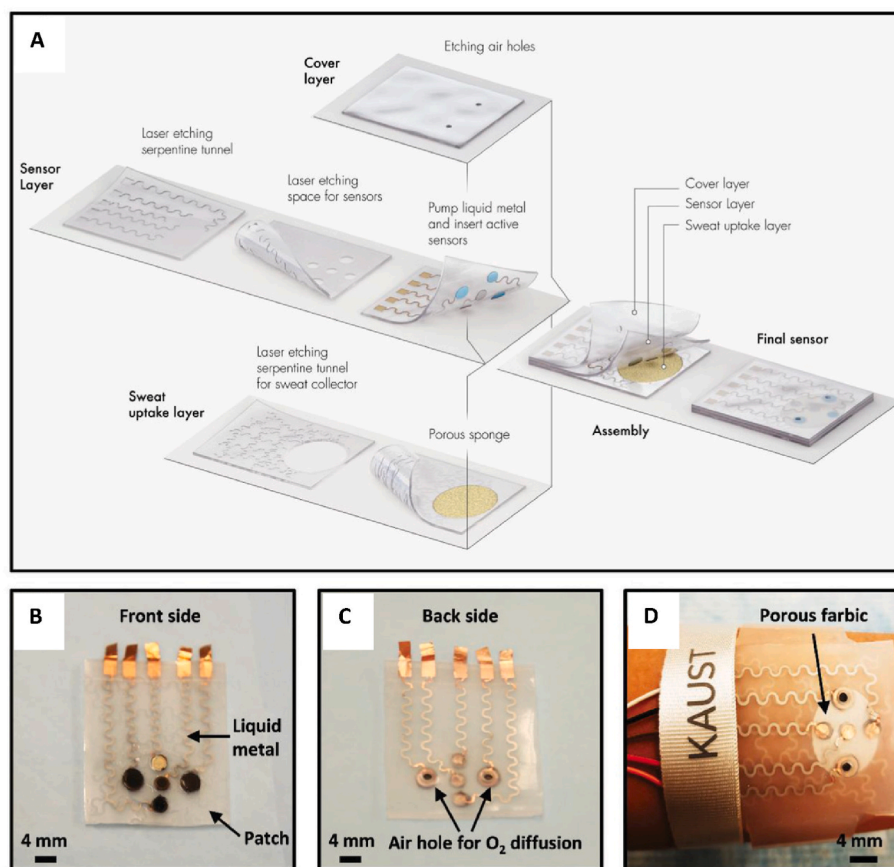
Fig. 20. Schematic drawings and corresponding images of a wearable biosensor patch. **(A)** Schematic illustration of the sensor patch system, which is composed of a sweat-uptake layer, a sensor layer, and a cover layer. **(B)** Front-side optical image of the sensor array (left and right), reference electrode (top), counter electrode (middle), and pH sensor (bottom). **(C)** Back-side optical image of the sensor array. **(D)** Optical images of the sensor wristband laminated on human skin. Reproduced with permission from Ref. [65]. *Copyright © 2019, Wiley-VCH.*

oxidase mixture (Fig. 25) [18]. Finally, graphene oxide and Prussian Blue mixed into carbon/polyurethane ink was also used to modify silver yarn embroidered into textile to serve as working and counter electrodes, where the working electrode was additionally functionalized with a LOx/chitosan mixture to impart selectivity to lactate. The electrochemical cell was then completed with a reference electrode made by coating silver yarn with an Ag,AgCl paste [75].

Apart from weaved-in or sewed-on conductive threads, textile was also used as an alternative to a plastic film substrate to make more comfortable-to-wear biosensors. For example, conductive inks were screen-printed onto a fabric in a similar processes as used for T-shirt artwork printing [76] and embedded into a wearable platform featuring a fluid-management device and electrical connection to a potentiostat. Another example was the use of Janus textile (Fig. 26) to control fluid permeation and wettability of specific areas of the wearable patch. The electrode system embedded in the Janus textiles and modified with corresponding enzymes allowed sensitive and real-time detection of glucose (40–18 μM) and lactate (around 10 mM) [77].

Recent publications in sweat biomarker monitoring reported a high level of sophistication in integrating biosensors into more complex multimodal platforms. Materials were carefully designed to conform to the human body and to expand the biomarker options to detect alcohol [78,79], lactate, caffeine (a chemical sensor, not a biosensor reported in Ref. [79]) [79], nicotine [80], and ascorbic acid [81]. Typically, such platforms included additional modalities, *e.g.* ultrasound transduced to measure blood pressure and heart rate simultaneously with biomarkers (Fig. 27) [79] or a fully characterized battery to enable a self-powered wearable device [82]. A number of platforms focused on sensing multiple analytes [78,79,83], also at an affordable price [83].

A significant fraction of publications reported fabrication of microfluidic devices for efficient fluid management and quantification, integrated with biosensors for various biomarkers. For example, a platform made of PDMS combining a microfluidic modality with a flexible substrate was used for impedimetric detection of cortisol in sweat (Fig. 28) by Lee et al. [84]. The biosensor was created by first growing ZnO nanorods with a hydrothermal method onto a patterned substrate followed by deposition of gold to obtain a nanostructured surface of the electrode. Cortisol antibody was then immobilized at the gold surface via formation of a self-assembled monolayer to impart selectivity and sensitivity of the biosensor to cortisol, while the remaining surface was blocked with ethanolamine to prevent non-specific absorption. The biosensor was then integrated with a microfluidic platform and tested in vivo as an epidermal patch. Significant steps were taken to miniaturise the microfluidic devices for detection of glucose while keeping a high degree of integration with microelectronics and battery-free powering of the device (Fig. 29) [85–87]. Platforms featuring soft microfluidics and hybrid colorimetric/biofuel cell systems were developed by Bandodkar et al. [86] for real-time sensing of the concentration of lactate and glucose, simultaneously with inorganic ions, sweat rate, and total sweat loss to give a potential user a comprehensive and high quality health status. Coupling GOx and LOx [86,88] or LOx and bilirubin oxidase [89] was a typical approach in construction of biofuel cells due to the clinical relevance of the analytes used as fuel and the relatively good robustness of the corresponding enzymes. The power output or current generated by the biofuel cell serves as an analytical signal of the platform to the corresponding enzyme substrates: glucose, lactate, or bilirubin. Apart from biofuel cell powering, NFC was reported to be useful for powering the amperometric detection of glucose [87] and cortisol [85], featuring
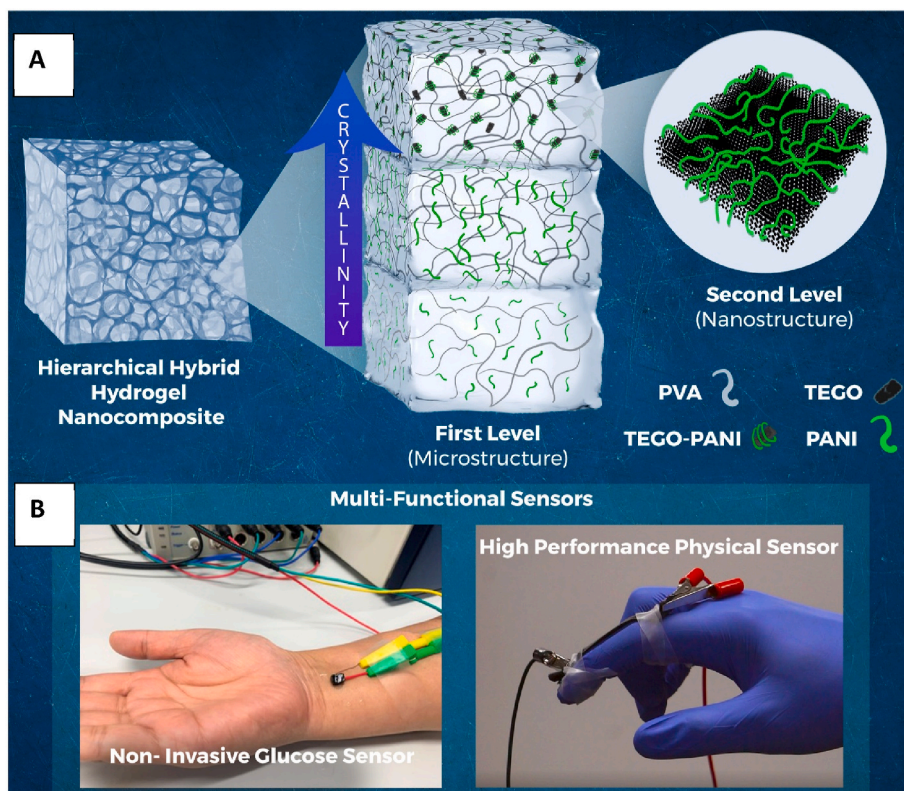
Fig. 21. (A) Schematic illustration of the hierarchical hybrid hydrogel nanocomposite with length scale decreasing from left to right. The first level of hierarchy exists at micrometer length scale and depicts three phases existing within the 3D mesh of the porous hydrogel. It consists of a dilute solvent rich phase within the voids, a transition region having PANI entangled within PVA and finally, a PVA and nanomaterial rich region of high crystallinity within the core of solid fibres in the 3D mesh. Simultaneously, at the second level (existing at nanometric scale), the material consists of highly expanded PANI crystallized on TEGO basal planes. **(B)** Images of the multi-functional sensor prototypes developed using the novel hydrogel, namely an amperometric biosensor for non-invasive detection of glucose concentration through sweat (left) and a high-performance physical sensor developed for detection of a multitude of human-body motion (right). Reproduced with permission from Ref. [70]. *Copyright © 2021, Elsevier.*
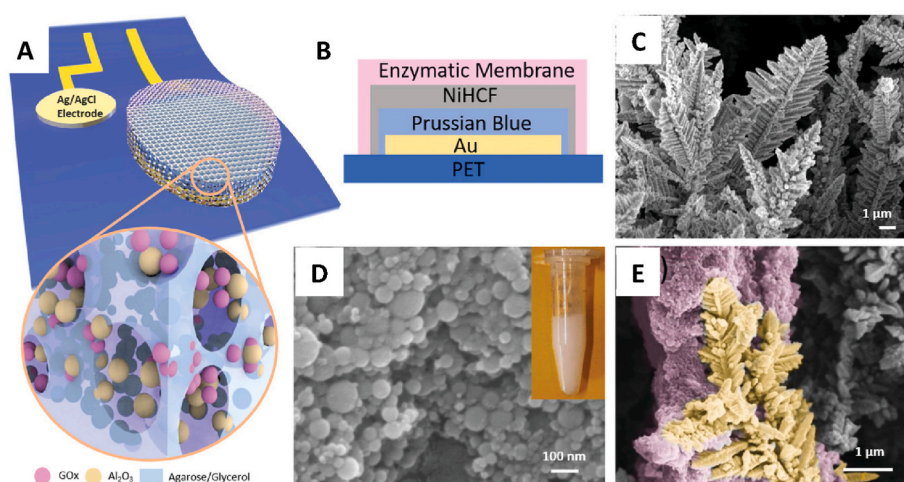

Fig. 22. (A) Schematic illustration of nanotextured glucose sensors with a porous enzymatic membrane. **(B)** Cross-section schematics of the working electrode. **(C)** SEM image of nanotextured NiHCF/PB/Au electrode. **(D)** SEM image of porous membranes (inset: photo of the membrane emulsion). **(E)** SEM image of porous membrane anchored to the nanotextured electrode. Reproduced with permission from Ref. [72]. *Copyright © 2019, Wiley-VCH.*

enzymatic and immunochemical biosensors, respectively.

In the field of wearable platforms fabrication, efforts were made to create self-powered devices employing, for example, sweat evaporation as the power source giving power output depending on lactate concentration [90]. Another example of self-powered device was a photo-electrochemical sensor that converted ambient light into an electrochemically measurable signal proportional to glucose concentration [91]. The analytical performance of the wearable platforms is presented in Table 4.

While electrochemical transduction was the most used mechanism of converting chemical information into a physically measurable signal, colorimetric probes were also widely used to detect glucose in sweat
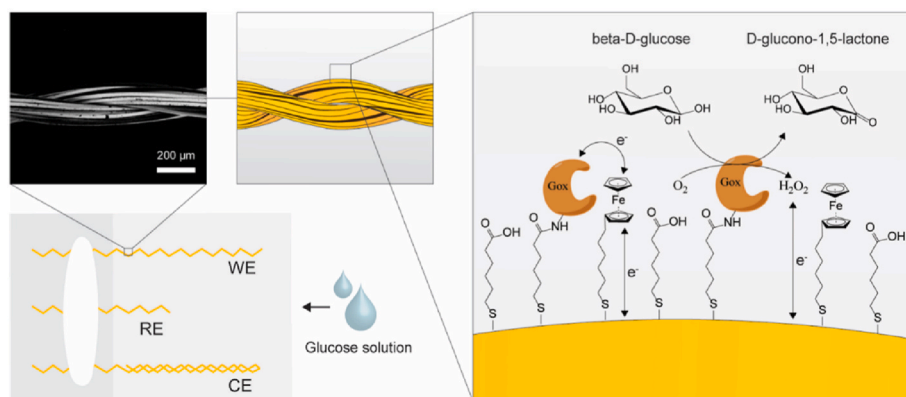
Fig. 23. Schematic representation of one of the devices with an inset SEM of an unstitched Au thread and a schematic (not to scale) of the chemistry of the glucose detection taking place on the functionalized Au/FHT/MHA/MHA-GOx filaments. Reproduced with permission from Ref. [73]. *Copyright © 2021, Elsevier.*
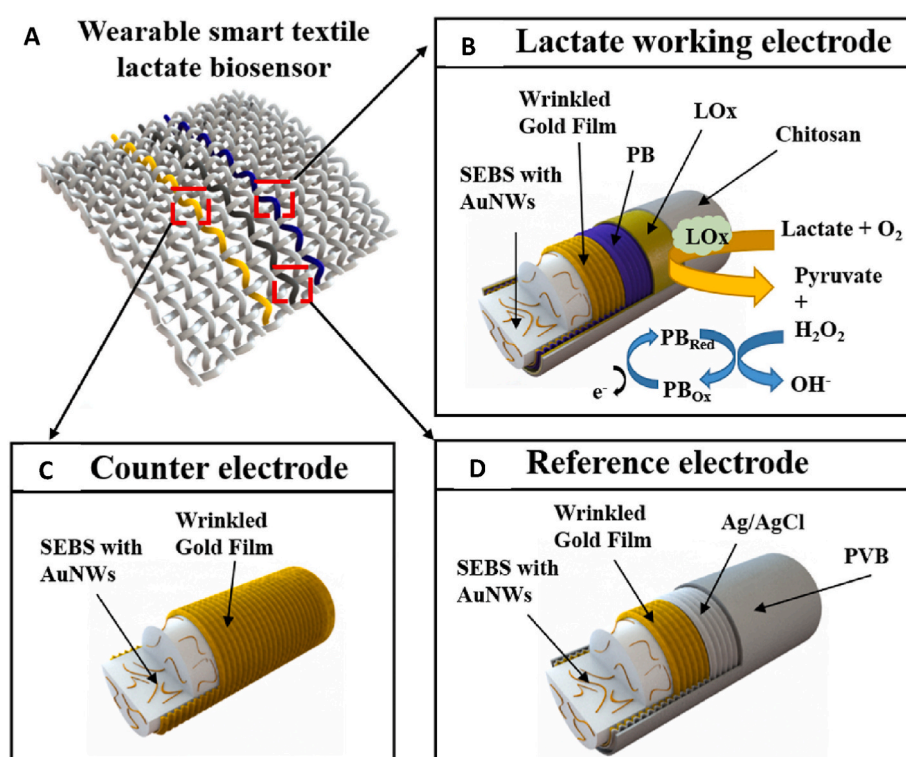

Fig. 24. (A) Scheme of a wearable smart textile electrochemical biosensor for lactate monitoring. **(B)** Morphology and sensing mechanism of the lactate working electrode. **(C)** Morphology of elastomeric gold fibre acting as a counter electrode. **(D)** Morphology of PVB coated Au/Ag/AgCl reference electrode. (For interpretation of the references to color in this figure legend, the reader is referred to the Web version of this article.) Reproduced with permission from Ref. [74]. *Copyright © 2021, Elsevier.*

within microfluidic devices. The most typical approach was to use a hydrogen peroxide sensitive dye as a colour indicator. To realize a dye approach, it was necessary to carefully design a microfluidic platform, for example by equipping it with check valves. Check valves helped to collect microliter volumes of sweat into the detecting reservoir containing GOx/peroxidase/o-dianisidine for colorimetric determination of sweat glucose and for preventing the analyte and dye backflow (Fig. 30A) [92]. Colorimetric readout was developed by Hartel et al. [88] by creating a resettable electrochromic biosensor based on Prussian Blue (Fig. 30B).

Apart from single-color implementation, that can be hard to read, efforts were made to improve the readability of the optical response by the naked eye. For example, GOx-horseradish peroxidase was coupled with potassium iodide and gold nanorods and integrated into a

microfluidic wearable device with multicolor colorimetric response to changes in glucose concentration in sweat. The multicolor readout was available either for semi-quantification by naked eyes or quantitative analysis with a smartphone, using a mathematical model correlating glucose concentration with the red green blue (RGB) value of a pixel point in the device [93]. Single-use soft microfluidic platforms with colorimetric readout were developed for multianalyte detection of creatinine and urea along with pH to give information about kidney function of a potential user (Fig. 31) [94]. Similarly, glucose, lactate, pH, and chloride ion concentration and temperature across a broad range of ambient lighting conditions [48] were detected with a simple, yet well characterized, smartphone readout [48,55,95]. Multimodal soft microfluidic platforms were also developed for detection of alcohol and ammonia [55] as well as cortisol, glucose, and ascorbic acid [95] using
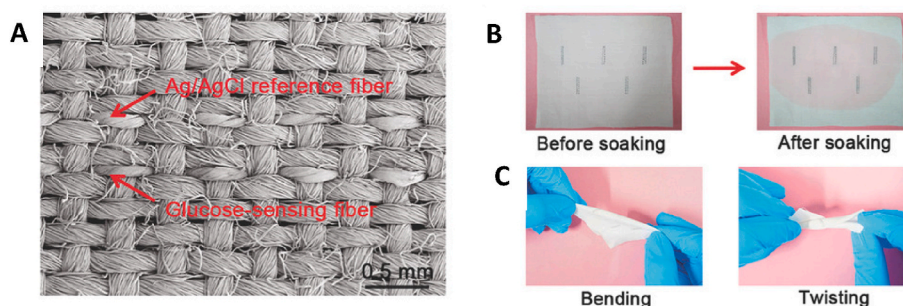
Fig. 25. Performance and characterization of the electrochemical fabric through the integration of different kinds of sensing fibres. **(A)** SEM image of glucose-sensing and Ag/AgCl reference fibres in the fabric. **(B)** Photograph of a 4.5 cm × 6 cm electrochemical fabric before and after soaking (with simulated sweat). **(C)** Photograph of a 4.5 cm × 6 cm electrochemical fabric under bending and twisting. Reproduced with permission from Ref. [18]. *Copyright © 2018, Wiley-VCH.*
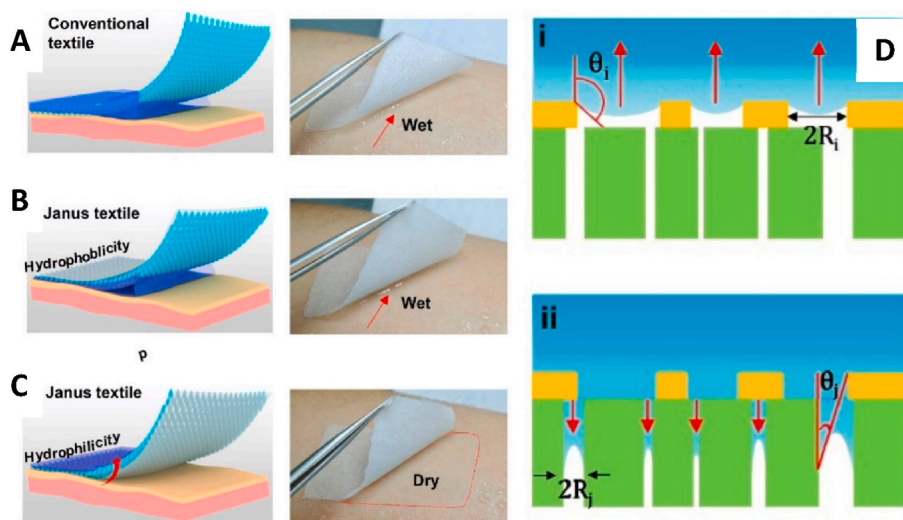

Fig. 26. Unidirectional sweat pumping on Janus textiles. Schematics (**left**), and on-body sweat absorbance (**middle**), upon bare gauze **(A)**, hydrophobic layer **(B)**, and hydrophilic layer **(C)** of Janus textile faced on sweaty epidermis. **(D)** Schematic contact pumping theoretical model. The hydrostatic pressure decreases instantaneously at hydrophobic−superhydrophilic (green-yellow) contact points (**i** and **ii**), causing spontaneous water transport. Reproduced with permission from Ref. [77]. *Copyright © 2020, American Chemical Society.* (For interpretation of the references to color in this figure legend, the reader is referred to the Web version of this article.)

enzymatic colorimetric and fluorimetric assays along with monitoring of sweat rate and conductivity using galvanic skin response.

In addition to colorimetric and fluorimetric transduction mechanisms, luminescence was used to detect uric acid, glucose, and alcohol utilizing enzyme-embedded gold nanocluster assemblies wrapped by MnO_2 nanosheets as the probe [96]. Another luminescent material used luminescent porous silica (PSi) obtained by etching from anodization of a boron-doped silicon wafer [97]. PSi was then decorated with carbon quantum dots and bimetallic Au and Ag nanoparticles to enhance the initial fluorescence intensity of PSi and catalyze the PSi oxidation triggered by hydrogen peroxide. The obtained composite was further coupled with glucose oxidase immobilized with chitosan to create a patch on adhesive polyurethane film. The readout was realized via taking photos with a smartphone and simple image processing.

Wearable biosensors were also made disposable and easy to fabricate from every-day materials such as water bottle polyester and nail polish that would come as a recycling option [98]. The sensitivity of such a biosensor made via classical immobilization of GOx in a chitosan matrix was reported to be *ca* 13 nA/(μM•cm^2) with a limit of detection 9.2 μM.

As seen in Table 4, the analytical performance and the stability of the biosensors greatly depends on the enzyme used and the method of enzyme immobilization. In general, the most stable and most frequently used enzyme is glucose oxidase that sustains one year of storage

reported in some cited articles and much longer in the commercial test strips. When evaluating the biosensor performance, it is important to note also that some analytes, such as lactate, may occur even at a higher concentration in sweat than in blood, while the situation for glucose is the opposite [2].

A tremendous amount of research work during the last five years was focused on sweat analysis, although the clinical relevance of sweat as a high-quality sample that reflects body metabolism is still arguable. Interestingly, recent studies of sweat revealed over 200 unique proteins, indicating that sweat can indeed be used for profiling antibodies and immune biomarkers [99] (in addition to small molecules), rendering sweat a potentially rich source of information about the human body.

2.1.3.1. Non-enzymatic biomarker sensors. Among non-enzymatic biomarker sensors, recent publications illustrate electrocatalytic sensors typically using integrated microfluidics and modified working electrodes in order to detect the oxidation or reduction current of biomarkers, such as caffeine [79] and vitamin C [81].

A nanoporous gold (NPG) based electrochemical glucose sensor [100] showed a high sensitivity of 253 μA/(mM•cm^2) and good selectivity against interfering biomolecules. In another study, a sensor based on the conducting polymer PEDOT:PSS hydrogel was used for accurate detection of uric acid in human sweat showing an ultrahigh sensitivity of
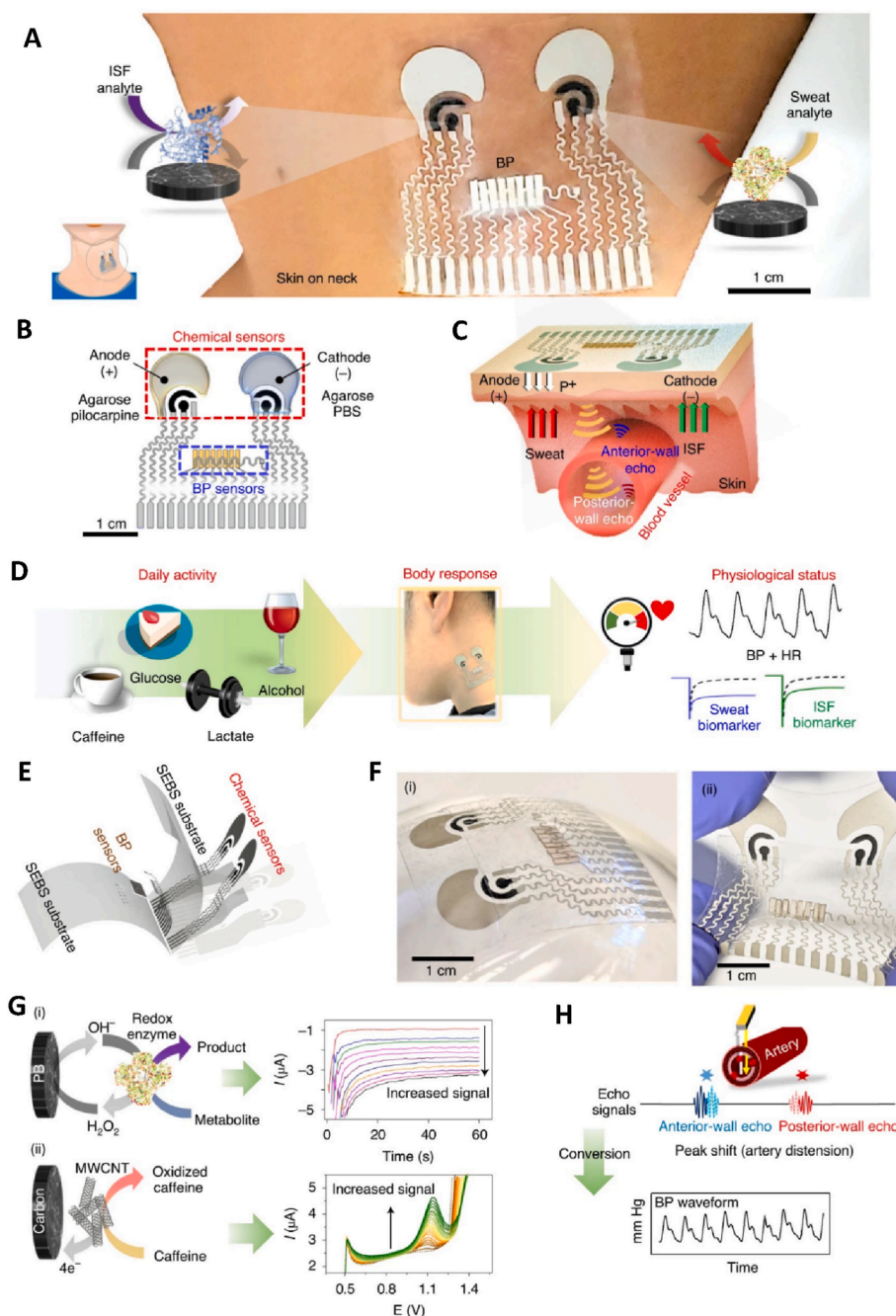
Fig. 27. Characterization of a multimodal wearable sensor. **(A–C)** Studies of the signal interference crosstalk between the ISF electrochemical and BP sensors. **(D–G)** Studies of the signal interference crosstalk between the sweat electrochemical sensor and BP transducer, photos of the sensor under normal conditions (left) and a 20 % vertical strain (right). **(H)** Envelopes of the raw echo signals before and after every 200 cycles of vertical stretching up to 1000 cycles. For a full description see the original article. Reproduced with permission from Ref. [79]. *Copyright © 2021, Nature Portfolio.*

875 μA/(mM•cm^2) and a low limit of detection (LOD) down to 1.2 μM [101]. Additionally, optical modality in combination with microfluidic devices were suggested to detect *e.g.* acetone, CO_2 and ammonia emitted through skin using a gradient-based colorimetric sensor array [102].

Molecularly imprinted polymer (MIP)-based sensors stand as a separate category of chemical sensors where the molecular recognition is based on the complementarity between the shape, size and functional groups of the biomarker and the imprinted cavities at the sensor surface. For example, a lactate MIP sensor with imprint of lactate was formed by polymerizing 3-aminophenyl boronic acid on graphene PVDF electrodes. The obtained MIP sensor was used in combination with differential pulse voltammetry (DPV) and yielded an electrochemical

response to lactate with a sensitivity of 5.18 μA/(mM•cm^2) and good specificity in the presence of glucose, urea and uric acid [103].

2.2. Dermal interstitial fluid

Interstitial fluid (ISF), also known as tissue fluid, is a clear, colourless fluid that fills the space between cells in tissues throughout the human body. ISF consists of a water solution or suspension of sugars, salts, fatty acids, amino acids, coenzymes, hormones, neurotransmitters, white blood cells and cell waste-products. ISF helps to transport nutrients and oxygen for metabolism in cells and removes waste products and surplus fluid from tissue. Furthermore, ISF allows for the transfer of signals and
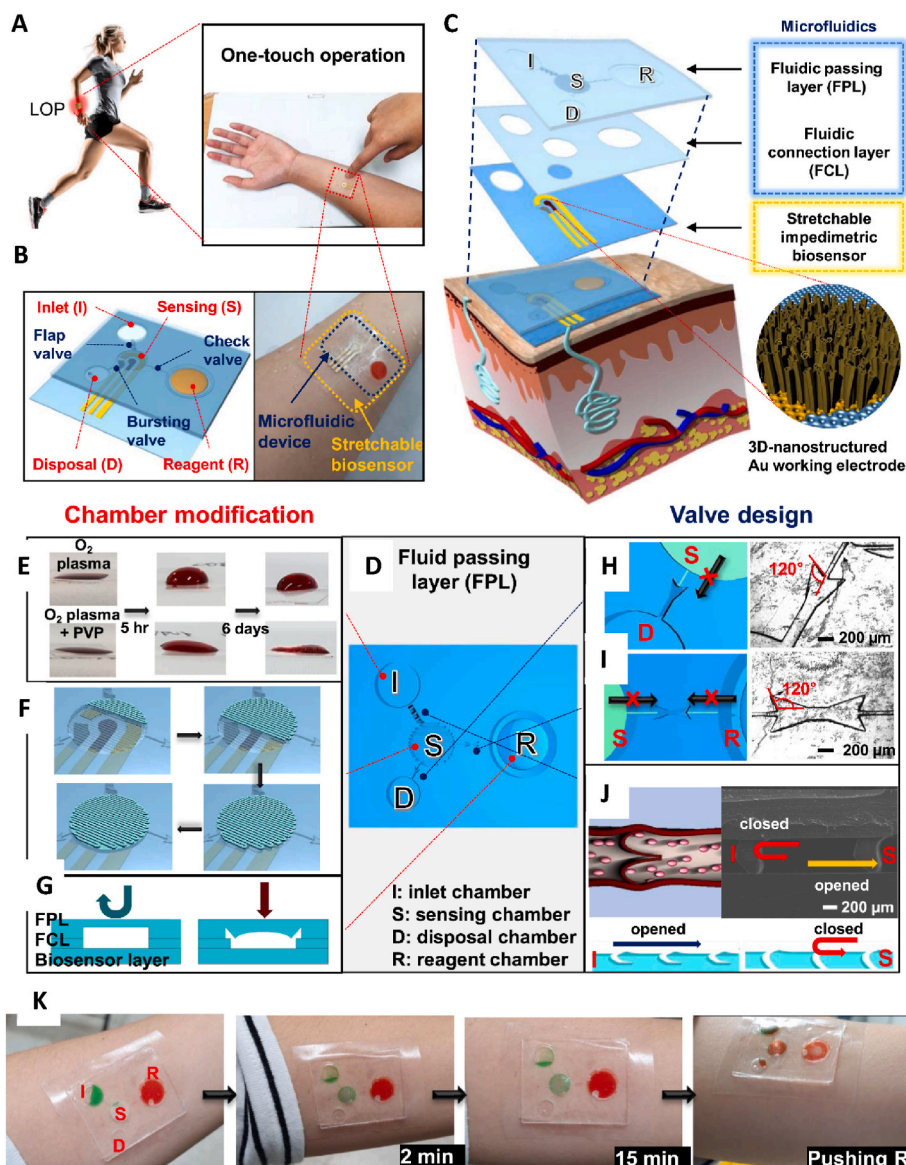
Fig. 28. Lab on a patch with microfluidic and electrochemical sensing components for wearable point-of-care technology. For the full description see the original article. Reproduced with permission from Ref. [84]. *Copyright © 2020, Elsevier.*
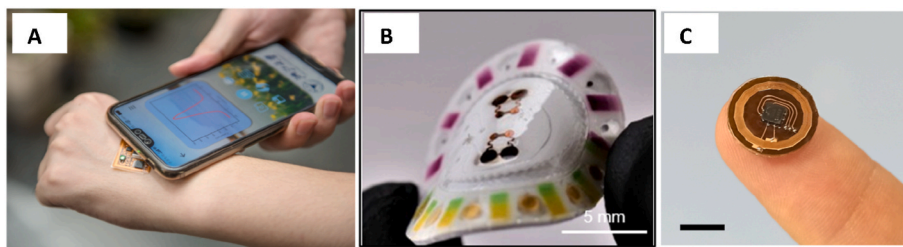

Fig. 29. (A) Integrated wireless, battery-free, and flexible detection system with NFC-enabled smartphone. Reproduced with permission from Ref. [85]. *Copyright © 2021, Elsevier.* **(B)** Microfluidic patch with embedded sensors for simultaneous electrochemical, colorimetric, and volumetric analysis of sweat. Reproduced with permission from Ref. [86]. *Copyright © 2019, American Association for the Advancement of Science.* **(C)** Glucose tag on a fingertip (scale bar: 6 mm). Reproduced with permission from Ref. [87]. *Copyright © 2022, Elsevier.*

information between cells.

In the last five years, several biosensing platforms were proposed for non-invasive monitoring of glucose in interstitial fluid, as summarized in Table 5. Unlike sweat, ISF is in direct dynamic equilibrium with blood but is not readily available at the surface of the skin. Typically, non-invasive sampling of ISF is achieved by applying a small electric current to the skin surface. The applied current induces electroosmotic flow through the negatively charged upper layer of skin, *stratum corneum*, towards the cathode. Electroosmotic flow carries neutral molecules, such as glucose, together with ISF to the surface of the skin.
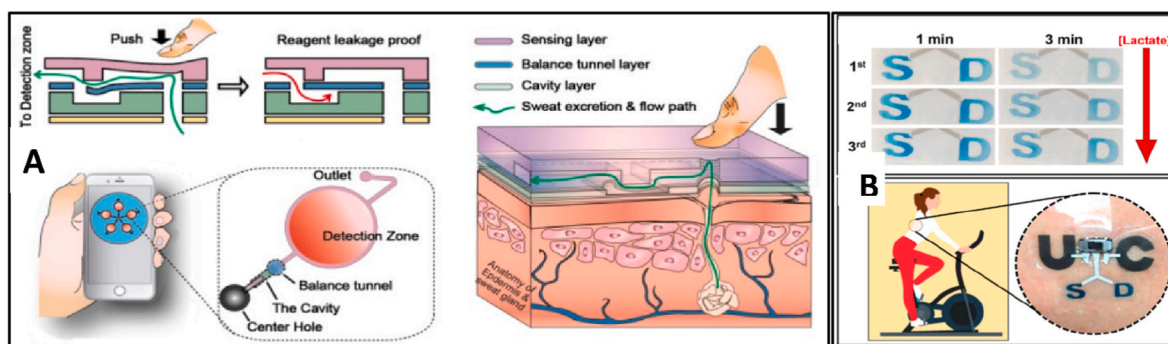
Fig. 30. (A) Schematic drawing of the structure and function of the integrated microfluidic check valve, sweat secretion from the human eccrine gland and the sweat collection by the sensor, and smartphone-based data visualization and acquisition of sweat glucose detection. The right side demonstrates the arrangement of the functionalized modules on the wearable microfluidic chip-based sensing device. Reproduced with permission from Ref. [92]. *Copyright © 2019, American Chemical Society.* **(B)** Resettable sweat-powered wearable electrochromic biosensor. For a full figure description see original publication. Reproduced with permission from Ref. [88]. *Copyright © 2022, Elsevier.*
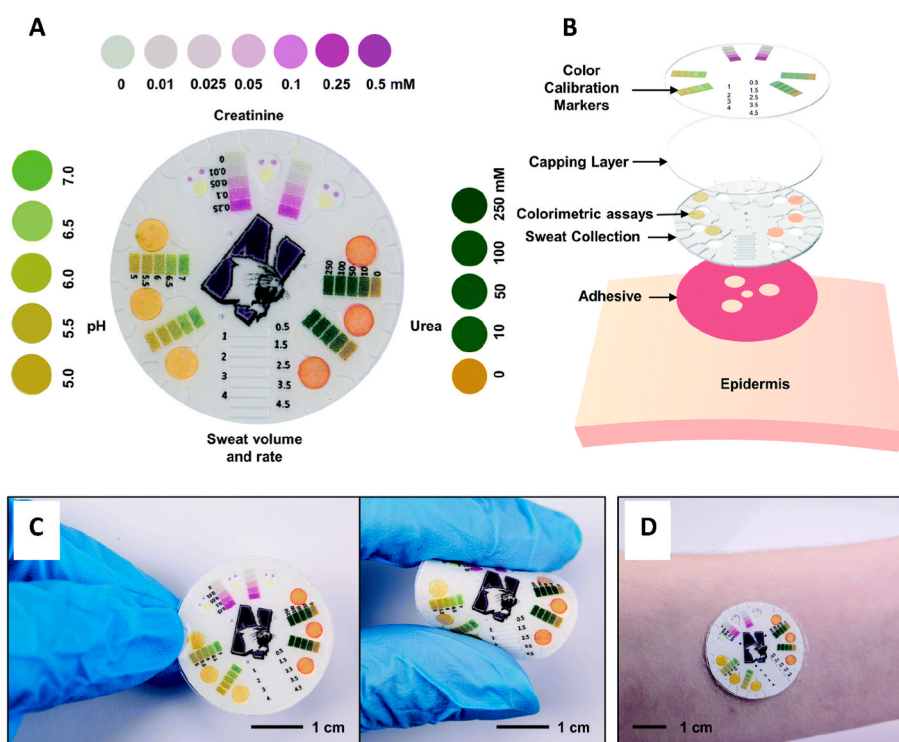

Fig. 31. Overview, schematic illustration, and optical images of an epidermal microfluidic sweat sensor. **(A)** Overview of the functionality of the colorimetric detection scheme with insets at the right, left and top that illustrate the range of colours across a corresponding relevant range for sweat. **(B)** Exploded view illustration of the different layers and components of the system. **(C)** Image of a device in a flat (left) and bent (right) state. **(D)** Image of a device mounted on the forearm. Reproduced with permission from Ref. [94]. *Copyright © 2019, Royal Society of Chemistry.* (For interpretation of the references to color in this figure legend, the reader is referred to the Web version of this article.)

Additionally, there is some contribution from the movement of charged species in the electrical field due to electrophoresis [7]. The method of extraction of ISF using electric current is called reverse iontophoresis, as "reverse" is opposed to iontophoresis, which is a drug delivery method whereby drug molecules are delivered to the deeper layers of skin at the anode. An enhanced version of reverse iontophoresis is called magnetohydrodynamic extraction (MHD) [104], which uses a magnetic field of *ca* 300 mT in addition to the applied electric current. The Lorenz force, resulting from the interaction between the magnetic and electric fields, acts on ISF enhancing its flow towards the skin surface by 13 times compared to reverse iontophoresis (Fig. 32) [104].

The enhancement in extraction obtained by MHD makes sampling of ISF more efficient, potentially improving the correlation between glucose concentrations in blood and in the extracted ISF. Since sampling via reverse iontophoresis is rather inconsistent from person to person, and less efficient compared with MHD extraction, several attempts have been made recently [105] and in the past to introduce an internal standard, such as *e.g.* measurement of Na^+ concentration, to compensate for differences in skin permeability. To do that, the concentration of Na^+ ions is monitored using a pair of ion-selective electrodes at both sides of the iontophoretic setup, anode and cathode, to determine the difference in Na^+ concentration and thus the extracted volume of ISF at each electrode. As opposed to past efforts, such differential determination of Na^+ concentration makes it possible to introduce a correction due to the skin differences. In addition to the internal standard used for quantitation of analyte in ISF, overall biosensor fabrication methods

Table 5
Analytical performance of wearable biosensors for glucose determination in ISF.

Biosensor implementation	Analytical sensitivity to glucose, nA/ ($\mu M \bullet cm^2$)	Limit of detection, μM	Tested shelf life/ Operational stability	Reference
Graphene/PtNP/Au/ PB GOx/Nafion inkjet printed	9.3	6.5	-/1 day	[105]
C/PB/screen printed, drop cast GOx/ chitosan/ collagenated nanofibre	85	7	-/-	[7]
Graphene fibres with deposited Prussian Blue GOx/chitosan	1539.53[a]	N/A	-/-	[107]
Gr/CNTs GOx	524.26[b]	N/A	-/-	[108]

PtNP – platinum nanoparticles, PB – Prussian Blue, GOx – glucose oxidase, CNTs – carbon nanotubes, Gr – graphene.

[a] Not mentioned whether the current density is calculated per geometric or electrochemical surface area, the numbers may therefore significantly vary.

[b] Current density is calculated per geometric surface area.

demonstrate the use of nanomaterials, such as graphene and Pt nanoparticles in combination with Prussian Blue [105]. Nanomaterials are employed to increase the electrochemically active surface area and to enhance the electron transfer between enzyme and electrode surface. New methods to attach enzyme to a permeable carrier were reported to improve the transport and conversion of reactants to hydrogen peroxide [7]. Furthermore, manipulations with extraction methods were used to both increase skin permeability and biosensor sensitivity by, e.g. thermal activation [105].

Typically, the composition of ISF is close to that of blood plasma. However, upon the extraction of ISF through the skin, the concentration of analytes can decrease by two orders of magnitude [106] due to the sieving effect of tight skin layers, such as dermis. Therefore, the analytical performance of the biosensors measuring glucose concentration in blood is usually insufficient for measuring glucose concentration in the extracted ISF. Efforts were taken to improve the analytical sensitivity of the glucose biosensors by increasing the surface area of the working electrode by using e.g. graphene fibres with deposited Prussian Blue in the form of a wearable textile electrode [107]. The analytical sensitivity of such electrodes is very large due to the large conducting surface area. Similarly, a graphene/CNT non-woven electrode was used to enhance the current response of the biosensor with GOx deposited directly onto CNT bundles [108]. Although authors claim that CNT works as a mediator for electron transfer from the catalytic center of GOx to the electrode, most likely the electron transfer happens via flavine adenine dinucleotide (FAD) released from enzyme as an impurity or due to surface-induced denaturation of GOx [109]. These types of electrodes [107,108] used no hydrogel featuring dry extraction electrodes and can be considered as a step towards textile-based wearable biosensors.

The most typical reported form-factor of the biosensors for detection of analytes in ISF is a patch that is mounted to the skin with an adhesive. Recent publications on wearable biosensors for ISF sampling and testing focus on the development of multimodal (hemodynamic and biomarker, Fig. 27) [79], multisample (sweat and ISF, Fig. 33) [78], and multi-analyte wearable platforms for health monitoring. The sensing platforms are based on a careful choice of materials to combine e.g. rigid acoustic and electrochemical transducers in one platform that is yet pliable and conforming to the human body. Towards this goal, stretchable silver ink was developed using styrene-ethylene-butylene-styrene (SEBS) block copolymer as a binder. The glucose biosensor was the only sensor operating with ISF and it used a mix of Nafion, chitosan, glutaraldehyde, and BSA to immobilize proteins, prevent their migration, and create a viscous environment for the enzyme folding. Such a wearable platform allowed to monitor biomarkers and their change in response to stimuli
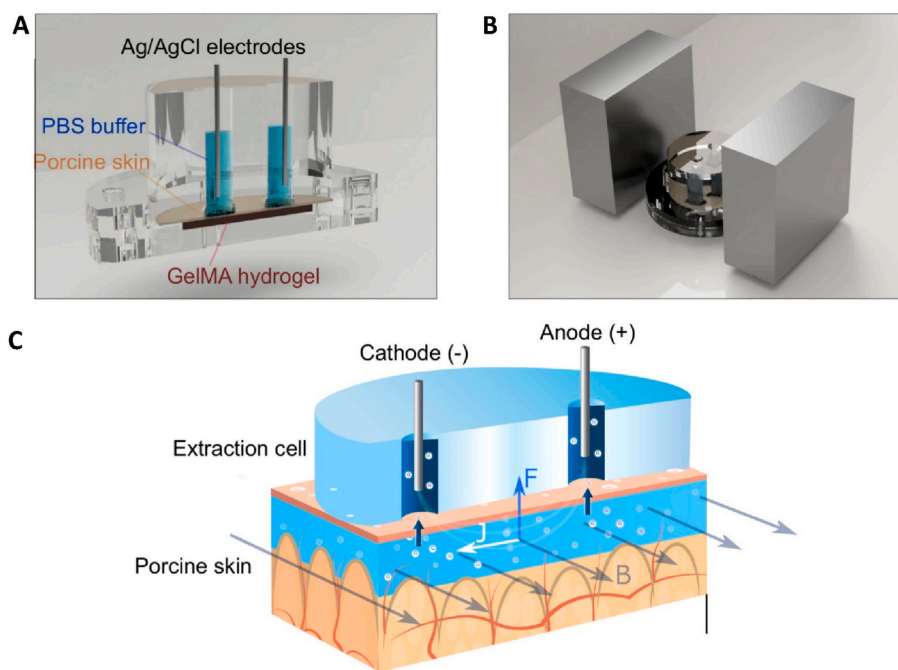

Fig. 32. (A) 3D model construction of MHD with the extraction cell cut out to reveal the main parts of the cell: GelMA hydrogel at the bottom, porcine skin on top of the hydrogel, electrode wells filled with buffer (PBS, 10 mM, pH 7.4) and Ag/AgCl electrodes (ø = 1 mm, length = 2.5 cm). **(B)** The extraction chamber is positioned between two neodymium magnets (size: 70 mm × 70 mm × 30 mm). **(C)** Schematic picture of glucose extraction using MHD. An electric current is established between the two electrode chambers filled with buffer solution. The electric current induces electro-osmotic flow from the anode through the skin towards the cathode. A current density profile (J) in the presence of a magnetic field (B) generates a Lorentz force (F) that drives the interstitial fluid towards the skin surface. Reproduced with permission from Ref. [104]. *Copyright © 2021, Nature Portfolio.*
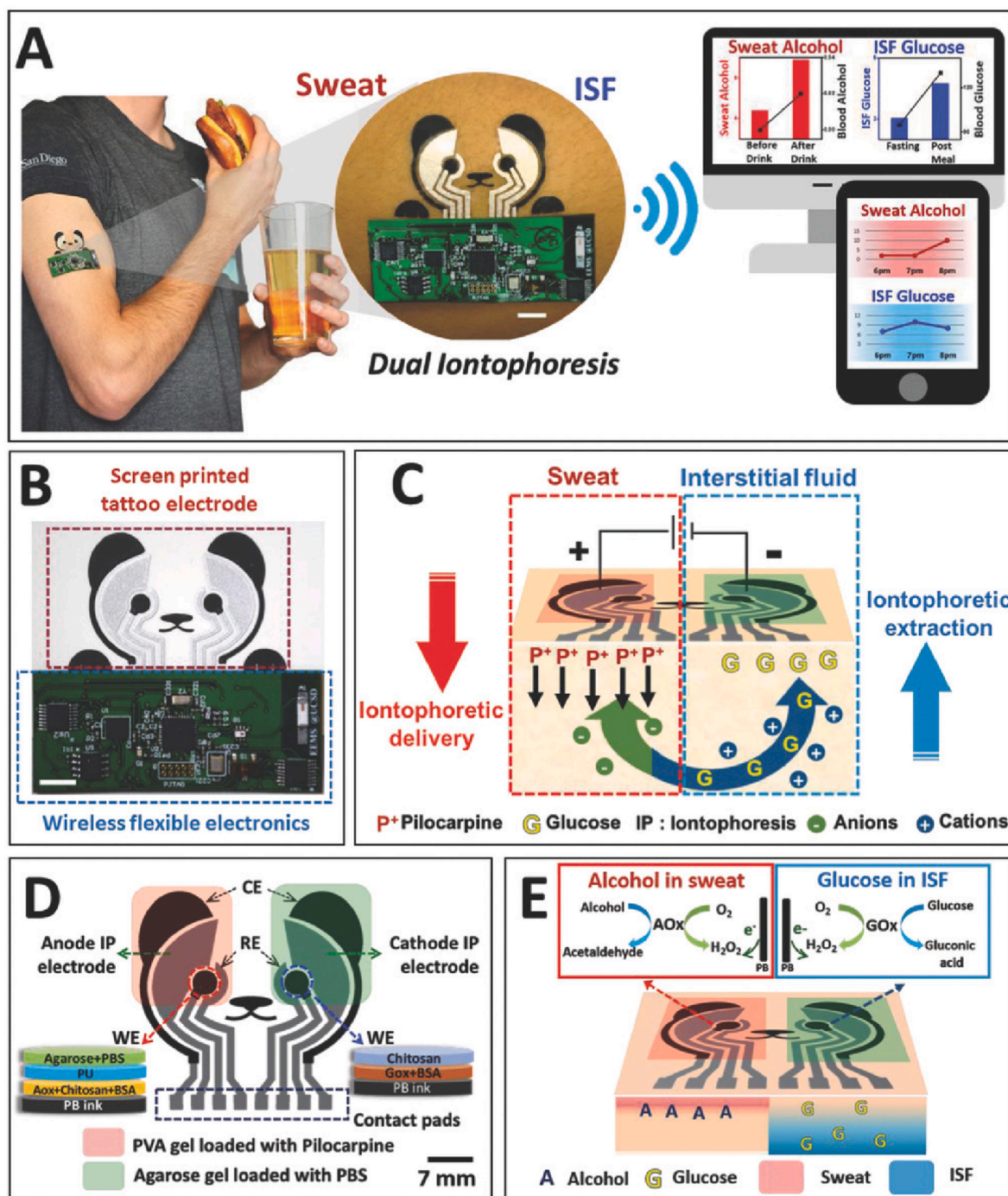
Fig. 33. The concept of simultaneous noninvasive sampling and monitoring of ISF and sweat using temporary tattoos (stickers). For the full description of the figure see the original article. Reproduced with permission from Ref. [78]. *Copyright © 2018, Wiley-VCH.*

such as exercise, alcohol and caffeine consumption [78,79] and demonstrated rather good correlation between the measured sensor response to glucose and the concentration of glucose in blood (Pearson coefficient = 0.9 [79]). Although the analytical performance parameters for the biosensors were not specifically reported in the works [78,79], the reported calibration plots suggest that the sensitivity is around 20–50 nA/(μM•cm^2), which is typical for biosensors with similar formulation.

2.3. Other dermal samples

Recently, a promising biosensor platform was developed for detecting tumours and pathogens by combining flexible microfluidic technology with isothermal nucleic acid amplification in a form factor of a bandage (Fig. 34). The wearable microfluidic sensor used recombinase polymerase amplification of nucleic acids, triggered by human body heat (30–37 °C). The detection of nucleic acids with an optical fluorimetric readout featured a limit of detection of 100 copies of deoxyribonucleic acid (DNA)/μL and a sensitivity −0.5194 ΔCt/decade. The assay used SYBR Green I as a fluorescent dye excited with a mini UV–vis torch (λ_{ex} = 365 nm) and fluorescence was read with a smartphone as the detector [110].

A standalone type of epidermal biosensor detecting volatile organic compounds emitted via skin was reported only in one work, where the
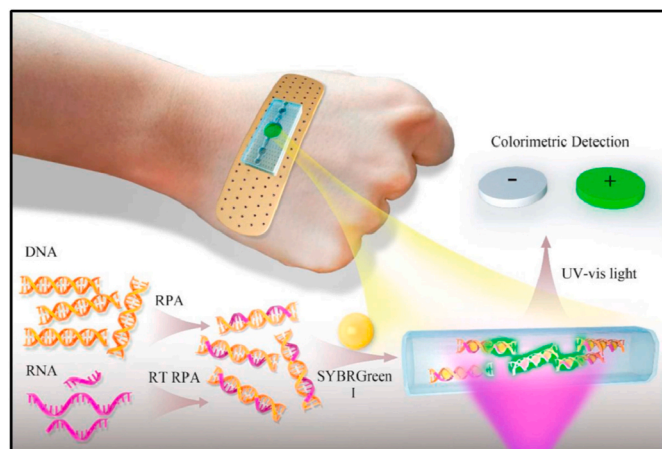
Fig. 34. Bandage-like wearable flexible microfluidic recombinase polymerase amplification sensor for the rapid visual detection of nucleic acids, Reproduced with permission from Ref. [110]. *Copyright © 2019, Elsevier.*

authors developed a bio-sniffer headset for determination of alcohol. The biosensor utilized reduced nicotine adenine dinucleotide (NADH) produced in the enzymatic reaction involving alcohol dehydrogenase

and oxidised nicotine adenine dinucleotide (NAD$^+$) immobilized in a PTFE membrane using PMEH (poly-[2-methacryloyloxyethyl phosphorylcholine]-*co*-[2-ethylhexyl methacrylate]). NADH autofluorescence emission was detected with a complementary metal–oxide–semiconductor (CMOS) camera [111].

3. Oral cavity (saliva)

Saliva is a clear and slightly viscous fluid secreted by the salivary glands located in the mouth and throat. Saliva plays a crucial role in oral health and has several important functions, such as lubrication, digestion, antimicrobial protection, taste and smell, and in aiding speech. Saliva analysis can be used as a diagnostic tool in certain medical and dental conditions to provide information about various health markers (hormone levels, drug levels, specific antibodies) and for assessing the oral health, disease detection, and monitoring the response to treatment. Since saliva can be non-invasively collected in larger (ml) volumes, there is less need for wearable on-body measurements of saliva, when compared to sweat and ISF.

As sodium intake is correlated with hypertension, Lee et al. presented intraoral, wireless hybrid electronics for real-time monitoring of sodium ions in saliva [112]. The stretchable, hybrid electronic system consisted of chip-scale components, microstructured sodium sensors, stretchable interconnects, and a low-profile, ultrasoft, breathable, and microporous
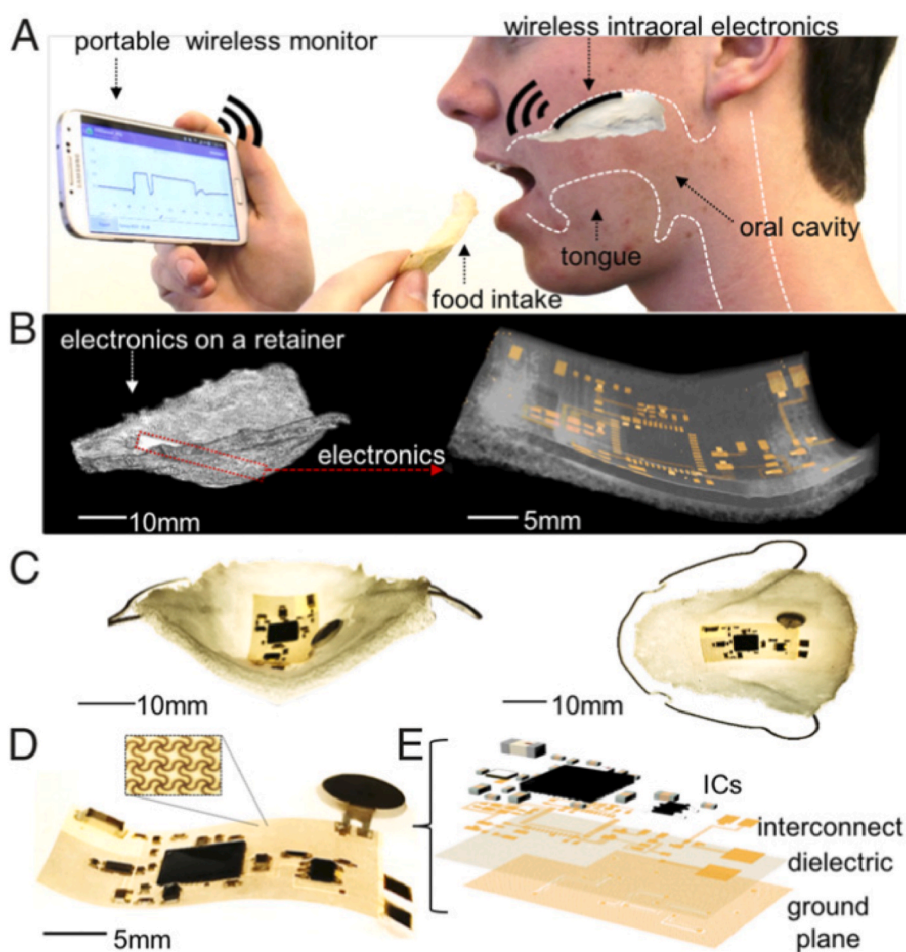

Fig. 35. System architectures and device composition. **(A)** Overview of the intraoral electronics displaying quantification of sodium intake via real-time monitoring. **(B)** X-ray micrographs of an ultrathin intraoral electronics, conformally laminated on an oral retainer (Left), and colorized image of circuit interconnects (Right) on a porous membrane. **(C)** Photos of the electronics [backside view (Left) and top view (Right)], configured in a stretchable structure with a retainer. **(D)** Zoomed-in photo of the wireless electronics. **(E)** Exploded view illustration of the multilayer composition of the electronics in D, including ICs, mesh interconnects, dielectric layer, and ground plane. Reprinted with permission from Ref. [112]. *Copyright © 2019 The Authors, some rights reserved. Distributed under a Creative Commons Attribution NonCommercial, NoDerivs License 4.0 (CC BY-NC-ND).*

membrane. The Na^+ sensor was made by layering of palladium and a Na^+ ISM on a copper substrate. The reference electrode was Ag/AgCl deposited on a copper substrate. The sensors and accompanying electronics were embedded into biocompatible elastomers (SF15 and Eco30) (Fig. 35).

Monitoring electrolytes is critical for newborns and babies in the intensive care unit. Recently, Lim et al. presented a smart wireless bioelectronic pacifier (Fig. 36) for real-time continuous monitoring of Na^+ and K^+ levels in infant's saliva [113]. The working electrodes were obtained by covering an Ag wire with carbon black mixed with an Ecoflex (CB-Ecoflex) layer followed by deposition of the respective ISMs. The reference electrode was Ag/AgCl/PVB. The microfluidic channels were made using a mixture of PDMS and PDMS- polyethylene glycol (PEG) co-polymer on a silicon wafer. The sensors in the device showed good stability and a sensitivity of 52 and 57 mV/dec for the sodium and potassium sensor, respectively. The feasibility and performance of the device was studied in vivo. Integrating chemical sensors in a pacifier is an elegant approach towards non-invasive monitoring of biomarkers in babies.

4. Ocular cavity (tears)

Tear fluid, also known as tears or lacrimal fluid is a clear, watery fluid that is produced by the lacrimal glands located in the upper outer part of the eye. Tears play a critical role in maintaining the health and function of the eyes, and they serve several important functions, such as lubrication, antimicrobial protection, cornea nourishment, and maintaining the quality of vision.

Detection of analytes in tears has been a long-sought modality of wearable devices, especially considering the possibility of integrating chemical sensors and biosensors into contact lenses. However, the technology has proven to be challenging in establishing a reliable correlation between concentration of analytes in tears and blood. Hence, determination of analytes in tear fluids by using chemical sensors is still very rare.

Moreddu et al. described the concept of laser-inscribed contact lens sensors for the determination of pH, nitrite, glucose, and protein in tear samples [114]. The microfluidic system was inscribed in commercial contact lenses by laser ablation (Fig. 37). It should be stressed that the device was tested only in vitro using artificial tear samples and colorimetric readout. The obtained linear range was 6–8 for pH and 0–200 μM for nitrite with sensitivities of 12.23 nm/pH and 0.03 nm/μM for pH and
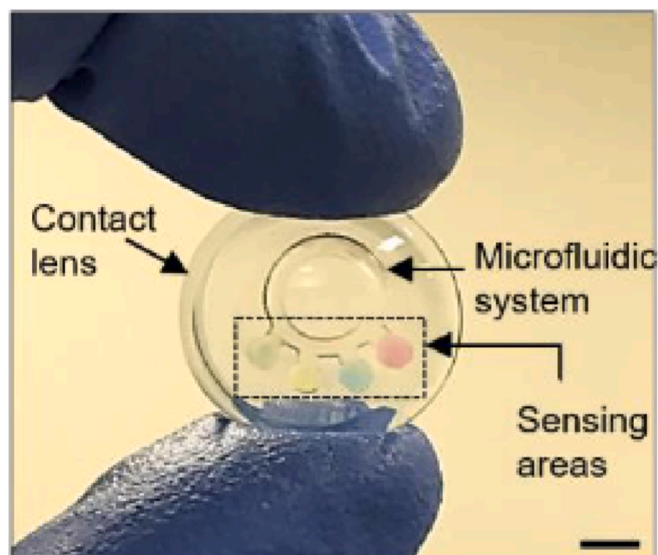

Fig. 37. Contact lens sensing platform with a microfluidic system and sensing zones. Adapted with permission from Ref. [114]. *Copyright © 2020, Elsevier.*

nitrite, respectively.

Recent efforts in making wearable biosensors for analysing tears were focused on a few areas, as summarized in Table 6. Examples include the development of biopolymers for coating NovioSense biosensors and proving their clinical performance towards electrochemical glucose monitoring in tears [115], developing electrochemical biosensors integrated into spectacles for monitoring glucose, vitamins, and alcohol [116], and developing microfluidic contact lenses with colorimetric readout with the help of a smartphone [114]. Utilization of tears as a sample is certainly hampered by the sensitivity of the human eye towards even minute foreign objects, which makes it challenging to perform chemical sensing in close vicinity to the eye. When considering the widespread use of contact lenses, integrating the biosensor into a contact lens seems to be feasible from the user perspective [114], while placing a sensor stick under the lower eyelid sounds less attractive for the user [115]. Connecting the biosensor to eyeglasses with a fluidic device for collecting tears allows the biosensor to be further away from the eye, which should be more comfortable for the wearer of the device [116].

5. Conclusions and outlook

Non-invasive on-body chemical sensing of multiple biomarkers is a vital field of research with major challenges as well as opportunities. Based on the scientific literature from the last five years, it can be concluded that a vast majority of chemical sensors and biosensors for non-invasive on-body measurements rely on electrochemical and optical
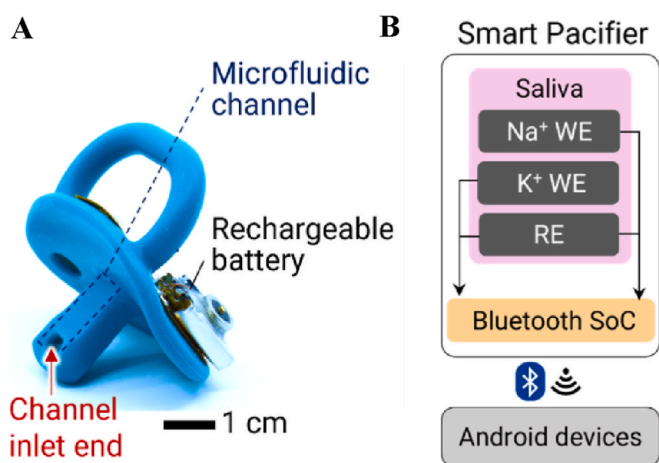

Fig. 36. Smart pacifier system for electrolyte monitoring. **(A)** Side view of the pacifier showing a microfluidic channel, an inlet end for delivering saliva and measuring ion concentration. **(B)** Illustration of the sensor's components of the smart pacifier with data recording on a portable device. Adapted with permission from Ref. [113]. *Copyright © 2022, Elsevier.*

Table 6
Analytical performance of biosensors for monitoring biomarkers in tears.

Biosensor implementation	Analyte	Analytical sensitivity	Limit of detection	Reference
Pt/Ir/Parylene/GOx/BSA/PEG/glutaraldehyde/Nafion	Glucose	0.7 μA/mM[a]	N/A	[115]
C/PB/Alcohol oxidase/BSA/chitosan/glutaraldehyde	Alcohol	1 nA/mM[a]	N/A	[116]
GOx/PB/carbon	Glucose	N/A	N/A	[116]
GOx, peroxidase, and 3,3′,5,5′-tetramethylbenzidine, colorimetric	Glucose	1.4 nm/mM	1.84 mM	[114]

[a] Estimation based on graphical data provided in the article.

transduction for determination of electrolytes, pH, glucose, and lactate in sweat. Electrochemical sensors, such as potentiometric ion/pH sensors and enzymatic biosensors give a reversible response and are therefore suitable for continuous monitoring, while optical sensors are generally single-use devices. It is not surprising that potentiometric ion sensors in the form of solid-contact ion-selective electrodes, combined with solid-state reference electrodes, continue to be a major technology for determination of electrolyte ions, such as Na^+, K^+ and Cl^-. Here, plasticized polymeric membranes containing appropriate ionophores are mostly used for ion sensing, while polyaniline is frequently used for pH sensing. Wearable electrochemical biosensors are dominated by glucose and lactate sensors based on the enzymes glucose oxidase and lactate oxidase, respectively. These established and proven sensing principles are often combined with innovative sensor design and microfluidic sample handling, especially for sweat that is currently the most popular non-invasive sample. While the planar sensor design is suitable for mass production by printing technologies, new research directions include also wearable sensors in the form of fibres and fabric, as well as self-healable sensors.

During the last five year, sweat is by far the most popular sample type for non-invasive on-body sensing, while interstitial fluid (ISF) is used mainly for glucose monitoring. Reverse iontophoresis and magnetohydrodynamics (MHD) are the dominating non-invasive sampling methods for ISF. Chemical sensors based on mass and thermal transduction are rarely used for non-invasive monitoring, and the same is true for alternative samples like saliva and tears. Saliva can be quite easily collected in larger volumes, which means that wearable on-body measurements of saliva is not necessarily the first choice. Utilization of tears as a sample is challenging, due to small volumes and the discomfort caused by sensors in or close to the eye.

5.1. Challenges

Further progress in the field of non-invasive on-body chemical sensing will require extensive research and development to address several challenges related to chemical sensor technology and non-invasive sampling of biofluids. The basic analytical performance of the chemical sensors must comply with the requirements of the intended application regarding selectivity, sensitivity, detection limit, response time, signal reversibility and stability. These requirements are generally fulfilled for many types of wearable sensors for electrolytes, pH, glucose and lactate, while determination of *e.g.* hormones at extremely low concentration levels is still challenging. Importantly, the analytical performance must remain sufficiently stable during the entire measurement time (hours–days), because recalibration is not feasible in the case of on-body measurements. This essentially means that in the end calibration-free chemical sensors and biosensors exhibiting exceptionally good biocompatibility and stability will be needed. Since chemical sensing involves direct contact between the active sensor surface and the sample, potential biofouling of the sensor material is also a major challenge, which is related to biocompatibility and reliability of the sensor. When the sensor is in direct contact with skin, it becomes important to consider any potential leakage of active sensor components that may cause skin irritation or other adverse health effects. For example, ion-selective membranes based on plasticized poly(vinyl chloride) may release plasticizer, ionophore and other active compounds when used for prolonged times. Microfluidics that prevents direct contact between the sensor and skin may solve this issue. When it comes to commercial applications, the shelf-life of the sensor is extremely important. From a user perspective, the chemical sensor must be affordable, safe, and comfortable to use. Ideally, the chemical sensor would be just removed from the package and attached to the body without any need for conditioning or calibration. Finally, the sensor output from the analyzed sample must correlate with the concentration of the analyte in blood in a timely manner. This is a requirement that finally determines whether the sensor will be commercialised or not.

Obviously, the technical requirements for wearable on-body chemical sensors are exceptionally stringent and success will require a truly interdisciplinary approach. Despite great research achievements over the last five years, as summarized in this review, much work is still needed to develop chemical sensors and biosensors that work reliably when applied for on-body measurements. Sensor parameters, such as shelf-life and operational stability are not always available in scientific publications. A maximum shelf-life of one year was reported for a glucose biosensor for sweat monitoring with an operational stability of 25 h. Such performance parameters are promising for practical applications. Other works reported a maximum operational stability of 15 days for glucose biosensors intended for sweat monitoring, while the shelf-life was not mentioned.

5.2. Opportunities

When non-invasive on-body chemical sensing of various biomarkers becomes a reality, it will have a huge impact on our everyday lives. As the chemical sensor technologies improve further, non-invasive chemical analysis of body fluids will make it convenient for anybody to monitor their health status in real time. Regular tracking of biomarkers at the molecular level will help to manage various diseases and it will have a major impact on preventive healthcare. Taking glucose as an example, the advantages for people suffering from diabetes is obvious. Furthermore, it will become feasible for anybody to track their glucose level and to make any necessary changes in lifestyle and nutrition long before diabetes sets in. This will reduce personal suffering and at the same time reduce the cost of public healthcare. Similarly, by regular monitoring of *e.g.* cortisol levels, early signs of stress and burnout can be detected and alleviated by lifestyle adjustments. Consequently, successful non-invasive on-body chemical sensing of multiple biomarkers will definitely redefine healthcare and will have a large impact on our everyday lives.

CRediT authorship contribution statement

Zhanna Boeva: Writing – original draft, Writing – review & editing. **Zekra Mousavi:** Writing – original draft, Writing – review & editing. **Tomasz Sokalski:** Writing – original draft, Writing – review & editing. **Johan Bobacka:** Writing – original draft, Writing – review & editing.

Declaration of competing interest

The authors declare the following financial interests/personal relationships which may be considered as potential competing interests: Johan Bobacka reports a relationship with GlucoModicum Ltd that includes: board membership, employment, and equity or stocks. Zhanna Boeva reports a relationship with GlucoModicum Ltd that includes: employment and equity or stocks.

Data availability

The review is based on already published data for which permission from the publishers have been obtained.

References

[1] J. Heikenfeld, A. Jajack, J. Rogers, P. Gutruf, L. Tian, T. Pan, R. Li, M. Khine, J. Kim, J. Wang, J. Kim, Wearable sensors: modalities, challenges, and prospects, Lab Chip 18 (2018) 217–248, https://doi.org/10.1039/C7LC00914C.

[2] J. Heikenfeld, A. Jajack, B. Feldman, S.W. Granger, S. Gaitonde, G. Begtrup, B. A. Katchman, Accessing analytes in biofluids for peripheral biochemical monitoring, Nat. Biotechnol. 37 (2019) 407–419, https://doi.org/10.1038/s41587-019-0040-3.

[3] T. Ray, J. Choi, A. Bandodkar, S. Krishnan, P. Gutruf, L. Tian, R. Ghaffari, J. Rogers, Bio-integrated wearable systems: a comprehensive review, Chem. Rev. 119 (2019) 5461–5533, https://doi.org/10.1021/acs.chemrev.8b00573.

[4] W. Gao, H. Ota, D. Kiriya, K. Takei, A. Javey, Flexible electronics toward wearable sensing, Acc. Chem. Res. 52 (2019) 523–533, https://doi.org/10.1021/acs.accounts.8b00500.

[5] J. Kim, A. Campbell, B. de Avila, J. Wang, Wearable biosensors for healthcare monitoring, Nat. Biotechnol. 37 (2019) 389–406, https://doi.org/10.1038/s41587-019-0045-y.

[6] J.R. Sempionatto, J.A. Lasalde-Ramírez, K. Mahato, J. Wang, W. Gao, Wearable chemical sensors for biomarker discovery in the omics era, Nat. Rev. Chem 6 (2022) 899–915, https://doi.org/10.1038/s41570-022-00439-w.

[7] E. Kemp, T. Palomäki, I.A. Ruuth, Z.A. Boeva, T.A. Nurminen, R.T. Vänskä, L. K. Zschaechner, A.G. Pérez, T.A. Hakala, M. Wardale, E. Haeggström, J. Bobacka, Influence of enzyme immobilization and skin-sensor interface on non-invasive glucose determination from interstitial fluid obtained by magnetohydrodynamic extraction, Biosens. Bioelectron. 206 (2022) 114123, https://doi.org/10.1016/j.bios.2022.114123.

[8] S.J. Montain, S.N. Cheuvront, H.C. Lukaski, Sweat mineral-element responses during 7 h of exercise-heat stress, Int. J. Sport Nutr. Exerc. Metab. 17 (2007) 574–582, https://doi.org/10.1123/ijsnem.17.6.574.

[9] A.H.B. Wu (Ed.), Tietz Clinical Guide to Laboratory Tests, fourth ed., Saunders/Elsevier, St. Louis, Mo, 2006.

[10] L.B. Baker, Physiology of sweat gland function: the roles of sweating and sweat composition in human health, Temperature 6 (2019) 211–259, https://doi.org/10.1080/23328940.2019.1632145.

[11] I. Alvear-Ordenes, D. García-López, J.A. De Paz, J. González-Gallego, Sweat lactate, ammonia, and urea in rugby players, Int. J. Sports Med. 26 (2005) 632–637, https://doi.org/10.1055/s-2004-830380.

[12] K. Aoyama, Y. Okino, H. Yamazaki, R. Kojima, M. Uchibori, Y. Nakanishi, Y. Ota, Saliva pH affects the sweetness sense, Nutrition 35 (2017) 51–55, https://doi.org/10.1016/j.nut.2016.10.018.

[13] F. Gao, C. Liu, L. Zhang, T. Liu, Z. Wang, Z. Song, H. Cai, Z. Fang, J. Chen, J. Wang, M. Han, J. Wang, K. Lin, R. Wang, M. Li, Q. Mei, X. Ma, S. Liang, G. Gou, N. Xue, Wearable and flexible electrochemical sensors for sweat analysis: a review, Microsyst. Nanoeng. 9 (2023) 1, https://doi.org/10.1038/s41378-022-00443-6.

[14] M.C. Brothers, M. DeBrosse, C.C. Grigsby, R.R. Naik, S.M. Hussain, J. Heikenfeld, S.S. Kim, Achievements and challenges for real-time sensing of analytes in sweat within wearable platforms, Acc. Chem. Res. 52 (2019) 297–306, https://doi.org/10.1021/acs.accounts.8b00555.

[15] Y. Marunaka, Roles of interstitial fluid pH in diabetes mellitus: glycolysis and mitochondrial function, World J. Diabetes 15 (2015) 125–135, https://doi.org/10.4239/wjd.v6.i1.125.

[16] J.H. Yoon, S.-M. Kim, Y. Eom, J.M. Koo, H.-W. Cho, T.J. Lee, K.G. Lee, H.J. Park, Y.K. Kim, H.-J. Yoo, S.Y. Hwang, J. Park, B.G. Choi, Extremely fast self-healable bio-based supramolecular polymer for wearable real-time sweat-monitoring sensor, ACS Appl. Mater. Interfaces 11 (2019) 46165–46175, https://doi.org/10.1021/acsami.9b16829.

[17] J.H. Yoon, S.-M. Kim, H.J. Park, Y.K. Kim, D.X. Oh, H.-W. Cho, K.G. Lee, S. Y. Hwang, J. Park, B.G. Choi, Highly self-healable and flexible cable-type pH sensors for real-time monitoring of human fluids, Biosens. Bioelectron. 150 (2020) 111946, https://doi.org/10.1016/j.bios.2019.111946.

[18] L. Wang, L. Wang, Y. Zhang, J. Pan, S. Li, X. Sun, B. Zhang, H. Peng, Weaving sensing fibers into electrochemical fabric for real-time health monitoring, Adv. Funct. Mater. 28 (2018) 1804456, https://doi.org/10.1002/adfm.201804456.

[19] T. Terse-Thakoor, M. Punjiya, Z. Matharu, B. Lyu, M. Ahmad, G.E. Giles, R. Owyeung, F. Alaimo, M. Shojaei Baghini, T.T. Brunyé, S. Sonkusale, Thread-based multiplexed sensor patch for real-time sweat monitoring, Npj Flex. Electron. 4 (2020) 1–10, https://doi.org/10.1038/s41528-020-00081-w.

[20] C. Zhao, X. Li, Q. Wu, X. Liu, A thread-based wearable sweat nanobiosensor, Biosens. Bioelectron. 188 (2021) 113270, https://doi.org/10.1016/j.bios.2021.113270.

[21] X. Hou, Y. Zhou, Y. Liu, L. Wang, J. Wang, Coaxial electrospun flexible PANI//PU fibers as highly sensitive pH wearable sensor, J. Mater. Sci. 55 (2020) 16033–16047, https://doi.org/10.1007/s10853-020-05110-7.

[22] J. Xu, Z. Zhang, S. Gan, H. Gao, H. Kong, Z. Song, X. Ge, Y. Bao, L. Niu, Highly stretchable fiber-based potentiometric ion sensors for multichannel real-time analysis of human sweat, ACS Sens. 5 (2020) 2834–2842, https://doi.org/10.1021/acssensors.0c00960.

[23] B.S. Napier, G. Matzeu, M.L. Presti, F.G. Omenetto, Dry spun, bulk-functionalized rGO fibers for textile integrated potentiometric sensors, Adv. Mater. Technol. 7 (2022) 2101508, https://doi.org/10.1002/admt.202101508.

[24] S.Y. Oh, S.Y. Hong, Y.R. Jeong, J. Yun, H. Park, S.W. Jin, G. Lee, J.H. Oh, H. Lee, S.-S. Lee, J.S. Ha, Skin-attachable, stretchable electrochemical sweat sensor for glucose and pH detection, ACS Appl. Mater. Interfaces 10 (2018) 13729–13740, https://doi.org/10.1021/acsami.8b03342.

[25] A. Alizadeh, A. Burns, R. Lenigk, R. Gettings, J. Ashe, A. Porter, M. McCaul, R. Barrett, D. Diamond, P. White, P. Skeath, M. Tomczak, A wearable patch for continuous monitoring of sweat electrolytes during exertion, Lab Chip 18 (2018) 2632–2641, https://doi.org/10.1039/C8LC00510A.

[26] M. McCaul, A. Porter, R. Barrett, P. White, F. Stroiescu, G. Wallace, D. Diamond, Wearable platform for real-time monitoring of sodium in sweat, ChemPhysChem 19 (2018) 1531–1536, https://doi.org/10.1002/cphc.201701312.

[27] H.Y.Y. Nyein, L.-C. Tai, Q.P. Ngo, M. Chao, G.B. Zhang, W. Gao, M. Bariya, J. Bullock, H. Kim, H.M. Fahad, A. Javey, A wearable microfluidic sensing patch for dynamic sweat secretion analysis, ACS Sens. 3 (2018) 944–952, https://doi.org/10.1021/acssensors.7b00961.

[28] J.R. Sempionatto, A. Martin, L. García-Carmona, A. Barfidokht, J.F. Kurniawan, J. R. Moreto, G. Tang, A. Shin, X. Liu, A. Escarpa, J. Wang, Skin-worn soft microfluidic potentiometric detection system, Electroanalysis 31 (2019) 239–245, https://doi.org/10.1002/elan.201800414.

[29] M. Parrilla, I. Ortiz-Gómez, R. Cánovas, A. Salinas-Castillo, M. Cuartero, G. A. Crespo, Wearable potentiometric ion patch for on-body electrolyte monitoring in sweat: toward a validation strategy to ensure physiological relevance, Anal. Chem. 91 (2019) 8644–8651, https://doi.org/10.1021/acs.analchem.9b02126.

[30] W. He, C. Wang, H. Wang, M. Jian, W. Lu, X. Liang, X. Zhang, F. Yang, Y. Zhang, Integrated textile sensor patch for real-time and multiplex sweat analysis, Sci. Adv. 5 (2019) eaax0649, https://doi.org/10.1126/sciadv.aax0649.

[31] Q. Zhai, L.W. Yap, R. Wang, S. Gong, Z. Guo, Y. Liu, Q. Lyu, J. Wang, GeorgeP. Simon, W. Cheng, Vertically aligned gold nanowires as stretchable and wearable epidermal ion-selective electrode for noninvasive multiplexed sweat analysis, Anal. Chem. 92 (2020) 4647–4655, https://doi.org/10.1021/acs.analchem.0c00274.

[32] L. Mou, Y. Xia, X. Jiang, Epidermal sensor for potentiometric analysis of metabolite and electrolyte, Anal. Chem. 93 (2021) 11525–11531, https://doi.org/10.1021/acs.analchem.1c01940.

[33] X. Xuan, C. Pérez-Ràfols, C. Chen, M. Cuartero, G.A. Crespo, Lactate biosensing for reliable on-body sweat analysis, ACS Sens. 6 (2021) 2763–2771, https://doi.org/10.1021/acssensors.1c01009.

[34] L. Chen, F. Chen, G. Liu, H. Lin, Y. Bao, D. Han, W. Wang, Y. Ma, B. Zhang, L. Niu, Superhydrophobic functionalized $Ti_3C_2T_x$ MXene-based skin-attachable and wearable electrochemical pH sensor for real-time sweat detection, Anal. Chem. 94 (2022) 7319–7328, https://doi.org/10.1021/acs.analchem.2c00684.

[35] K. Lin, J. Xie, Y. Bao, Y. Ma, L. Chen, H. Wang, L. Xu, Y. Tang, Z. Liu, Z. Sun, S. Gan, L. Niu, Self-adhesive and printable tannin–graphene supramolecular aggregates for wearable potentiometric pH sensing, Electrochem, Commun. Now. 137 (2022) 107261, https://doi.org/10.1016/j.elecom.2022.107261.

[36] Y. Tang, S. Gan, L. Zhong, Z. Sun, L. Xu, C. Liao, K. Lin, X. Cui, D. He, Y. Ma, W. Wang, L. Niu, Lattice proton intercalation to regulate WO_3-based solid-contact wearable pH sensor for sweat analysis, Adv. Funct. Mater. 32 (2022) 2107653, https://doi.org/10.1002/adfm.202107653.

[37] R. Hoekstra, P. Blondeau, F.J. Andrade, IonSens: a wearable potentiometric sensor patch for monitoring total ion content in sweat, Electroanalysis 30 (2018) 1536–1544, https://doi.org/10.1002/elan.201800128.

[38] Q. An, S. Gan, J. Xu, Y. Bao, T. Wu, H. Kong, L. Zhong, Y. Ma, Z. Song, L. Niu, A multichannel electrochemical all-solid-state wearable potentiometric sensor for real-time sweat ion monitoring, Electrochem. Commun. 107 (2019) 106553, https://doi.org/10.1016/j.elecom.2019.106553.

[39] A. Ghoorchian, M. Kamalabadi, M. Moradi, T. Madrakian, A. Afkhami, H. Bagheri, M. Ahmadi, H. Khoshsafar, Wearable potentiometric sensor based on $Na_{0.44}MnO_2$ for non-invasive monitoring of sodium ions in sweat, Anal. Chem. 94 (2022) 2263–2270, https://doi.org/10.1021/acs.analchem.1c04960.

[40] M. Bariya, Z. Shahpar, H. Park, J. Sun, Y. Jung, W. Gao, H.Y.Y. Nyein, T.S. Liaw, L.-C. Tai, Q.P. Ngo, M. Chao, Y. Zhao, M. Hettick, G. Cho, A. Javey, Roll-to-Roll gravure printed electrochemical sensors for wearable and medical devices, ACS Nano 12 (2018) 6978–6987, https://doi.org/10.1021/acsnano.8b02505.

[41] H.Y.Y. Nyein, M. Bariya, L. Kivimäki, S. Uusitalo, T.S. Liaw, E. Jansson, C.H. Ahn, J.A. Hangasky, J. Zhao, Y. Lin, T. Happonen, M. Chao, C. Liedert, Y. Zhao, L.-C. Tai, J. Hiltunen, A. Javey, Regional and correlative sweat analysis using high-throughput microfluidic sensing patches toward decoding sweat, Sci. Adv. 5 (2019) eaaw9906, https://doi.org/10.1126/sciadv.aaw9906.

[42] G. Xu, C. Cheng, Z. Liu, W. Yuan, X. Wu, Y. Lu, S.S. Low, J. Liu, L. Zhu, D. Ji, S. Li, Z. Chen, L. Wang, Q. Yang, Z. Cui, Q. Liu, Battery-free and wireless epidermal electrochemical system with all-printed stretchable electrode array for multiplexed in situ sweat analysis, Adv. Mater. Technol. 4 (2019) 1800658, https://doi.org/10.1002/admt.201800658.

[43] B. Gil, S. Anastasova, G. Yang, A smart wireless ear-worn device for cardiovascular and sweat parameter monitoring during physical exercise: design and performance results, Sensors 19 (2019) 1616, https://doi.org/10.3390/s19071616.

[44] M. Bariya, Li, R. Ghattamaneni, C.H. Ahn, H.Y.Y. Nyein, L.-C. Tai, A. Javey, Glove-based sensors for multimodal monitoring of natural sweat, Sci. Adv. 6 (2020), https://doi.org/10.1126/sciadv.abb8308 eabb8308.

[45] M.S. Kil, S.J. Kim, H.J. Park, J.H. Yoon, J.-M. Jeong, B.G. Choi, Highly stretchable sensor based on fluid dynamics-assisted graphene inks for real-time monitoring of sweat, ACS Appl. Mater. Interfaces 14 (2022) 48072–48080, https://doi.org/10.1021/acsami.2c10638.

[46] M.L. Zamora, J.M. Dominguez, R.M. Trujillo, C.B. Goy, M.A. Sánchez, R. E. Madrid, Potentiometric textile-based pH sensor, Sens. Actuators B Chem. 260 (2018) 601–608, https://doi.org/10.1016/j.snb.2018.01.002.

[47] S.B. Kim, Y. Zhang, S.M. Won, A.J. Bandodkar, Y. Sekine, Y. Xue, J. Koo, S. W. Harshman, J.A. Martin, J.M. Park, T.R. Ray, K.E. Crawford, K. Lee, J. Choi, R. L. Pitsch, C.C. Grigsby, A.J. Strang, Y. Chen, S. Xu, J. Kim, A. Koh, J.S. Ha, Y. Huang, S.W. Kim, J.A. Rogers, Super-absorbent polymer valves and colorimetric chemistries for time-sequenced discrete sampling and chloride analysis of sweat via skin-mounted soft microfluidics, Small 14 (2018) 1703334, https://doi.org/10.1002/smll.201703334.

[48] J. Choi, A.J. Bandodkar, J.T. Reeder, T.R. Ray, A. Turnquist, S.B. Kim, N. Nyberg, A. Hourlier-Fargette, J.B. Model, A.J. Aranyosi, S. Xu, R. Ghaffari, J.A. Rogers, Soft, Skin-integrated multifunctional microfluidic systems for accurate colorimetric analysis of sweat biomarkers and temperature, ACS Sens. 4 (2019) 379–388, https://doi.org/10.1021/acssensors.8b01218.

[49] N. Promphet, P. Rattanawaleedirojn, K. Siralertmukul, N. Soatthiyanon, P. Potiyaraj, C. Thanawattano, J.P. Hinestroza, N. Rodthongkum, Non-invasive textile based colorimetric sensor for the simultaneous detection of sweat pH and lactate, Talanta 192 (2019) 424–430, https://doi.org/10.1016/j.talanta.2018.09.086.

[50] K. Zhang, J. Zhang, F. Wang, D. Kong, Stretchable and superwettable colorimetric sensing patch for epidermal collection and analysis of sweat, ACS Sens. 6 (2021) 2261–2269, https://doi.org/10.1021/acssensors.1c00316.

[51] Z. Zhao, Q. Li, L. Chen, Y. Zhao, J. Gong, Z. Li, J. Zhang, A thread/fabric-based band as a flexible and wearable microfluidic device for sweat sensing and monitoring, Lab Chip 21 (2021) 916–932, https://doi.org/10.1039/D0LC01075H.

[52] H. Yu, J. Sun, Sweat detection theory and fluid driven methods: a review, Nanotechnol. Precis. Eng. 3 (2020) 126–140, https://doi.org/10.1016/j.npe.2020.08.003.

[53] C. Liu, T. Xu, D. Wang, X. Zhang, The role of sampling in wearable sweat sensors, Talanta 212 (2020) 120801, https://doi.org/10.1016/j.talanta.2020.120801.

[54] J. Francis, I. Stamper, J. Heikenfeld, E.F. Gomez, Digital nanoliter to milliliter flow rate sensor with in vivo demonstration for continuous sweat rate measurement, Lab Chip 19 (2019) 178–185, https://doi.org/10.1039/C8LC00968F.

[55] S.B. Kim, J. Koo, J. Yoon, A. Hourlier-Fargette, B. Lee, S. Chen, S. Jo, J. Choi, Y. S. Oh, G. Lee, S.M. Won, A.J. Aranyosi, S.P. Lee, J.B. Model, P.V. Braun, R. Ghaffari, C. Park, J.A. Rogers, Soft, skin-interfaced microfluidic systems with integrated enzymatic assays for measuring the concentration of ammonia and ethanol in sweat, Lab Chip 20 (2020) 84–92, https://doi.org/10.1039/C9LC01045A.

[56] H. Shi, Y. Cao, Y. Zeng, Y. Zhou, W. Wen, C. Zhang, Y. Zhao, Z. Chen, Wearable tesla valve-based sweat collection device for sweat colorimetric analysis, Talanta 240 (2022) 123208, https://doi.org/10.1016/j.talanta.2022.123208, 123208.

[57] A. Hauke, P. Simmers, Y.R. Ojha, B.D. Cameron, R. Ballweg, T. Zhang, N. Twine, M. Brothers, E. Gomez, J. Heikenfeld, Complete validation of a continuous and blood-correlated sweat biosensing device with integrated sweat stimulation, Lab Chip 18 (2018) 3750–3759, https://doi.org/10.1039/C8LC01082J.

[58] N.B. Twine, R.M. Norton, M.C. Brothers, A. Hauke, E.F. Gomez, J. Heikenfeld, Open nanofluidic films with rapid transport and no analyte exchange for ultra-low sample volumes, Lab Chip 18 (2018) 2816–2825, https://doi.org/10.1039/C8LC00186C.

[59] M.A. Komkova, A.A. Eliseev, A.A. Poyarkov, E.V. Daboss, P.V. Evdokimov, A. A. Eliseev, A.A. Karyakin, Simultaneous monitoring of sweat lactate content and sweat secretion rate by wearable remote biosensors, Biosens. Bioelectron. 202 (2022) 113970, https://doi.org/10.1016/j.bios.2022.113970, 113970.

[60] A. Wiorek, M. Parrilla, M. Cuartero, G.A. Crespo, Epidermal patch with glucose biosensor: pH and temperature correction toward more accurate sweat analysis during sport practice, Anal. Chem. 92 (2020) 10153–10161, https://doi.org/10.1021/acs.analchem.0c02211.

[61] S. Yoon, H. Yoon, M.A. Zahed, C. Park, D. Kim, J.Y. Park, Multifunctional hybrid skin patch for wearable smart healthcare applications, Biosens. Bioelectron. 196 (2022) 113685, https://doi.org/10.1016/j.bios.2021.113685, 113685.

[62] S. Ferri, K. Kojima, K. Sode, Review of glucose oxidases and glucose dehydrogenases: a bird's eye view of glucose sensing enzymes, J. Diabetes Sci. Technol. 5 (2011) 1068–1076, https://doi.org/10.1177/193229681100500507.

[63] J. Xiao, C. Fan, T. Xu, L. Su, X. Zhang, An electrochemical wearable sensor for levodopa quantification in sweat based on a metal-Organic framework/graphene oxide composite with integrated enzymes, Sens. Actuators B Chem. 359 (2022), https://doi.org/10.1016/j.snb.2022.131586.

[64] M. Li, L. Wang, R. Liu, J. Li, Q. Zhang, G. Shi, Y. Li, C. Hou, H. Wang, A highly integrated sensing paper for wearable electrochemical sweat analysis, Biosens. Bioelectron. 174 (2021) 112828, https://doi.org/10.1016/j.bios.2020.112828.

[65] Y. Lei, W. Zhao, Y. Zhang, Q. Jiang, J.H. He, A.J. Baeumner, O.S. Wolfbeis, Z. L. Wang, K.N. Salama, H.N. Alshareef, A MXene-based wearable biosensor system for high-performance in vitro perspiration analysis, Small 15 (2019), https://doi.org/10.1002/SMLL.201901190.

[66] V. Myndrul, E. Coy, N. Babayevska, V. Zahorodna, V. Balitskyi, I. Baginskiy, O. Gogotsi, M. Bechelany, M.T. Giardi, I. Iatsunskyi, MXene nanoflakes decorating ZnO tetrapods for enhanced performance of skin-attachable stretchable enzymatic electrochemical glucose sensor, Biosens. Bioelectron. 207 (2022) 114141, https://doi.org/10.1016/j.bios.2022.114141, 114141.

[67] H. Yoon, J. Nah, H. Kim, S. Ko, M. Sharifuzzaman, S.C. Barman, X. Xuan, J. Kim, J.Y. Park, A chemically modified laser-induced porous graphene based flexible and ultrasensitive electrochemical biosensor for sweat glucose detection, Sens. Actuators B Chem. 311 (2020) 127866, https://doi.org/10.1016/j.snb.2020.127866.

[68] X. Cheng, B. Wang, Y. Zhao, H. Hojaiji, S. Lin, R. Shih, H. Lin, S. Tamayosa, B. Ham, P. Stout, K. Salahi, Z. Wang, C. Zhao, J. Tan, S. Emaminejad, A mediator-free electroenzymatic sensing methodology to mitigate ionic and electroactive interferents' effects for reliable wearable metabolite and nutrient monitoring, Adv. Funct. Mater. 30 (2020), https://doi.org/10.1002/adfm.201908507.

[69] H. Xia, H. Tang, B. Zhou, Y. Li, X. Zhang, Z. Shi, L. Deng, R. Song, L. Li, Z. Zhang, J. Zhou, Mediator-free electron-transfer on patternable hierarchical meso/macro porous bienzyme interface for highly-sensitive sweat glucose and surface electromyography monitoring, Sens. Actuators B Chem. 312 (2020) 127962, https://doi.org/10.1016/j.snb.2020.127962, 127962.

[70] V. Garg, T. Gupta, S. Rani, S. Bandyopadhyay-Ghosh, S.B. Ghosh, L. Qiao, G. Liu, A hierarchically designed nanocomposite hydrogel with multisensory capabilities towards wearable devices for human-body motion and glucose concentration detection, Compos. Sci. Technol. 213 (2021) 108894, https://doi.org/10.1016/j.compscitech.2021.108894.

[71] E.V. Karpova, E.V. Shcherbacheva, A.A. Galushin, D.V. Vokhmyanina, E. E. Karyakina, A.A. Karyakin, Noninvasive diabetes monitoring through continuous analysis of sweat using flow-through glucose biosensor, Anal. Chem. 91 (2019) 3778–3783, https://doi.org/10.1021/ACS.ANALCHEM.8B05928.

[72] Y. Lin, M. Bariya, H.Y.Y. Nyein, L. Kivimäki, S. Uusitalo, E. Jansson, W. Ji, Z. Yuan, T. Happonen, C. Liedert, J. Hiltunen, Z. Fan, A. Javey, Porous enzymatic membrane for nanotextured glucose sweat sensors with high stability toward reliable noninvasive health monitoring, Adv. Funct. Mater. 29 (2019) 1902521, https://doi.org/10.1002/adfm.201902521.

[73] A. Piper, I. Öberg Månsson, S. Khaliliazar, R. Landin, M.M. Hamedi, A disposable, wearable, flexible, stitched textile electrochemical biosensing platform, Biosens. Bioelectron. 194 (2021) 113604, https://doi.org/10.1016/j.bios.2021.113604.

[74] R. Wang, Q. Zhai, T. An, S. Gong, W. Cheng, Stretchable gold fiber-based wearable textile electrochemical biosensor for lactate monitoring in sweat, Talanta 222 (2021) 121484, https://doi.org/10.1016/j.talanta.2020.121484, 121484.

[75] A. Khan, M. Winder, G. Hossain, Modified graphene-based nanocomposite material for smart textile biosensor to detect lactate from human sweat, Biosens. Bioelectron. X 10 (2022) 100103, https://doi.org/10.1016/j.biosx.2021.100103, 100103.

[76] L. Zheng, Y. Liu, C. Zhang, A sample-to-answer, wearable cloth-based electrochemical sensor (WCECS) for point-of-care detection of glucose in sweat, Sens. Actuators B Chem. 343 (2021), https://doi.org/10.1016/j.snb.2021.130131.

[77] X. He, S. Yang, Q. Pei, Y. Song, C. Liu, T. Xu, X. Zhang, Integrated smart Janus textile bands for self-pumping sweat sampling and analysis, ACS Sens. 5 (2020) 1548–1554, https://doi.org/10.1021/ACSSENSORS.0C00563.

[78] J. Kim, J. Sempionatto, S. Imani, M. Hartel, A. Barfidokht, G. Tang, A. Campbell, P. Mercier, J. Wang, Simultaneous monitoring of sweat and interstitial fluid using a single wearable biosensor platform, Adv. Sci. 5 (2018), https://doi.org/10.1002/advs.201800880.

[79] J.R. Sempionatto, M. Lin, L. Yin, E. De la paz, K. Pei, T. Sonsa-ard, A.N. de Loyola Silva, A.A. Khorshed, F. Zhang, N. Tostado, S. Xu, J. Wang, An epidermal patch for the simultaneous monitoring of haemodynamic and metabolic biomarkers, Nat. Biomed. Eng. 5 (2021) 737–748, https://doi.org/10.1038/S41551-021-00685-1.

[80] L.-C. Tai, C.H. Ahn, H.Y.Y. Nyein, W. Ji, M. Bariya, Y. Lin, L. Li, A. Javey, Nicotine monitoring with a wearable sweat band, ACS Sens. 5 (2020) 1831–1837, https://doi.org/10.1021/acssensors.0c00791.

[81] J. Sempionatto, A. Khorshed, A. Ahmed, A. Silva, A. Barfidokht, L. Yin, K. Goud, M. Mohamed, E. Bailey, J. May, C. Aebischer, C. Chatelle, J. Wang, Epidermal enzymatic biosensors for sweat vitamin C: toward personalized nutrition, ACS Sens. 5 (2020) 1804–1813, https://doi.org/10.1021/acssensors.0c00604.

[82] J. Zhao, Y. Lin, J. Wu, H.Y.Y. Nyein, M. Bariya, L.-C. Tai, M. Chao, W. Ji, G. Zhang, Z. Fan, A. Javey, A fully integrated and self-powered smartwatch for continuous sweat glucose monitoring, ACS Sens. 4 (2019) 1925–1933, https://doi.org/10.1021/acssensors.9b00891.

[83] T. Sun, J. Hui, L. Zhou, B. Lin, H. Sun, Y. Bai, J. Zhao, H. Mao, A low-cost and simple-fabricated epidermal sweat patch based on "cut-and-paste" manufacture, Sens. Actuators B Chem. 368 (2022) 132184, https://doi.org/10.1016/j.snb.2022.132184, 132184.

[84] H.-B. Lee, M. Meeseepong, T.Q. Trung, B.-Y. Kim, N.-E. Lee, A wearable lab-on-a-patch platform with stretchable nanostructured biosensor for non-invasive immunodetection of biomarker in sweat, Biosens. Bioelectron. 156 (2020) 112133, https://doi.org/10.1016/j.bios.2020.112133, 112133.

[85] C. Cheng, X. Li, G. Xu, Y. Lu, S.S. Low, G. Liu, L. Zhu, C. Li, Q. Liu, Battery-free, wireless, and flexible electrochemical patch for in situ analysis of sweat cortisol via near field communication, Biosens. Bioelectron. 172 (2021) 112782, https://doi.org/10.1016/j.bios.2020.112782, 112782.

[86] A.J. Bandodkar, P. Gutruf, J. Choi, K.H. Lee, Y. Sekine, J.T. Reeder, W.J. Jeang, A. J. Aranyosi, S.P. Lee, J.B. Model, R. Ghaffari, C.J. Su, J.P. Leshock, T. Ray, A. Verrillo, K. Thomas, V. Krishnamurthi, S. Han, J. Kim, S. Krishnan, T. Hang, J. A. Rogers, Battery-free, skin-interfaced microfluidic/electronic systems for simultaneous electrochemical, colorimetric, and volumetric analysis of sweat, Sci. Adv. 5 (2019), https://doi.org/10.1126/SCIADV.AAV3294.

[87] H. Mirzajani, T. Abbasiasl, F. Mirlou, E. Istif, M.J. Bathaei, Ç. Dağ, O. Deyneli, D. Yazıcı, L. Beker, An ultra-compact and wireless tag for battery-free sweat glucose monitoring, Biosens. Bioelectron. 213 (2022) 114450, https://doi.org/10.1016/j.bios.2022.114450, 114450.

[88] M.C. Hartel, D. Lee, P.S. Weiss, J. Wang, J. Kim, Resettable sweat-powered wearable electrochromic biosensor, Biosens. Bioelectron. 215 (2022) 114565, https://doi.org/10.1016/j.bios.2022.114565, 114565.

[89] R.A. Escalona-Villalpando, E. Ortiz-Ortega, J.P. Bocanegra-Ugalde, S.D. Minteer, J. Ledesma-García, L.G. Arriaga, Clean energy from human sweat using an enzymatic patch, J. Power Sources 412 (2019) 496–504, https://doi.org/10.1016/j.jpowsour.2018.11.076.

[90] H. Guan, T. Zhong, H. He, T. Zhao, L. Xing, Y. Zhang, X. Xue, A self-powered wearable sweat-evaporation-biosensing analyzer for building sports big data, Nano Energy 59 (2019) 754–761, https://doi.org/10.1016/J.NANOEN.2019.03.026.

[91] Y. Liu, L. Zhong, S. Zhang, J. Wang, Z. Liu, An ultrasensitive and wearable photoelectrochemical sensor for unbiased and accurate monitoring of sweat glucose, Sens. Actuators B Chem. 354 (2022) 131204, https://doi.org/10.1016/j.snb.2021.131204, 131204.

[92] J. Xiao, Y. Liu, L. Su, D. Zhao, L. Zhao, X. Zhang, Microfluidic chip-based wearable colorimetric sensor for simple and facile detection of sweat glucose, Anal. Chem. 91 (2019) 14803–14807, https://doi.org/10.1021/ACS.ANALCHEM.9B03110.

[93] S. He, H. Lian, X. Cao, B. Liu, X. Wei, Cascaded enzymatic reaction-mediated multicolor pixelated quantitative system integrated microfluidic wearable analytical device (McPiQ-μWAD) for non-invasive and sensitive glucose diagnostics, Sens. Actuators B Chem. 369 (2022) 132345, https://doi.org/10.1016/j.snb.2022.132345, 132345.

[94] Y. Zhang, H. Guo, S.B. Kim, Y. Wu, D. Ostojich, S.H. Park, X. Wang, Z. Weng, R. Li, A.J. Bandodkar, Y. Sekine, J. Choi, S. Xu, S. Quaggin, R. Ghaffari, J.A. Rogers, Passive sweat collection and colorimetric analysis of biomarkers relevant to kidney disorders using a soft microfluidic system, Lab Chip 19 (2019) 1545–1555, https://doi.org/10.1039/C9LC00103D.

[95] S. Kim, B. Lee, J.T. Reeder, S.H. Seo, S.U. Lee, A. Hourlier-Fargette, J. Shin, Y. Sekine, H. Jeong, Y.S. Oh, A.J. Aranyosi, S.P. Lee, J.B. Model, G. Lee, M.H. Seo, S.S. Kwak, S. Jo, G. Park, S. Han, I. Park, H.I. Jung, R. Ghaffari, J. Koo, P.V. Braun, J.A. Rogers, Soft, skin-interfaced microfluidic systems with integrated immunoassays, fluorometric sensors, and impedance measurement capabilities, Proc. Natl. Acad. Sci. U. S. A. 117 (2020) 27906–27915, https://doi.org/10.1073/PNAS.2012700117.

[96] Z. Zhou, T. Shu, Y. Sun, H. Si, P. Peng, L. Su, X. Zhang, Luminescent wearable biosensors based on gold nanocluster networks for "turn-on" detection of Uric acid, glucose and alcohol in sweat, Biosens. Bioelectron. 192 (2021) 113530, https://doi.org/10.1016/j.bios.2021.113530, 113530.

[97] Y. Cui, W. Duan, Y. Jin, F. Wo, F. Xi, J. Wu, Ratiometric fluorescent nanohybrid for noninvasive and visual monitoring of sweat glucose, ACS Sens. 5 (2020) 2096–2105, https://doi.org/10.1021/acssensors.0c00718.

[98] R.V. Blasques, J.S. Stefano, J.R. Camargo, L.R. Guterres e Silva, L.C. Brazaca, B.C. Janegitz, Disposable Prussian blue-anchored electrochemical sensor for enzymatic and non-enzymatic multi-analyte detection, Sens. Actuators Rep. 4 (2022) 100118, https://doi.org/10.1016/j.snr.2022.100118.

[99] B.A. Katchman, M. Zhu, J. Blain Christen, K.S. Anderson, Eccrine sweat as a biofluid for profiling immune biomarkers, PROTEOMICS – clin, Appl 12 (2018) 1800010, https://doi.org/10.1002/prca.201800010.

[100] C.W. Bae, P.T. Toi, B.Y. Kim, W.I. Lee, H.B. Lee, A. Hanif, E.H. Lee, N.-E. Lee, Fully stretchable capillary microfluidics-integrated nanoporous gold electrochemical sensor for wearable continuous glucose monitoring, ACS Appl. Mater. Interfaces 11 (2019) 14567–14575, https://doi.org/10.1021/acsami.9b00848.

[101] Z. Xu, J. Song, B. Liu, S. Lv, F. Gao, X. Luo, P. Wang, A conducting polymer PEDOT:PSS hydrogel based wearable sensor for accurate uric acid detection in human sweat, Sens. Actuators B Chem. 348 (2021), https://doi.org/10.1016/j.snb.2021.130674.

[102] J. Yu, D. Wang, V. Tipparaju, W. Jung, X. Xian, Detection of transdermal biomarkers using gradient-based colorimetric array sensor, Biosens. Bioelectron. 195 (2022), https://doi.org/10.1016/j.bios.2021.113650.

[103] P. Kanokpaka, L.-Y. Chang, B.-C. Wang, T.-H. Huang, M.-J. Shih, W.-S. Hung, J.-Y. Lai, K.-C. Ho, M.-H. Yeh, Self-powered molecular imprinted polymers-based triboelectric sensor for noninvasive monitoring lactate levels in human sweat, Nano Energy 100 (2022) 107464, https://doi.org/10.1016/j.nanoen.2022.107464, 107464.

[104] T.A. Hakala, A. García Pérez, M. Wardale, I.A. Ruuth, R.T. Vänskä, T.A. Nurminen, E. Kemp, Z.A. Boeva, J.-M. Alakoskela, K. Pettersson-Fernholm, E. Hæggström, J. Bobacka, Sampling of fluid through skin with magnetohydrodynamics for noninvasive glucose monitoring, Sci. Rep. 11 (2021) 7609, https://doi.org/10.1038/s41598-021-86931-7.

[105] Z. Pu, X. Zhang, H. Yu, J. Tu, H. Chen, Y. Liu, X. Su, R. Wang, L. Zhang, D. Li, A thermal activated and differential self-calibrated flexible epidermal biomicrofluidic device for wearable accurate blood glucose monitoring, Sci. Adv. 7 (2021) 199–226, https://doi.org/10.1126/SCIADV.ABD0199/SUPPL_FILE/ABD0199_SM.PDF.

[106] C. McCormick, D. Heath, P. Connolly, Towards blood free measurement of glucose and potassium in humans using reverse iontophoresis, Sens. Actuators B Chem. 166–167 (2012) 593–600, https://doi.org/10.1016/j.snb.2012.03.016.

[107] S. Cai, C. Xu, D. Jiang, M. Yuan, Q. Zhang, Z. Li, Y. Wang, Air-permeable electrode for highly sensitive and noninvasive glucose monitoring enabled by graphene fiber fabrics, Nano Energy 93 (2022) 106904, https://doi.org/10.1016/j.nanoen.2021.106904, 106904.

[108] Y. Yao, J. Chen, Y. Guo, T. Lv, Z. Chen, N. Li, S. Cao, B. Chen, T. Chen, Integration of interstitial fluid extraction and glucose detection in one device for wearable non-invasive blood glucose sensors, Biosens. Bioelectron. 179 (2021) 113078, https://doi.org/10.1016/j.bios.2021.113078, 113078.

[109] P. Bollella, E. Katz, Enzyme-based biosensors: tackling electron transfer issues, Sensors 20 (2020) 3517, https://doi.org/10.3390/s20123517.

[110] B. Yang, J. Kong, X. Fang, Bandage-like wearable flexible microfluidic recombinase polymerase amplification sensor for the rapid visual detection of nucleic acids, Talanta 204 (2019) 685–692, https://doi.org/10.1016/j.talanta.2019.06.031.

[111] T. Arakawa, R. Ishikawa, K. Iitani, K. Toma, Y. Iwasaki, K. Mitsubayashi, Headset bio-sniffer with wireless CMOS camera for percutaneous ethanol vapor from the ear canal, Biosens. Bioelectron. X. 11 (2022) 100169, https://doi.org/10.1016/j.biosx.2022.100169.

[112] Y. Lee, C. Howe, S. Mishra, D.S. Lee, M. Mahmood, M. Piper, Y. Kim, K. Tieu, H.-S. Byun, J.P. Coffey, M. Shayan, Y. Chun, R.M. Costanzo, W.-H. Yeo, Wireless, intraoral hybrid electronics for real-time quantification of sodium intake toward hypertension management, Proc. Natl. Acad. Sci. 115 (2018) 5377–5382, https://doi.org/10.1073/pnas.1719573115.

[113] H.-R. Lim, S.M. Lee, S. Park, C. Choi, H. Kim, J. Kim, M. Mahmood, Y. Lee, J.-H. Kim, W.-H. Yeo, Smart bioelectronic pacifier for real-time continuous monitoring of salivary electrolytes, Biosens. Bioelectron. 210 (2022) 114329, https://doi.org/10.1016/j.bios.2022.114329.

[114] R. Moreddu, J.S. Wolffsohn, D. Vigolo, A.K. Yetisen, Laser-inscribed contact lens sensors for the detection of analytes in the tear fluid, Sens. Actuators B Chem. 317 (2020) 128183, https://doi.org/10.1016/j.snb.2020.128183.

[115] A.E. Kownacka, D. Vegelyte, M. Joosse, N. Anton, B.J. Toebes, J. Lauko, I. Buzzacchera, K. Lipinska, D.A. Wilson, N. Geelhoed-Duijvestijn, C.J. Wilson, Clinical evidence for use of a noninvasive biosensor for tear glucose as an alternative to painful finger-prick for diabetes management utilizing a biopolymer coating, Biomacromolecules 19 (2018) 4504–4511, https://doi.org/10.1021/acs.biomac.8b01429.

[116] J.R. Sempionatto, L.C. Brazaca, L. García-Carmona, G. Bolat, A.S. Campbell, A. Martin, G. Tang, R. Shah, R.K. Mishra, J. Kim, V. Zucolotto, A. Escarpa, J. Wang, Eyeglasses-based tear biosensing system: non-invasive detection of alcohol, vitamins and glucose, Biosens. Bioelectron. 137 (2019) 161–170, https://doi.org/10.1016/j.bios.2019.04.058.